

# **PYROMETALLURGICAL RECOVERY OF COBALT FROM WASTE REVERBARATORY FURNACE SLAG BY DC PLASMA-ARC FURNACE TECHNOLOGY**

**BY: WEZI BANDA**

**DEGREE of MASTERS of SCIENCE  
In  
ENGINEERING  
(Extractive Metallurgy)**

**at the**

**University of Stellenbosch**

**Supervisor: Mr. JJ Eksteen**



**PYROMETALLURGICAL RECOVERY OF COBALT FROM  
WASTE REVERBARATORY FURNACE SLAG BY DC  
PLASMA-ARC FURNACE TECHNOLOGY**

**by**

**Wezi Banda**

**Thesis presented in partial fulfilment of the requirements for the degree of Master  
of Science in Engineering (Extractive Metallurgy) in the Department of Chemical  
Engineering at the University of Stellenbosch.**

**Supervisor: Mr. J. J. Eksteen**

**December 2001**

## **Declaration**

I, the undersigned, hereby declare that the work contained in this thesis is my own original work and has not previously, in its entirety or in part, been submitted at any university for a degree.

## Abstract

Slag cleaning has become a common practice at many smelters in the nonferrous industry to maximize recovery of valuable metals. However, during the carbothermic reduction of nonferrous slag to recover cobalt, in particular, iron is recovered predominantly. High iron levels present a problem for the subsequent treatment of the alloy as it may increase the solids loading to the filter and lead to increased reagent consumption during leaching. Finding an appropriate slag modifier that would selectively improve the recovery of cobalt against that of iron to the metallic alloy can solve this problem. In the present study the effects of lime ( $\text{CaO}$ ), rutile ( $\text{TiO}_2$ ), and fluorspar ( $\text{CaF}_2$ ) on the recovery of cobalt from waste nonferrous slag have been investigated under reducing conditions at  $1500^\circ\text{C}$ . The selective recovery of cobalt compared to the recovery of iron at different levels of flux additions is discussed in this study, to show the selectivity of these fluxes. It is also shown in the study that the recovery of cobalt does not only depend on the oxygen partial pressure and temperature but on the slag composition as well.

The slags used in the experiments were a) synthetic slag prepared from chemically pure reagents and its composition was derived from that of the industrial nonferrous slag composition typical of reverbaratory furnace and b) actual slag obtained from an old slag dump situated on the Zambian Copperbelt region. The investigation has shown that  $\text{TiO}_2$  addition leads to the most selective cobalt recoveries in all cases. On the other hand, both  $\text{CaO}$  and  $\text{CaF}_2$  lead to higher overall cobalt recoveries. The effect of  $\text{TiO}_2$  on the slag chemistry leads to the formation of iron titanate compounds in the slag unlike  $\text{CaO}$ , which displaces “ $\text{FeO}$ ” from the fayalitic slag and thus increases the activity of  $\text{FeO}$  in the molten slag, which in turn affects the iron recoveries to the alloy product.  $\text{CaF}_2$  on the other hand, affects the fluidity of the slag leading to improved recoveries by improved settling of metals through the slag to the alloy product.

A 44V/1100A DC-plasma arc furnace was used to reduce slag to recover cobalt at about 13.5kVA power input. The major part of the study was conducted in a tube furnace and the findings were applied to the extraction of cobalt from slag using the plasma-arc furnace. It was found that the synthetic slag experiments could be used as a guide to understand the behaviour of cobalt during the carbothermic recovery of cobalt from silica saturated fayalitic slags. Cobalt recoveries were higher in the DC furnace than the



corresponding reduction experiments carried out in the tube furnace. However, significant amounts of silicon and carbon were detected in the metallic alloy product of the DC plasma-arc furnace.

## Opsomming

Slak suiwering is besig om standaard praktyk te word by vele smelters om die herwinning van waardevolle metale uit slak te maksimeer. Tydens die karbotermiese reduksie van slakke vanaf kopersmelters om kobalt te herwin, word beduidende hoeveelhede yster ook herwin. Hoë ystervlakke in die herwinde legering veroorsaak probleme met die stroom-af verwerking van die legering aangesien dit lei tot verhoogde reagensgebruik tydens loging en 'n verhoogde vastestof las of die filterstelsel. Die identifisering van 'n geskikte slak modifiseerder, wat die selektiwiteit van herwinning van kobalt relatief tot yster verhoog, sal hierdie probleem verminder. In hierdie tesis word die rol van kalk ( $\text{CaO}$ ), rutiel ( $\text{TiO}_2$ ) en vloeispaat ( $\text{CaF}_2$ ) toevoeging tot die selektiewe herwinning van kobalt uit afvalslakke ondersoek. Die karbotermiese reduksie van die slak vind by  $1500\text{ }^\circ\text{C}$  plaas. Dit word getoon dat bo-en-behalwe die suurstofpotensiaal en die bedryfstemperatuur, die slak-chemie 'n beduidende rol speel.

Die slakke gebruik in hierdie studie is: a) 'n sintetiese slak gemaak van chemies-suiwer rou-materiale (waarvan die samestelling afgelei is van die samestelling van tipiese reverbereeroond slakke), en b) monsters van die ware slak verkry vanaf 'n slakhoop van die Zambiese Kopergordel. Die studie het getoon dat  $\text{TiO}_2$  toevoeging gelei het tot die hoogste selektiwiteit in alle gevalle. Daarteenoor het  $\text{CaF}_2$  en  $\text{CaO}$  gelei tot hoër algehele herwinnings van kobalt.  $\text{TiO}_2$  toevoeging lei tot die vorming van ystertitanaat komplekse in die slak, teenoor  $\text{CaO}$  wat die "FeO" uit die fajaliet struktuur verplaas en die aktiwiteit van FeO in die slak verhoog en dus gevolglik herwinning van yster tot die legering beïnvloed.  $\text{CaF}_2$  verhoog egter die vloeibaarheid van die slak wat lei tot verhoogde herwinning deurdat die legering druppels makliker uitsak deur die slak.

'n 44V/1100A Gelykstroom-plasmaboogoond is gebruik om die kobalt te herwin uit die slak teen ongeveer 13.5 kVA Die grootste gedeelte van die studie is gedoen in 'n buisoond en die bevindings was dan toegepas op die ekstraksie van kobalt uit slak in die plasmaboogoond. Dit was gevind dat die sintetiese slak eksperimente gebruik kan word as 'n voorlopige gids om die gedrag van kobalt in silika-versadigde slakke tydens karbotermiese reduksie te verstaan. Kobalt herwinnings was oor die algemeen hoër in die plasmaboogoond as vir die ooreenstemmende reaksies in die buisoond. Daar het egter

beduidende hoeveelhede silikon en koolstof in die legering opgelos tydens die plasmabooggoond eksperimente.

## **Acknowledgements**

I would like to thank my supervisor, Mr. J. J. Eksteen, for providing me the opportunity to pursue this degree and his commitment and assistance rendered during the course of the study.

My sincere gratitude is extended to Anglovaal Mining limited (AVMIN) and Chambishi Metals Plc (an AVMIN subsidiary), for the contribution to the project both financially and materially.

To Max Pelser, I say thank you for the assistance and contribution to this study. I am indebted to the staff of the workshop in the Department of Chemical Engineering for their tireless effort in making graphite crucibles and the modifications to some equipment.

Lastly, but not the least I say thank you to my family, friends and colleagues who showed interest and patience during the period of the study.



*To my parents*

## Table of Contents

<i>Declaration.....</i>	<i>i</i>
<i>Abstract .....</i>	<i>ii</i>
<i>Opsomming .....</i>	<i>iv</i>
<i>Acknowledgements .....</i>	<i>vi</i>
<i>Table of Contents.....</i>	<i>viii</i>
<i>List of Figures.....</i>	<i>xii</i>
<i>List of Tables.....</i>	<i>xvi</i>

### CHAPTER ONE

<i>Introduction.....</i>	<i>1</i>
<i>1.1 General Occurrence of Cobalt .....</i>	<i>1</i>
<i>1.2 Research Outline .....</i>	<i>2</i>
1.2.1 Recovery of Co, Cu, and Ni from Copper Slags .....	4
1.2.2 The Structure of Silicate Slag.....	5
1.2.3 Thermodynamics of Slag.....	6
1.2.4 Reaction Mechanisms and Reduction Rates .....	7
<i>1.3 Objectives of the Study.....</i>	<i>8</i>

### CHAPTER TWO

<i>Literature Review.....</i>	<i>10</i>
<i>2.1 Background on Slags.....</i>	<i>11</i>
2.1.1 Composition and Structure of Slags .....	11
2.1.2 Physical Properties of Slags.....	14
a) Viscosity .....	14
b) Interfacial Phenomena.....	15
c) Transport Properties .....	19
<i>2.2 Nonferrous Smelter Slags.....</i>	<i>20</i>
2.2.1 Thermodynamics of Nonferrous Slags .....	21
2.2.2 Metals in Slag: Occurrence of Cobalt in slag.....	24
a) Physicochemical Losses .....	26
b) Mechanical Losses .....	27
<i>2.5 Recovery of Metals from Slag .....</i>	<i>27</i>
2.5.1 Methods of Metal Recovery from Slags.....	28



<b>2.5.2 Process Thermodynamics .....</b>	<b>29</b>
a) Activity coefficient of CoO in slag .....	30
b) Distribution of Cobalt in Slag and Metal Alloy .....	32
<b>2.5.3 Process Kinetics .....</b>	<b>33</b>
a) Reduction Rates .....	33
b) Reaction Mechanisms .....	35
<b>2.6 The Influence of Fluxing on Slag Properties and Cobalt Recovery .....</b>	<b>37</b>
<b>2.7 Thermodynamics of Metallic Phase.....</b>	<b>38</b>
<b>2.8 Recovery of Cobalt from Slag by DC Plasma Arc Technology.....</b>	<b>39</b>
2.8.1 History of Plasmas .....	39
2.8.2 Principles of Plasma Arcs .....	40
a) Heat Transfer Modes .....	40
b) Initiation of the Plasma Arc .....	41
2.8.3 Application: Specific Technology on Cobalt Extraction.....	43
2.8.4 Practical Problems Encountered with Plasma arc Furnaces .....	49
2.8.5 Role of Feed Charge Option: Through Electrode or Through Side Ports ....	51
<b>2.9 Summary .....</b>	<b>52</b>

## **CHAPTER THREE**

<b><i>Experimental.....</i></b>	<b>54</b>
<b>3.1 Materials and Equipment.....</b>	<b>54</b>
<b>3.1.1 Materials.....</b>	<b>54</b>
a) Preparation of Slags: Synthetic Slag .....	54
b) Preparation of Wüstite.....	56
b) Preparation of slags: Actual Slag .....	57
<b>3.1.2 Equipment .....</b>	<b>63</b>
a) Induction furnace.....	63
b) Tube Furnace.....	63
c) Bottom - Loading Furnace.....	64
d) Plasma Furnace .....	65
d) Crucibles.....	66
<b>3.2 Method.....</b>	<b>67</b>
<b>3.2.1 Tube Furnace Experiments .....</b>	<b>67</b>
a) Synthetic Slag Experiments.....	67
b) Actual Slag Experiments.....	68
<b>3.2.2 Plasma Furnace Experiments.....</b>	<b>69</b>
<b>3.2.3 Determination of Reaction Mechanisms and Reduction Rates .....</b>	<b>70</b>
<b>3.2.4 Analytical Procedures .....</b>	<b>71</b>
a) ICP.....	71
b) XRFS.....	71



c) XRD .....	71
d) Titrametric Analysis .....	72
<b>3.3 Preliminary Experiment .....</b>	<b>72</b>
<b>3.3.1 Determination of Graphite and Flux Amount .....</b>	<b>72</b>
<b>3.3.2 Setup of Slag Reduction Experiments .....</b>	<b>73</b>

## CHAPTER FOUR

### *Results and Discussion..... 74*

<b>4.1 Preliminary Experiments..... 74</b>	<b>74</b>
<b>4.1.1 Determination of Carbon Requirement .....</b>	<b>74</b>
<b>4.1.2 Effect of Amount of Reductant on the Recovery of Cobalt .....</b>	<b>75</b>
<b>4.1.3 Reduction Rates and Reaction Mechanisms .....</b>	<b>77</b>
<b>4.2 Final Experiments .....</b>	<b>79</b>
<b>4.2.1 Synthetic slag experiments.....79</b>	<b>79</b>
a) Effect of CaO on the Recovery of Co, Cu and Fe Metals from Slag .....	79
b) Effect of CaF <sub>2</sub> on the Recovery of Co, Cu and Fe Metals from Slag .....	80
c) Effect of TiO <sub>2</sub> on the Recovery of Co, Cu and Fe Metals from slag .....	81
<b>4.2.2 Actual Slag Experiments.....84</b>	<b>84</b>
a) Effect of CaO on the Recovery of Co, Cu and Fe Metals from Slag .....	84
b) Effect of CaF <sub>2</sub> on the Recovery of Co, Cu and Fe Metals from Slag .....	84
c) Effect of TiO <sub>2</sub> on the Recovery of Co, Cu and Fe Metals from Slag.....	85
<b>4.2.3 DC Plasma-arc Furnace Experiments .....</b>	<b>88</b>
a) Effect of CaO on recovery of Co, Cu and Fe Metals from Slag .....	88
b) Effect of CaF <sub>2</sub> on recovery of Co, Cu and Fe Metals from Slag.....	89
c) Effect of TiO <sub>2</sub> on the Recovery of Co, Cu and Fe Metals from Slag.....	89
<b>4.3 Effect of Slag Modifiers on Slag Composition and Recovery of Metals .....</b>	<b>91</b>
<b>4.3.1 Effect of Slag Modifiers on the Basicity of Slag.....91</b>	<b>91</b>
<b>4.3.2 Effect of Slag Modifiers on Recovery Ratio of Co to Fe in Metal Alloy .....</b>	<b>92</b>
<b>4.4 Thermodynamic Considerations .....</b>	<b>98</b>
a) Effect of CaO on Slag Composition.....	99
b) Effect of CaF <sub>2</sub> on Slag Composition.....	100
c) Effect of TiO <sub>2</sub> on Slag Composition .....	100
<b>4.4.1 Effect of Slag Modifier on Cobalt in Slag.....101</b>	<b>101</b>

## CHAPTER FIVE

### *Conclusions and Recommendations.....104*



*References*.....107

*Appendices*.....114

Appendix A.....114

Appendix B.....115

Appendix C.....120

## List of Figures

Figure 2.1. Stages in the breakdown of the lattice of molten silica brought about by the addition of an oxide of a divalent metal such as CaO. The shaded circles represent metal ions. The concentration of metal oxide increases from top to bottom. (Richardson, 1974) ..	13
Figure 2.2 Effect of FeO/SiO <sub>2</sub> ratio in slag on interfacial tensions between metal (alloy) and slags. Average matte grade is 46.4 wt% Cu. Linear least square (Mackey, 1982) .....	18
Figure 2.3 Effect of lime content on interfacial tensions between metal (mattes) and slags. Average silica content of slag 34 wt%; average matte grade is 45.4 wt% Cu. (Mackey, 1982) .....	19
Figure 2.4. CaO-FeO-SiO <sub>2</sub> equilibrium phase diagram (Biswas and Davenport, 1980) .....	22
Figure 2.5. The SiO <sub>2</sub> -FeO-Fe <sub>2</sub> O <sub>3</sub> system Partial liquidus diagram (Floyd and Mackey, 1981) .....	23
Figure 2.6. Fayalite homogeneous melt region showing composition range of some slags (Floyd and Mackey, 1981) .....	24
Figure 2.7 Predominance area diagram of system Cu-Co-Fe-S-O-SiO <sub>2</sub> at 1250°C (Imriš, 1982) .....	26
Figure 2.8 A schematic representation of mass transfer processes occurring between and within phases during slag cleaning operations (Floyd and Mackey, 1981) .....	34
Figure 2.9. Recovery of elements to the alloy as a function of the quantity of carbon added, at 1500°C (Jones <i>et al.</i> 1996) .....	35
Figure 2.10. Typical Potential distribution along an arc (Jerome Feinman, 1987) .....	41
Figure 2.11. Voltage-current characteristic for an arc and for voltage and current sources, respectively (Jerome Feinman, 1987) .....	43
Figure 2.12 Kinetics of slag cleaning (Curr, 1985) .....	46

Figure 2.13. Reduction kinetics of the slag by using coke and natural graphite (Yucel <i>et al.</i> , 1992).....	47
Figure 2.14 Varying Co and Cu recovery in the metallic matte against various power inputs (Yucel <i>et al.</i> , 1992).....	48
Figure 2.15. Cross section of the furnace with 50 kg slag smelting capacity (Yucel <i>et al.</i> , 1992).....	49
Figure 2.16. A schematic diagram of the DC-arc furnace used at Mintek (Curr <i>et al.</i> , 1983). ....	50
Figure 3.1 X-ray diffractogram of the “FeO” compound.....	57
Figure 3.2 Slag matrix with entrained phases (a) and (b) cumulates at x200 magnification .....	58
Figure 3.3 Metallic phase within the slag matrix, (a) transmitted light microscope image, (b) reflected light microscope image.....	59
Figure 3.4 A ferrite subphase, <i>f</i> , around metallic phase, <i>m</i> . (a) transmitted light microscope image, (b) reflected light microscope image. ....	59
Figure 3.5 Metallic phase within the metal phase appearing as light spots in (a) and some gray spots in (b). ....	59
Figure 3.6 Composition and microscopic image of slag marix.....	61
Figure 3.7 Image of the copper sulphide phase (white dots) within metallic the metalli phase ....	61
Figure 3.8 Image and composition of Cu-Fe-S system in the metallic phase .....	62
Figure 3.9 Image and composition of phase containing cobalt, Co-S-Cu-Fe phase within the metallic phase .....	62
Figure 3.10 A schematic diagram of the Induction furnace setup for the preparation of master slag (SiO <sub>2</sub> , CaO, Al <sub>2</sub> O <sub>3</sub> and MgO). 1. Induction Coil, 2. Graphite Crucible, 3. Slag Mixture, 4. Insulating Material, 5. Furnace Shell.....	63



Figure 3.11 A schematic diagram of the set-up of the tube furnace used in the experiments. 1. Cooling Water channel, 2. Rubber Seals, 3. Radiation Shield, 4. Platinum Wire, 5. Recrystallized Alumina Crucible, 6. Recrystallized Alumina Work Tube, 7. Bolt and Nut, 8. Gas Inlet, 9. Insulation Material, 10. Lanthanum Chromate Element, 11. Element Support Collar, 12. Gas Outlet .....	64
Figure 3.12 A schematic drawing of the setup for the determination of mechanisms and rates of reaction experiments .....	65
Figure 3.13 Schematic diagram of the DC plasma furnace used in extraction of cobalt from slag. 1. Cathode Terminal, 2. Cooling Water Channel, 3. Feed Port, 4. Graphite Electrode, 5 Refractory Material, 6. Graphite Crucible, 7. Anode Terminal, 8. Offgas Outlet, .....	66
Figure 4.1 The effect of reductant on the amount of metal alloy recovered at 1500°C.....	77
Figure 4.2 Determination of reduction rate of metal oxide in slag at 1500°C.....	78
Figure 4.3 The effect of CaO on cobalt, iron and copper recoveries .....	80
Figure 4.4 The effect of CaF <sub>2</sub> on cobalt, iron and copper recoveries.....	81
Figure 4.5 The effect of TiO <sub>2</sub> on cobalt, iron and copper recoveries .....	82
Figure 4.6 The effect of CaO on the reductive recovery of Co, Cu, and Fe from slag at 1500°C. ....	84
Figure 4.7 The effect of CaF <sub>2</sub> on the reductive recovery of Co, Cu, and Fe from slag at 1500°C. ....	85
Figure 4.8 The effect of TiO <sub>2</sub> on the reductive recovery of Co, Cu, and Fe from slag at 1500°C. ....	86
Figure 4.9 The effect of CaO on the reductive recovery of Co, Cu, and Fe from slag using a DC Plasma arc Furnace. ....	88
Figure 4.10 The effect of CaF <sub>2</sub> on the reductive recovery of Co, Cu, and Fe from slag using a DC Plasma arc Furnace. ....	89



Figure 4.11 The effect of $\text{TiO}_2$ on the reductive recovery of Co, Cu, and Fe from slag using a DC Plasma arc Furnace. ....	90
Figure 4.12 The effect of flux addition on the Co/Fe ratio in metal alloy during the carbothermic reduction of synthetic slag in a tube furnace at $1500^\circ\text{C}$ . ....	93
Figure 4.13 The effect of flux addition on the Co/Fe ratio in metal alloy during the carbothermic reduction of actual slag in a tube furnace at $1500^\circ\text{C}$ . ....	93
Figure 4.14 The effect of flux addition on the Co/Fe ratio in metal alloy during the carbothermic reduction of actual slag in a DC plasma-arc furnace. ....	94
Figure 4.15 Influence of CaO on iron-silicate slag. Calculated from HSC thermodynamic package .....	100
Figure 4.16 Influence of $\text{TiO}_2$ on iron-silicate slag. Calculated from HSC thermodynamic Package.....	101
Figure 4.17 Effect of slag modifiers on the Co distribution between slag and metal in synthetic slag at $1500^\circ\text{C}$ .....	102
Figure 4.18 Effect of slag modifiers on the Co distribution between slag and metal in synthetic slag at $1500^\circ\text{C}$ .....	102
Figure 1B Setup of Tube Furnace .....	115
Figure 2B. Setup of crucible for Tube Furnace experiments .....	115
Figure 3B Muffle Furnace Setup used in the rate reduction determination .....	116
Figure 4B Induction Furnace Setup used in the rate reduction determination .....	116
Figure 5B DC plasma-arc furnace setup used in the recovery of cobalt from slag .....	117

## List of Tables

Table 2.1 Surface energy of some fayalite slags (Minto and Davenport, 1973) .....	16
Table 2.2 Typical composition of copperbelt converter slag (Floyd and Mackey, 1981).....	21
Table 2.3 The activity of coefficient of CoO in iron silicate slags before and after recalculation. Components in ( ) are part of cobalt alloy (Teague, 2000). ....	31
Table 2.4 Bath resistance as a function of depth (Curr <i>et al.</i> , 1983) .....	43
Table 2.5 Analysis of Turkey (Kure) copper slag (Yucel <i>et al.</i> , 1992).....	47
Table 2.6 Arc smelting furnace power ratings (Açma <i>et al.</i> , 1993) .....	48
Table 3.1 Reagents used and their purity .....	55
Table 3.2 Composition of base slag .....	56
Table 3.3 Composition of the synthetic slag .....	65
Table 3.4 Composition of the actual slag .....	69
Table 3.5 Composition of the actual slag used in plasma furnace experiments.....	69
Table 3.6 Analysis of anthracite used in the plasma furnace experiments.....	70
Table 4.1 Calculation of carbon requirement .....	75
Table 4.2 Data from the initial experiments conducted at 1500°C.....	76
Table 4.3 Analysis of Metal contents of slag and alloy at the end of experiments-synthetic slag experiments .....	83

Table 4.4 Analysis of Metal content of alloy and slag at the end of Experiments-Actual slag experiments.....	87
Table 4.5 Analysis of Metal content of alloy at end of experiment and feed slag – Actual slag experiments in DC Plasma arc Furnace.....	95
Table 4.6 Analysis of slag at the end of experiment – Synthetic Slag Experiments in the tube Furnace .....	96
Table 4.7 Analysis of slag at the end of Experiments-Actual slag experiments .....	97
Table 1A Preparation of crucible and slag and the product of the plasma furnace .....	117
Table 1C Synthetic Slag Experiments Data .....	122
Table 2C Feed size characterisation for DC plasma furnace Experiments .....	123
Table 3C Analytical Results.....	124
Table 4C Recovery calculations for synthetic slag experiments in the tube furnace .....	125
Table 5C Recovery calculations for actual slag experiments in the tube furnace.....	126
Table 6C Recovery calculations for actual slag experiments in the DC plasma arc furnace .....	127
Table 7C DCV readings for plasma experiments.....	128
Table 8C DCV readings for plasma experiments.....	129
Table 9C DCV readings for plasma experiments.....	130



---

## CHAPTER ONE

### *Introduction*

#### **1.1 General Occurrence of Cobalt**

Cobalt is an anomalous metal that is frequently associated with the pyrometallurgical extraction of copper and/or nickel from sulphide ores because natural deposits containing cobalt are very rare. By virtue of its position on the periodic table, cobalt has properties similar to iron and nickel. During smelting of copper and/or nickel concentrates cobalt can either enter the slag like iron or enter the matte like nickel (or copper). Its chemical similarities with iron gives it the tendency to report to the slag in oxidizing environments like converting stage of copper smelting, and in reducing environments like in slag cleaning, it is reduced with copper and/or nickel, and iron.

The development in the production of cobalt dates back from 1900 and has grown from virtually zero to the current figure of 20,000 tonnes or more (Clark, 1999). This development has been due to the vast applications cobalt has found in industry: from colouring to high-speed tools. Cobalt has the ability to create superalloys when combined with other metals e.g. in tungsten carbide it is used as a bonding material for powders of tungsten and graphite. It is also used in the treatment of cancer in the form of radioactive cobalt. Other fields in which cobalt finds its market or application are cobalt colours, magnets and catalysts, and most recently in battery manufacturing. The increased interest in the recycling of cobalt has been necessitated by the commodity price for cobalt that has been competitive and stabilizing for the past decade. The stability in price stems from the new streams of cobalt production that are emerging.

The predication is that the demand for cobalt in any given year will depend on world economic conditions, (JOM, 2000). In near to medium term, the overall growth in cobalt demand is anticipated to be 3-6% per year. In the medium to long term, cobalt supply is expected to grow faster than demand, likely causing a general downward trend in cobalt prices. During the first 11 months of 1999 for instance, the average spot price of cobalt cathode varied between US\$8.50/lb and US\$21.25/lb.



With recent advancements in the technology of nonferrous metallurgy, metal values such as cobalt, which could not be recovered due to metallurgical reasons or economical reasons, can now be recovered from slag either as part of a smelting process or as a post-treatment of dumped slag. Nowadays, slags are “cleaned” to maximise the recovery of pay metals. The methods of cleaning of slags are dictated, to a larger extent, by the type of metal to be recovered. Pyrometallurgical processes include melting and settling (copper), reduction to matte or alloy (copper, cobalt, and nickel) and fuming (zinc, lead, and tin). Beneficiation processes include milling and flotation of slowly cooled slag (copper).

The environmental aspect of slag quality is another major advantage for slag cleaning (Norbert, 2000). Even if the economics (metal prices) or metal content does not economically warrant its recovery, slag cleaning might be justified to generate an environmentally stable slag which may be valorised for applications such as road construction and cement production.

Significant amounts of cobalt metal are contained in the slag dumps produced from copper-smelting operations in Zambia and the Democratic Republic of Congo during the past four to six decades. During the early years of copper smelting in reverbaratory furnaces, very little was done to control the losses of metal values to the slag and consequently, valuable metals, particularly cobalt, were dumped and have been reported in slags dating back to the mid 20<sup>th</sup> century. Going with the recent advancements in recovering metals from slags, a project is underway in the Democratic Republic of Congo to reprocess a slag dump at Lubumbashi, consisting of approximately 20 million tonnes of old furnace slag grading 2-3%Co. In Zambia, a process is underway to reprocess a similar quantity of slag consisting of 20 million tonnes at 0.76% Co and between 1.2% and 1.5%Cu (Mining Weekly, 1999).

## 1.2 Research Outline

The cleaning of smelter slags is a fairly new practice in the nonferrous smelting industry. The literature available (chapter two) with regard to understanding the slag chemistry and other physical properties and how they affect the metal recovery is scanty and is mostly



dealing with the smelting of copper and other nonferrous metals from their mineral ores and not so much on the slags coming from smelting processes. The extractive metallurgy of copper for instance, has experienced major advancements in understanding the effect the slag properties has on improving matte grade, control of copper losses to slag and minimizing the dissolution of impurities in the matte. The effect of fluxing this type of slag with silica or lime has been studied and thermodynamic data generated regarding the activities and activity coefficients of copper and slag components ( $\text{SiO}_2$ ,  $\text{FeO}$ ,  $\text{CaO}$ ). A review (chapter two) of the thermodynamics and chemistry of copper slags on the slag cleaning to recover copper and cobalt would be a significant contribution to the knowledge required for a better understanding of the behaviour of cobalt in slag cleaning.

A few workers (Norbert, 1998; Radhanath, 1998; Matusiewicz *et al.*, 1998) have looked at the occurrence of cobalt, its distribution in the slag and its recovery from slags. The recovery of Cu, Co, and magnetic iron from ancient copper slags, located in Kure, Turkey, using a DC-arc furnace has been reported by Açma *et al.* (1993). Banks *et al.*, (1975) examined the use of carbothermic reduction to recover copper and other nonferrous metals from smelter discard slags.

Current work being done on the recovery of cobalt from waste slags is based either on the Mintek carbothermic reduction process in a DC-arc furnace (Jones *et al.*, 1998) or on the Ausmelt top submerged lance technology (Matusiewicz *et al.*, 1998). Industrial scale operations to recover cobalt from waste copper slags using electric furnaces (direct and alternating current) are due to be commissioned in Zambia and the Democratic Republic of Congo (Norbert, 2000). However, other companies such as Atomic Energy Corporation of South Africa Ltd. (AEC) and Anglovaal Ltd. (now AVMIN) have done used DC Plasma arc furnaces in different fields other than cobalt the recovery of cobalt from slag.

The relative low cost of electricity in Southern Africa seems to be a key driving force for the choice of application of electrical furnaces over fuel-based furnaces such as Ausmelt-type furnaces. The applicability of electric furnaces for the recovery of cobalt from slags has been shown to be feasible. However, more research on the chemistry of the slag and



operating conditions associated with electric furnaces like DC plasma-arc with regard to slag cleaning operations is needed.

It has been shown in the literature reviewed (Chapter 2) that the amount of cobalt recovered differed according to the initial composition of the slag. The composition of the slag depends on the way the ore was treated, the type of process and whether the slag came from smelting furnaces or converters. Most slags of interest are rich in iron oxide and silica, and many have a bulk composition of approximately that of fayalite.

One of the key challenges lies in finding an additive that may modify the slag chemistry for optimal and selective recovery of cobalt (and copper to a lesser extent) over that of iron. Furthermore, a possible mechanism is required which would characterise the influence of these modifiers on the reductive recovery of cobalt from slag at plasma-smelting temperatures. Experiments to characterise the kinetics and mass transfer/mixing effects in a small scale DC plasma arc furnace would also be required.

### **1.2.1 Recovery of Co, Cu, and Ni from Copper Slags**

It is a general consensus among many researchers that metals in slags are encountered either as a dispersed phase of entrained metal phases (matte or pure metal) or as a dissolved species in the form of sulphide or oxide existing in a single homogeneous phase. Oxidic dissolved species are prevalent in slags from processes involving high-grade mattes typical of converter slags. If entrained metals are not too finely dispersed in the slag metals such as copper and nickel can be recovered from slag by settling, but for dissolved metals chemical reduction may be necessary to achieve significant recoveries.

Electric furnaces are most frequently used in copper smelting, however, other furnaces such as the Ausmelt-developed, oil-fired furnace at the Chinese Houma smelter and the El Teniente-developed Horno de Limpieza de Escoria furnace, are being used for copper slag cleaning, the latter after injection of a reductant for the recovery of copper from more oxidized slags (Norbert, 2000). The flotation of slowly cooled slags after suitable milling is another process very frequently encountered for the recovery of sulphide copper from copper slags, particularly from copper converting.



Whereas nickel follows copper in converting to a large extent, cobalt follows iron and invariably reports to the converter slag or to the smelter slags if converter slags are returned to the smelter. From these slags, cobalt can be recovered as an alloy or a matte by reductive smelting in an electric furnace. A review of recent studies (Chapter 2) have shown that reduction smelting by DC plasma-arc furnace can be applied as a post treatment of old copper smelter dump slag to recover cobalt metal.

To decrease cobalt losses in slags in Cu-Ni smelting, processes have been developed that are aimed at separating iron prior to the converting step. This is achieved in the Falconbridge process, in which iron and sulphur are partially oxidized by roasting as a first step, followed by reductive smelting to matte in an electric furnace (Norbert, 2000).

The recovery of metals from slag would need an understanding of the type and structure of the slags in which these metals exists. The slags arising from industrial furnaces (such as reverbaratory furnace) that process copper are characterised as silica-saturated silicate slags with substantial amount of iron (magnetite) and other metal oxides.

### 1.2.2 The Structure of Silicate Slag

Molten slags are oxide mixtures, which play a significant role in slag-metal reactions in many industrial processes. For a discussion of various properties of molten slags, the knowledge of their structure is essential.

A crystalline silicate is an arrangement of chains of silica ( $\text{SiO}_4$ ) tetrahedra linked to four others by bridging  $-\text{O}-$  (oxygen) bonds. When melted, it is supposed that some of the regularity of the arrangement of the tetrahedral units in the crystal lattice is lost. The introduction of basic oxides (or other network breakers) to such a melt introduces  $\text{O}^{2-}$  ions (in the case of basic oxides), which can combine with  $-\text{O}-$  to produce pairs of  $\text{O}^-$  ions attached to the silica matrix. This is said to continue until a certain critical value of the ratio of  $\text{O}^{2-}$  (or network breaker)/ $\text{SiO}_2$  is attained. Cations such as  $\text{Na}^+$ ,  $\text{Ca}^{2+}$ ,  $\text{Mg}^{2+}$ ,  $\text{Fe}^{2+}$ , tend to break the bonded oxygen and form non-bridging oxygens (NBO),  $\text{O}^-$ , and free oxygens,  $\text{O}^{2-}$ .



Other cations, which also form tetrahedra, are  $\text{Ti}^{4+}$ ,  $\text{Al}^{3+}$ ,  $\text{P}^{5+}$  and  $\text{Fe}^{3+}$ . These can be incorporated into silicate network as  $\text{TiO}_4^{4-}$ ,  $\text{AlO}_4^{5-}$ ,  $\text{PO}_4^{3-}$  and  $\text{FeO}_4^{5-}$ . Some cations are needed for electrical charge-balancing duties of the melt. Such cations (e.g.  $\text{Na}^{2+}$ ) do not participate in network-breaking thus the addition of  $\text{Al}_2\text{O}_3$  to a silicate melt may cause further polymerisation of the melt.

Copper slags arising from reverbaratory furnace are estimated on a  $\text{SiO}_2$ -‘FeO’-CaO ternary system in which all the oxides of iron are reported as “FeO” and,  $\text{MgO}$ ,  $\text{Al}_2\text{O}_3$ ,  $\text{K}_2\text{O}$  and  $\text{Na}_2\text{O}$  are reported as CaO. The slag is silica saturated (about 35%  $\text{SiO}_2$ ) with a significant amount of iron oxides (magnetite). The mineralogical studies of the slag have shown that cobalt is present in slag as  $\text{CoO}$ . Copper in the slag is mainly attributed to the presence of copper rich sulphides or entrained matte ( $\text{Cu-Fe-S}$ ) droplets. The cobalt oxide, and to a lesser extent, the copper oxide are associated with the silicate/oxide phases (Jones, 1997)

### 1.2.3 Thermodynamics of Slag

Slag is formed from the gangue minerals contained in the ores and from fluxing materials such as silica, lime, and fuel for burners. Slag has a lower density than metal alloy or matte and so it forms on top of matte or alloy in smelting processes. The important properties of a slag in smelting include good metal-slag separability, good fluidity of the slag, and ability to absorb unwanted elements from the sought metal. In addition, the slag shields the matte or alloy from the furnace gases that may cause reoxidation of the metal in the matte during a smelting process. The properties of the slag can be controlled to improve the grade of the metal alloy or matte. This is achieved by altering the physicochemical properties of the slag consequently, controlling the activities and activity coefficient of metal oxides in the slag. This in turn affects the solubility of metals and metal oxides in the matte or alloy and slag, respectively.

The distribution of cobalt between slag and matte depends on a number of thermodynamic parameters. The most significant one is the activity coefficient of cobalt oxide in the slag. Under the conditions of constant temperature and oxygen partial pressure, the activity coefficient of cobalt oxide is a function of slag composition and affects the extent to which cobalt dissolves in the matte. If the composition of the slag is



controlled so that the activity coefficient of cobalt oxide in the slag is increased, the solubility of cobalt oxide in the slag will be reduced and hence, the recovery of cobalt could be increased by forcing the cobalt present in the slag to dissolve in the matte (Teague, 2000).

#### 1.2.4 Reaction Mechanisms and Reduction Rates

In the reduction smelting of a slag with solid carbon, it is traditionally assumed that the limiting reaction is the gasification reaction of carbon. The gas plays two important roles; mass transfer of elements from metal to slag by escaping gases ( $\text{CO}_2$ ,  $\text{SO}_2$ , etc.) and reduction of oxides by reducing gas ( $\text{CO}$ ). Three phases (gas-liquid-solid) coexists only on their interface, therefore, in an overall reaction involving three or more phases, the rate controlling reaction is that which occurs at an interface between the two phases only. The reduction time of the slag can be limited by the amount of cobalt oxide contained in the slag. The following stages have been assumed to take place during a carbothermic reduction in which solid carbon is used.

- i) *metal-iron exchange:*  $(\text{MO}) + [\text{Fe}] = (\text{FeO}) + [\text{M}]$
- ii) *reduction of FeO in slag:*  $(\text{FeO}) + \text{CO} = [\text{Fe}] + \text{CO}_2$
- iii) *generation of CO gas:*  $\text{C} + \text{CO}_2 = 2\text{CO}$

where, ( ) refers to the slag phase and [ ] refers to the alloy/matte phase.

The cobalt oxide, and to a lesser extent, the copper oxide associated with the silicate/oxide phases, are reduced by Fe from the alloy to form metallic Co (and Cu), resulting in the formation of FeO in the slag. Given that this reaction occurs between the metal bath and the overlying slag, the exchange of Co and Cu with Fe will take place only at the slag/metal interface. An improvement in recoveries of valuable metals can be achieved by allowing greater quantities of slag to come into contact with the alloy (by mild gas stirring, for example), and increasing the length of contact time between slag and metal, within the constraints of economic and logistic feasibility. The amount of cobalt recovered during a carbothermic reduction of copper slags can be affected by the reduction time, the amount of reductant, and power applied to the furnace (Yucel *et al.*, 1992 and Ama *et al.*, 1992).



### 1.3 Objectives of the Study

As outlined above, an understanding of the role the slag modifiers play in reduction smelting of old copper smelter slag to recover cobalt is important to the industrial operations of today. The concentration or grade of cobalt in slag is lower (0.7 – 3 %) than that of iron (17 – 22 %) and thus, a more selective recovery process in favour of cobalt would be preferable.

The main objective of this study was to determine the optimal chemical conditions to recover cobalt from reverbaratory furnace slag by carbothermic reduction at 1500°C. This temperature (1500°C) was chosen for the following reasons:

- Intended industrial operations in a DC plasma arc would operate at temperatures above 1500°C.
- Most of the work that has been done previously with regard to the thermodynamics of cobalt in slag at matte smelting is in the range of 1200 to 1350°C. Operating at 1500°C would create an opportunity to explore the behaviour of cobalt at elevated temperatures.
- Above all, the alloy product of the reduction process is predominantly iron. To maintain a liquid state of the alloy (and the slag) during the smelting process, a temperature of 1500°C would be required.

To conduct this study the following issues were considered and addressed.

- A review of literature to highlight the economical, thermodynamic, kinetics and technological aspects of slag cleaning. The occurrence and behaviour of cobalt in slag at matte smelting and converting was reviewed.
- The existing operations and projects on slag cleaning with particular interest in cobalt recovery were reviewed.
- Preliminary experimental investigation of mechanisms and rate of reduction of iron-silicate slag (containing cobalt and copper) by solid carbon were performed to aid the interpretation of the reduction rates and mechanisms.
- The effects of lime (CaO), fluorspar (CaF<sub>2</sub>), and rutile (TiO<sub>2</sub>) as slag modifiers on the selective recovery of cobalt (and to some extent copper) were evaluated



experimentally. The mechanism by which lime, fluorspar and rutile affect the slag chemistry and structure is discussed.

- The experiments to reduce copper slag in a laboratory scale DC plasma arc furnace to recover cobalt were conducted.

The findings from the literature review are summarised in chapter 2 and the findings from the present study are summarised in Chapter 4.

## CHAPTER TWO

### *Literature Review*

The review of literature is aimed at establishing the composition of slags, recovery of metals from slags and thermodynamic behaviour of metal oxide in slag, particularly cobalt metal. The subject on slags is a wide topic and so only the slags relevant to nonferrous slags are reviewed. It should be noted that most of the literature reviewed on the behaviour of cobalt metal in slag is carried out on the conditions that relate to matte smelting. In other words the literature has to do more with slagging of cobalt than the recovery of cobalt from slag. However, there are a few researchers who have reported on the behaviour of cobalt during slag cleaning of nonferrous slag and their work is reviewed. The limited literature on slag cleaning could be due to it been a relatively new concept. There is much that is required for a clear understanding of slag cleaning under reductive smelting conditions. The use of electric furnaces particularly the DC plasma-arc type furnace, to recover cobalt and other base metals from slags will be reviewed.

The first part of this chapter describes the composition and structure of slag with emphasis on slag arising from the reverbaratory furnace, which has traditionally been the standard smelting furnace for copper sulphide minerals in copper production. The physical properties of slags and the metal losses during smelting are described in the first part. The behaviour of cobalt in slag is described in the second part along with the methods of recovery of cobalt from slags and the effect of modifying the composition of slag and selective recovery of cobalt. The thermodynamic properties of the alloy will be described too.

The final part of the chapter describes the recovery of cobalt from slags using dc electric furnace. The definition, history, properties and behaviour of the plasma are also described.



## 2.1 Background on Slags

Slags are formed in the smelting (melting and separation) of ores or refining of crude metals from gangue minerals contained in the ores and from fluxing material such as silica, lime and heavy fuel for burners. Since  $\text{SiO}_2$  is always present in any ore, slags are essentially silicate melts and sometimes a mixture of phosphates and borates. The slags are immiscible with metallic phases and thus make them separable from metallic phases. By virtue of the lower densities of slags compared to metallic and sulphide phases, slags form on top of the metallic phase during the smelting process. The importance of slag control in metallurgical processes include,

- i) Good separability: the two liquids of metallic alloy and slag must be completely immiscible with each other.
- ii) Ability to absorb impurities: the grade of the metal been recovered is affected by the unwanted elements that may be recovered along. To control this the slag must be controlled such that it is able to absorb such impurities from the sought metal. For instance in copper smelting, the amount of impurities to the matte like bismuth, arsenic, selenium, lead, etc are controlled by controlling the slag properties. Also, the costs of the proceeding processes are affected.
- iii) Slags also protect the metal from being contaminated by the environment and reduce excessive heat loss from the metal.

In order to give slags the desired properties such as melting point, viscosity, density, or chemical properties, other components, “fluxes”, are sometimes added. Common fluxes are lime and magnesia in iron and steelmaking, fluorspar in steel refining, and silica in copper smelting. In this study the term flux will be used to refer to compounds added to slag to modify and control the properties of the slag.

### 2.1.1 Composition and Structure of Slags

Since most mineral ores contain  $\text{SiO}_2$ , the composition of molten slags are chiefly silicates with the concentration of  $\text{SiO}_2$  varying from process to process. Also present in the melts are metallic oxides like  $\text{CaO}$ ,  $\text{MgO}$ , and  $\text{Al}_2\text{O}_3$ , which enter the slag by way of fluxes or as mineral ore constituents. The existence of iron in slag is in a form of magnetite or wüstite, depending on the oxygen potential of the slag. The source of iron in



slag is from the mineral ores, for example, in copper minerals iron is present in bornite ( $\text{Cu}_5\text{FeS}_4$ ) or chalcopyrite ( $\text{CuS} \cdot \text{FeS}$ ). Other components present include the  $\text{K}_2\text{O}$ ,  $\text{Na}_2\text{O}$ ,  $\text{Cr}_2\text{O}_3$ , and  $\text{P}_2\text{O}_5$ . Slags arising from industrial operations are complex and usually contain many components (multicomponent slags) that are difficult to quantify. The literature available on the composition of slag is confined to iron and steelmaking industry in most cases.

A crystalline silicate is an arrangement of chains of silica ( $\text{SiO}_4$ ) tetrahedron linked to four others by bridging  $-\text{O}-$  (oxygen) bonds. When melted, it is supposed that some of the regularity of the arrangement of the tetrahedral units in the crystal lattice is lost. The introduction of basic oxides (or other network breakers) to such a melt introduces  $\text{O}^{2-}$  ions (in the case of basic oxides), which can combine with  $-\text{O}-$  to produce pairs of  $-\text{O}^-$  ions attached to the silica matrix. This is said to continue until a certain critical value of the ratio of  $\text{O}^{2-}$  (or network breaker)/ $\text{SiO}_2$  is attained. Cations such as  $\text{Na}^+$ ,  $\text{Ca}^{2+}$ ,  $\text{Mg}^{2+}$ ,  $\text{Fe}^{2+}$ , tend to break the bonded oxygen and form non-bridging oxygens (NBO),  $\text{O}^-$ , and free oxygens,  $\text{O}^{2-}$ . Chain breakage according to Masson, (1965) as reviewed by Gaskell, (1981) is a depolymerisation reaction that occurs according to the reaction 2.1. Figure 2.1 shows an illustration of the structure of molten slag and the effect of oxide addition



The concept of ionisation and thus polymerisation or depolymerisation can be viewed from the properties of the periodic table. The oxides of the alkali metals (Li, Na, K, etc) are more ionic in nature than the alkaline earth metals (Be, Mg, Ca, etc), which in turn are more ionic than the transition metals. The oxides of the metals become progressively more covalent in nature across the periodic table from left to right. The strongly ionic oxides ionise most readily in melts (to  $\text{M}^+$  and  $\text{O}^{2-}$ ). This increases the available  $\text{O}^{2-}$  ions in the melt causing further depolymerisation due to the breakdown of pyrosilicate to orthosilicate (reaction 1.2).

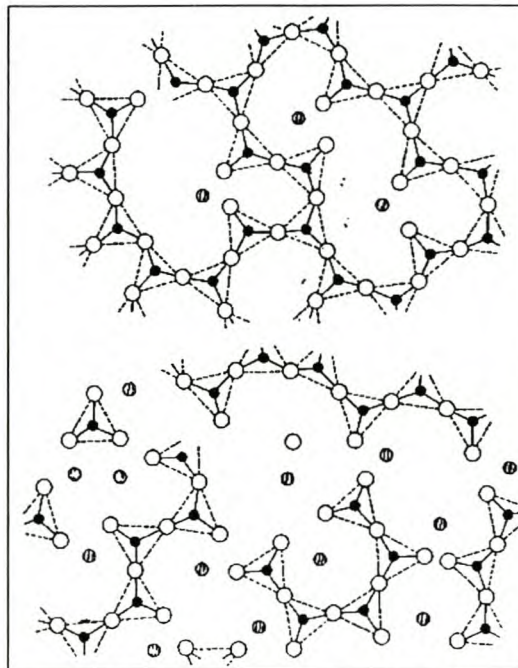


Other cations, which also form tetrahedra, are  $\text{Ti}^{4+}$ ,  $\text{Al}^{3+}$ ,  $\text{P}^{5+}$  and  $\text{Fe}^{3+}$ . These can be incorporated into silicate network as  $\text{TiO}_4^{4-}$ ,  $\text{AlO}_4^{5-}$ ,  $\text{PO}_4^{3-}$  and  $\text{FeO}_4^{5-}$ . Some cations are



needed for electrical charge-balancing duties of the melt. Such cations (e.g.  $\text{Na}^{2+}$ ) do not participate in network-breaking thus the addition of  $\text{Al}_2\text{O}_3$  to a silicate melt may cause further polymerisation of the melt (Sano, 1997).

In slags containing iron oxides,  $\text{Fe}^{2+}$  ions tend to operate as network breakers but  $\text{Fe}^{3+}$  ions can function as both network formers and breakers. The tendency of network forming increases as the  $(\text{Fe}^{3+}/(\text{Fe}^{3+} + \text{Fe}^{2+}))$  ratio increases. This is however not expected in reductive smelting because of low oxygen potential ( $p\text{O}_2$ ) in the system. In slags containing  $\text{TiO}_2$ ,  $\text{Ti}^{4+}$  can act as both network breaker and former, however for the range of 1-7%  $\text{TiO}_2$ , it operates as a network former. The addition of  $\text{CaF}_2$  to acidic, polymerised, silicate melts results in the depolymerisation of the melt but in basic melts it acts as a diluent.



**Figure 2.1.** Stages in the breakdown of the lattice of molten silica brought about by the addition of an oxide of a divalent metal such as  $\text{CaO}$ . The shaded circles represent metal ions. The concentration of metal oxide increases from top to bottom. (Richardson, 1974)

Thermodynamic properties of slag components and other oxides that may be present in the slag can be measured in laboratory experiments. However, these experiments are expensive and time consuming. Because of this, models have been developed to interpolate and extrapolate thermodynamic data and predict thermodynamic properties of different slag systems. Evaluated data for metals, mattes, and slags can be coupled with



Gibbs energy minimisation programs to calculate equilibrium conditions in multicomponent, multiphase industrial systems. Pelton (1997) has discussed the applicability of solution models to multiphase multicomponent systems. For example, a calculation of reduction of slag by carbon at 1700°C is performed with FACT system that uses the global Gibbs minimisation with automatic data retrieval to calculate equilibrium amounts and compositions. In this example by Pelton, the quasichemical model and slag sulphide capacity were used for the liquid slag, and a polynomial model was employed for the liquid metal phase. Detailed development of the models is not part of the scope of this work but reference is made to show the ease with which certain thermodynamic properties can be calculated with optimised thermodynamic data (Pelton, 1997).

Several slags have been optimised to cover a range of multicomponent multiphase slag systems. The data optimised for the models has been confined to iron and steelmaking slags and matte smelting covering copper, nickel, lead and zinc smelting. Applicability of such thermodynamic software to slag systems with regard to cobalt recovery has not been optimised fully according to Pelton (*personal communication*, 2000).

### 2.1.2 Physical Properties of Slags

Physical properties such as density, viscosity, thermal and electrical conductivity and heat capacity are necessary in process engineering calculations and the analysis of reaction rates, kinetics and transport phenomena. From a fundamental point of view, properties such as viscosity and conductivity can help provide insight into slag structure.

#### *a) Viscosity*

A fayalitic slag high in silica has a higher viscosity than a corresponding slag in which the silica has been diluted with a metal oxide such as FeO, Fe<sub>2</sub>O<sub>3</sub>, or CaO. The high viscosity of silica slags is a result of the presence of the three-dimension network of polymeric silicate anions. This network is broken down by the addition of metal oxides. Viscosities of slags have temperature coefficients, which typically follow the Arrhenius equation. For fayalitic slags the influence of temperature is more marked at high silica concentrations on account of depolymerisation of silicate anions. The Mackey (1982) has shown that most workers agree that the presence of Fe<sub>2</sub>O<sub>3</sub> in liquid melts tend to lower



the viscosity of fayalite slag. The addition of CaO always decrease the viscosity of smelting slags and it is more marked for the high SiO<sub>2</sub> melts due to CaO modifying the Si-O bonds rather than the Fe-O.

The influence of temperature and composition on a large number of complex iron-silicate slags, high in Al<sub>2</sub>O<sub>3</sub> and CaO and typical of the Zambian Copperbelt, was measured many years ago in a classic study by Roberts (1959) and Higgins and Jones (1963) and reviewed by Mackey (1982). These investigators found the following trends for the slags of composition 41.5% SiO<sub>2</sub>, 26.6% FeO, 9.6% Al<sub>2</sub>O<sub>3</sub>, 22.3% CaO:

- the addition of Al<sub>2</sub>O<sub>3</sub> increases viscosity,
- the addition of CaO or MgO causes a decrease in viscosity, however with MgO, the temperature at which a steep increase in viscosity, occurs is higher with lower levels of additive,
- the partial replacement of CaO with MgO causes a decrease in viscosity up to about 6% MgO above which MgO increases viscosity and
- the addition of FeO, Fe<sub>3</sub>O<sub>4</sub> or Fe<sub>2</sub>O<sub>3</sub> reduced viscosity.

Copper sulphide and copper metal (with its inherent cobalt content) have a higher density and are immiscible with slag. Thus any copper in this phase will have a tendency to settle from the molten slag into the metal bath. It is therefore important that the viscosity of the slag is reduced to improve recoveries. This can be achieved by increased temperature or flux additions, and/or increasing the settling time to allow smaller droplets to fall.

The viscosity of liquid slag is an important physical property. It influences the transfer of heat and mass across the slag phase (Kucharski, 1989). Viscosity is a factor influencing the dispersion of gas bubbles in slag and has a bearing on slag foaming too. The presence of solids, which increases slag viscosity, or the presence of active surface polymers at the gas/slag interface encourages slag foaming. High slag viscosity and a high rate of metal drop ejection into the slag phase favours emulsion formation (Mackenzie, 1975).

### ***b) Interfacial Phenomena***

The interfacial phenomena on kinetic factors are important in processing. The main four factors determining the rate of processing are:



- i) chemical equilibria which are approached at the interfaces and so influence the concentration difference between the interface and the bulk phases,
- ii) the interfacial areas of reacting phases,
- iii) the chemical kinetics and,
- iv) the mass transfer rates at the interfaces.

Faster and effective processing can be achieved by increasing the interfacial areas per m<sup>3</sup> of the reactor. Effective stirring within the reacting phases ensures effective mass transfer rates on either side of the interfaces. In industrial electric furnaces, like the DC transferred arc mechanism, the stirring of the mixture is attained by the gaseous compounds that evolve from the chemical reactions and thus creating buoyancy driven flow in the slag. It is believed that the force of the arc will create a stirring effect on the melt.

Mackey (1982) reports that the surface energy of silicate slags is not very temperature sensitive. In the SiO<sub>2</sub>-CaO-FeO system, the partial replacement of FeO with CaO at a constant SiO<sub>2</sub> level increases the surface energy. Interfacial energy data for several slag-matte systems were compiled as part of a study on the entrapment and flotation of matte drops in reverbaratory slags Table 2.1, Minto and Davenport (1972, 1973, 1974). The last role of the data could be used to estimate the surface energy of the slags used in this study.

**Table 2.1** Surface energy of some fayalite slags (Minto and Davenport, 1973).

Composition, %				Temp., °C	Average Surface Energy, ergs/cm <sup>2</sup>
SiO	FeO	Fe O	CaO		
21.6	69.5	9.5	-	1340-1400	434
26.7	66.3	7.0	-	1250	416
30.0	70.0	-	-	1250	435
33.0	67	-	-	1250	445
33	61	-	7	1250	465
43	44	-	14	1250	440

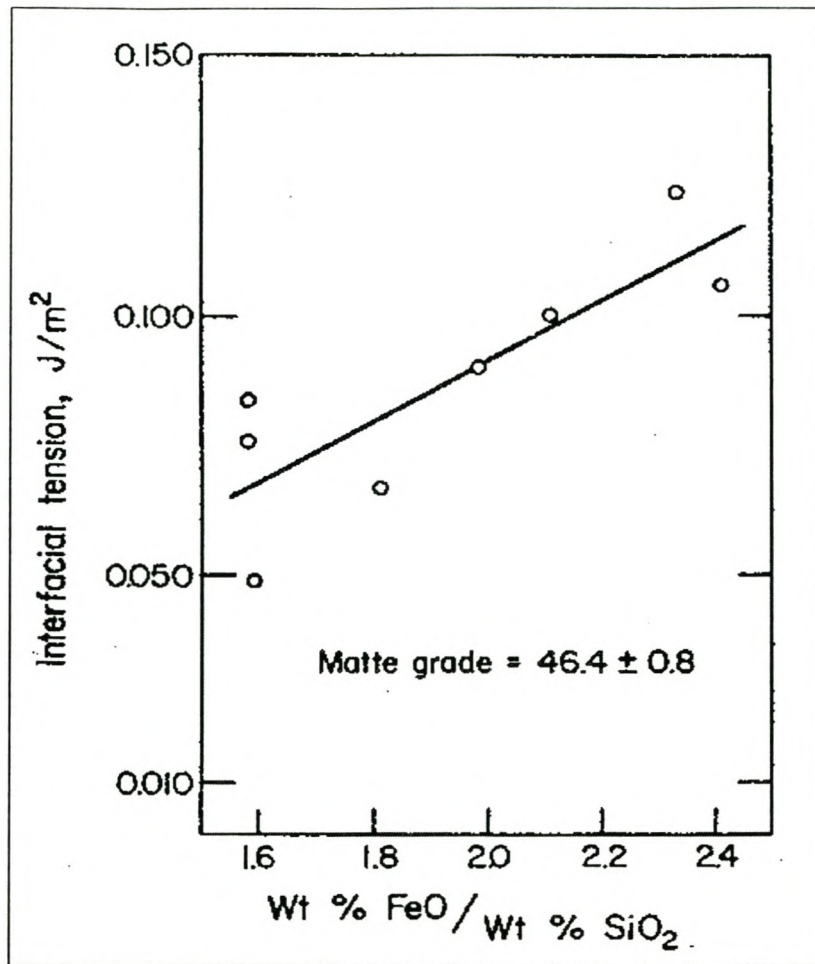
Mattes have surface tension of between 0.32 and 0.36 J/m<sup>2</sup>. Elliot *et al.* (1982) studied and measured the surface tensions and densities of Cu-Fe mattes in equilibrium with  $\gamma$ -iron and iron silicate slags. The interfacial tensions between mattes and iron-silicate slags varied from 0.02 J/m<sup>2</sup> for low-grade mattes (~20 wt % Cu) to 0.1 J/m<sup>2</sup> for high-grade



mattes (~80 wt % Cu). Their findings were that the surface tension of iron-silicates slags is lowered in the presence of sulphur.

On the wetting characteristics of slags, Elliot (1982) reports that there appears to be a reasonably good correlation between the values of the spreading coefficient (driving force for spreading of the liquid over the surface to achieve complete wetting) and the flotation coefficient (flotation of metal values by rising bubbles) and the matte grade, and also with the lime content of the slag. It was found that the addition of up to 10% CaO, partially replaces FeO in iron-silicate slags and increases the surface tension of the slags. Lime addition increased the spreading coefficient but did not affect the flotation coefficient.

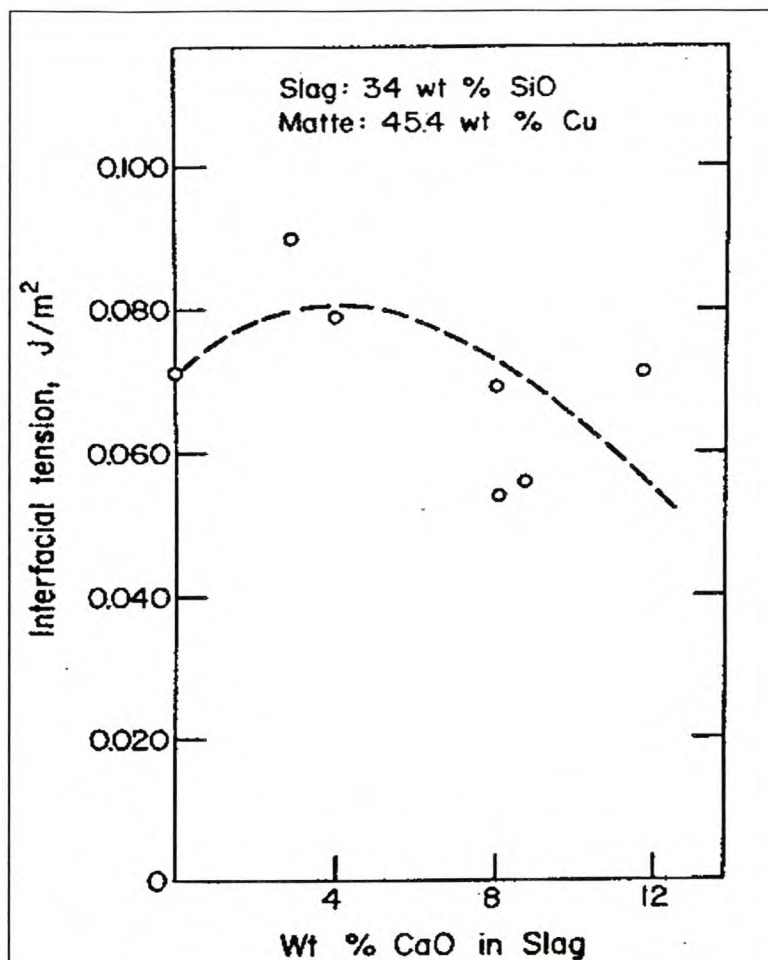
The interfacial tensions of the slag-metal interfaces are intermediate between those for metals and slags separately (Richardson, 1982). For a CaO-SiO<sub>2</sub>-Al<sub>2</sub>O<sub>3</sub> slag and liquid iron, the work of adhesion is 700-800 mJ/m<sup>2</sup> and the corresponding interfacial tension is about 1400 mJ/m<sup>2</sup>. The greater this adhesion, the lower the interfacial tension and the greater the spreading tendency of the slag on the metal. This adhesion of the slag to metal tends to increase (and hence the interfacial tension to decrease) in the presence of solutes common to both slag and metal, for example, C in Fe, C<sup>2-</sup> in slag; Fe<sup>2+</sup> in slag, Fe in metal and when the reaction is occurring between two phases.



**Figure 2.2** Effect of FeO/SiO<sub>2</sub> ratio in slag on interfacial tensions between metal (alloy) and slags. Average matte grade is 46.4 wt% Cu. Linear least square (Mackey, 1982)

According to Richardson (1982), the interfacial phenomena may have no effect on the equilibria between metals, slags and gases, but that it may exert some profound effects on the rates of reaction which occur across interfaces involving these phases. The interfacial phenomena may also affect the coalescence of metal drops in slags and influence the foaming of slags and nucleation of gases in metals.





**Figure 2.3** Effect of lime content on interfacial tensions between metal (mattes) and slags. Average silica content of slag 34 wt%; average matte grade is 45.4 wt% Cu. (Mackey, 1982)

### *c) Transport Properties*

The electrical conductivity of slags is one of the fundamental parameters affecting electric furnace smelters and is an important factor influencing the choice of slag chemistry. In silica-saturated slags such as reverbaratory slags, conduction is largely ionic (as opposed to electronic) but this decreases with slags of lower silica content (and increasing FeO content). The overall electric conductivity of converter slags would be expected to be higher than that of the reverbaratory or flash furnace slags because of higher iron content. Addition of CaO to iron silicate melts lowers its conductivity (Mackey, 1982). CaO is presumed to dissociate into equal numbers of  $\text{Ca}^{2+}$  and  $\text{O}^{2-}$  ions that tend towards neutrality. In  $\text{SiO}_2\text{-Al}_2\text{O}_3\text{-CaO}$  melts, conductivity increases with increasing basicity. Acidic slags are defined as slags with little or no free  $\text{O}^{2-}$  ions and so makes them more ionic and more conductive than basic slags, which have free  $\text{O}^{2-}$  ions (Gilchrist, 1980). These seemingly contradictory observations arise due to the presence of

electrically, ionically conductive and non-conductive components which interact non-linearly.

The conductance of silicate melts is normally raised by the addition of metal oxides since conduction mechanism is primarily ionic. In cases where the metal oxide is an electronic conductor such as FeO and CoO, which conduct by virtue of the presence of cations of variable valance, conduction becomes more ionic as the concentration of silica increases. At the same time, the proportion of the higher valence cation (e.g.  $\text{Fe}^{3+}$ ,  $\text{Co}^{3+}$ ) decreases, provided the oxygen potential is kept constant. For melt composition of the type  $2\text{FeO} \cdot \text{SiO}_2$  the electrical conduction  $\kappa$ , is  $5 \text{ ohm}^{-1} \text{ cm}^{-1}$  at  $1400^\circ\text{C}$  (Richardson, 1974).

Electrical conductive determines the slag resistivity and therefore the power dissipation,  $I^2R$ , and heating of the slag. The more conductive the slag becomes, the less does the  $I^2R$  heating in the slag itself contribute to slag heating. Slags tend to become more ionically conductive as temperature increases or as  $\text{SiO}_2$  concentration increases (rendering them acidic). This is not desired in electric furnaces because it affects the heat distribution in the melt. The remedy to this problem could be to increase the addition of CaO (or other flux) or increase the arc resistance by increasing the arc length and running at higher voltages. The latter increases the  $I^2R$  power dissipation to the melt. This increases the amount of heat transferred to the melt in the bath.

## 2.2 Nonferrous Smelter Slags

Non-ferrous slags are slags arising from smelting operations that process metals other than iron. The slags originating from reverbaratory furnace are estimated on a  $\text{SiO}_2$ -‘FeO’-CaO ternary system in which all the oxides of iron are reported as ‘FeO’ and,  $\text{MgO}$ ,  $\text{Al}_2\text{O}_3$ ,  $\text{K}_2\text{O}$  and  $\text{Na}_2\text{O}$  are reported as CaO. The system  $\text{FeO}-\text{Fe}_2\text{O}_3-\text{CaO}-\text{SiO}_2$  forms the basis for the composition of the converter slag. The reverbaratory furnace is considered as a melting settling furnace unlike a converter furnace where most oxidation of copper (white metal stage) takes place by oxygen blow. The oxygen potential in the converter is higher than that in the reverbaratory furnace and so most of the iron is present as magnetite in converter slag. The slag from these two furnaces is silica saturated (about 35%  $\text{SiO}_2$ ) typical of copper matte smelting, with a significant amount



of iron oxides. As mentioned earlier, the composition of the matte smelting slag is influenced and determined by the matte grade, the fluxes added and the highly oxidising atmosphere in the converter.

The composition figures in Table 2.2 are typical of the converter slag obtained from copperbelt in Zambia. Iron in slag exists as magnetite and as fayalite in slag matrix.

**Table 2.2** Typical composition of copperbelt converter slag (Floyd and Mackey, 1981)

%Cu	%Co	%SiO <sub>2</sub>	%Fe	%Fe <sub>3</sub> O <sub>4</sub>	%Al <sub>2</sub> O <sub>3</sub>	%CaO	%MgO	%S	%Bi	%Pb
5.75	2.57	21.98	44.95	33.68	2.95	1.02	0.7	2.36	0.009	0.0042

The ionic theory of slags is applicable to copper slags to describe their structure and composition (Mackey, 1982). In most copper smelting slags, cations are generally in dilute range and are dispersed.

### 2.2.1 Thermodynamics of Nonferrous Slags

Slag systems of copper smelting have been classified on the FeO-CaO-SiO<sub>2</sub> system. Matousek (1993) studied copper smelting slags and classified industrial slags as smelting slags and converting slags. According to him the smelting slag comprises those slags with iron to silica ratios of 1 and the converting slag has iron to silica ratio of 2. Thermodynamic properties of these slags have been studied and reported by several other workers. Biswas and Davenport (1980), reported that the phase relationship for reverbaratory slags could be approximated on the CaO-FeO-SiO<sub>2</sub> phase diagram as shown in Figure 2.4. The use of this diagram is facilitated by reporting all the iron as “FeO”, and by combining Al<sub>2</sub>O<sub>3</sub>, CaO and MgO as a total “CaO”. On the other hand the phase relationships for converter slags can be estimated on FeO-Fe<sub>2</sub>O<sub>3</sub>-SiO<sub>2</sub>.

The partial liquidus diagram for FeO-Fe<sub>2</sub>O<sub>3</sub>-SiO<sub>2</sub> system is illustrated in Figure 2.5 showing the composition of various smelting slags. An examination of industrial reverbaratory slags on this basis indicates that they are all situated in the low temperature valley of the CaO-FeO-SiO<sub>2</sub> system. They also tend towards SiO<sub>2</sub> saturation, that is, they contain 35% or more SiO<sub>2</sub>. Matousek (1993) shows that there is a relationship between the industrial slags of primary importance and the system FeO-Fe<sub>2</sub>O<sub>3</sub>-SiO<sub>2</sub> by relating the oxidation states of the two potentials. The presence of minor amounts of CaO, MgO,

$\text{Al}_2\text{O}_3$  and other metal oxides expand the melt field region permitting fully liquid slags to form. Oxygen potential of the silica-saturated slags at  $1250^\circ\text{C}$  was calculated by relating the iron ratios (ferric to ferrous) and iron to silica ratio. The resulting equation, Equation 2.1 showed no dependence of slag oxidation state on temperature for fixed ferric/ferrous ratios and silica content.

$$\log P_{\text{O}_2} = -3.29 + 3.92 \log \left( \frac{\text{Fe}^{3+}}{\text{Fe}^{2+}} \right) - 1.05 \left( \frac{\% \text{Fe}}{\% \text{SiQ}} \right) \quad [2.3]$$

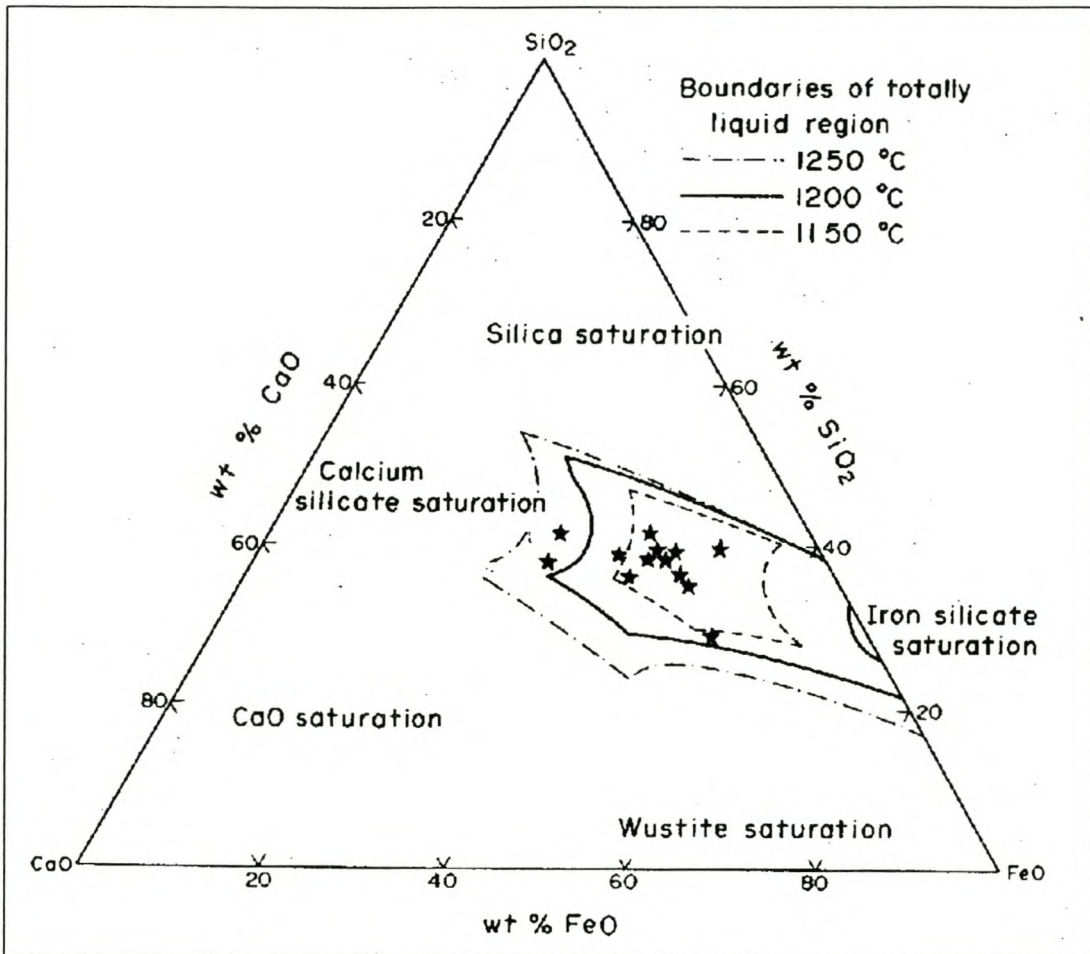


Figure 2.4. CaO-FeO-SiO<sub>2</sub> equilibrium phase diagram (Biswas and Davenport, 1980).



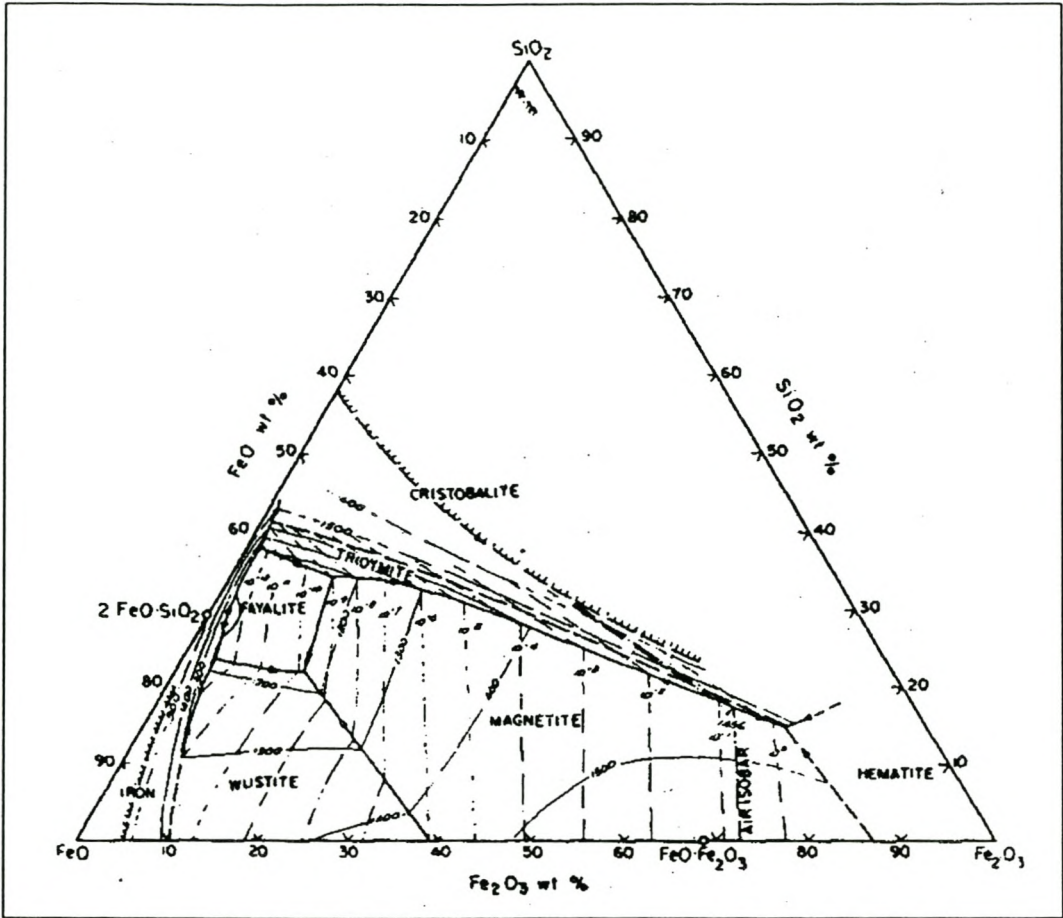


Figure 2.5. The SiO<sub>2</sub>-FeO-Fe<sub>2</sub>O<sub>3</sub> system Partial liquidus diagram (Floyd and Mackey, 1981).

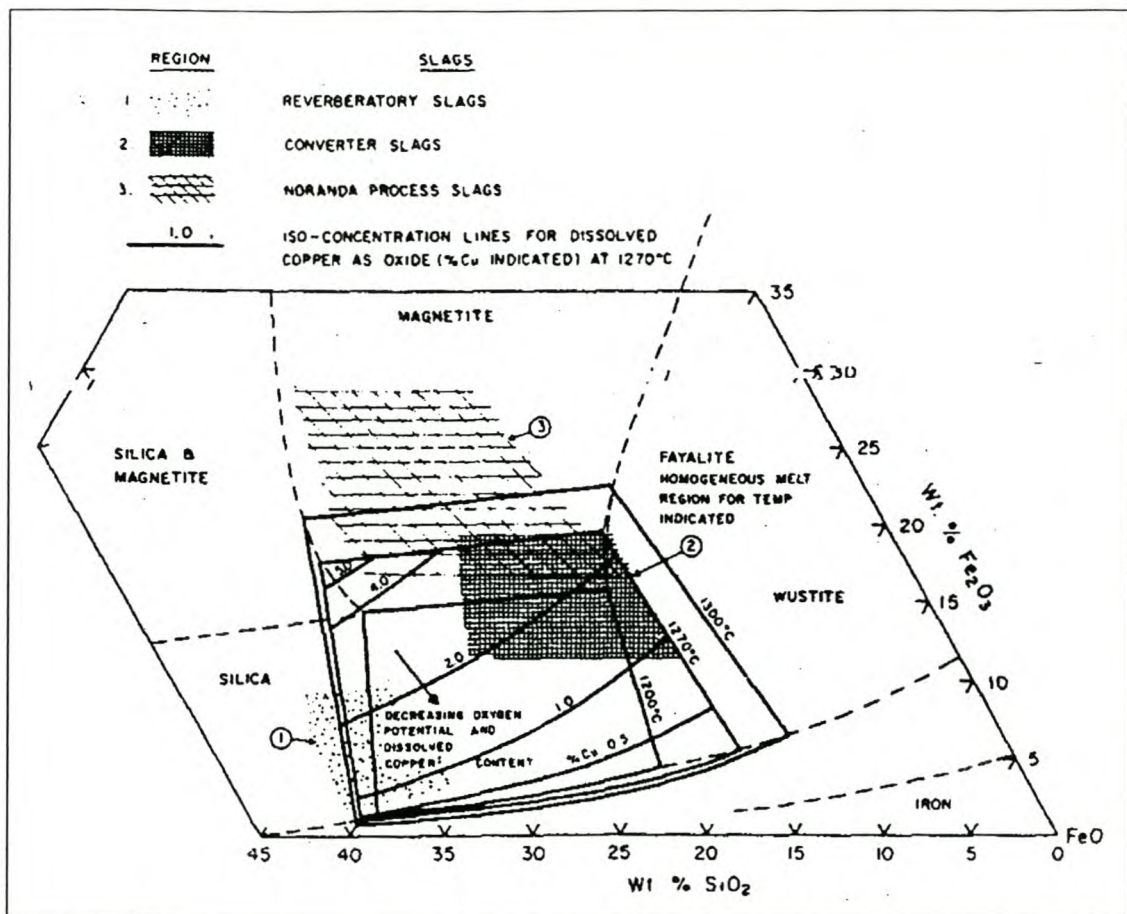


Figure 2.6. Fayalite homogeneous melt region showing composition range of some slags (Floyd and Mackey, 1981).

### 2.2.2 Metals in Slag: Occurrence of Cobalt in slag

The losses of metal values during slag cleaning have been studied for some years now. The literature of particular interest to this study is that concerning the dissolution of cobalt in slag. Mackey (1982), and Floyd and Mackey (1981) showed that the dissolution of copper and other elements like Co, Ni, Zn, Pb, was both oxidic and sulphidic. This is in agreement with findings by Imriš (1982) in the Rokana slags that showed that the dissolution of copper and cobalt in slag occurred as oxidic and sulphidic phases. The way in which metal values are lost to slag has been studied and is said to occur mechanically and physico-chemically. These two mechanisms of metal dissolution are described later in the section in the next section.

The dissolution of cobalt in slag have been studied by Imriš (1982) and Pirard (1991) who investigated two different copper slags from Rokana, Zambia and Küre, Turkey



respectively. Both their findings confirm that most of the cobalt in slag is present in oxidic phases. Imriš showed the existence of cobaltous oxide and sulphide by examining the predominance area diagrams of the Co-S-O and Cu-Fe-S-O-SiO<sub>2</sub> systems at 1200°C Figure 2.7. The conclusion from his work was that about 55% and 74% of cobalt in reverbaratory and converter slags, respectively, is dissolved as cobaltous oxide representing the physicochemical losses in slags. Tests done on the Rokana slags included flotation of finely ground slag, microscopic examination and microanalysis of solid slags from flotation test of quenched reverbaratory and converter slags. The remaining percentages represented an entrained sulphide that is lost mechanically.

On the other hand, the study by Pirard (1991), despite its limitation to Kure slags only, the behaviour of cobalt in slag during slag crystallisation (solidification) can be said to depend on the affinity of Co for the different phases of the slag. A model of cobalt precipitation that represented a molten slag with 0.44% wt% Co content was used to describe the behaviour of cobalt in slag. The distribution of cobalt after crystallisation was found to be highest in hercynites (FeO.Al<sub>2</sub>O<sub>3</sub>) which accumulated 0.86 wt% Co, then 0.54 wt% Co in fayalite (2FeO.SiO<sub>2</sub>) the remaining 0.15 wt% Co (in liquidus) was collected in leucite (KAlSi<sub>2</sub>O<sub>6</sub>), wüstite (FeO), sulphides and metal. Pirard's findings were that 96% of losses of cobalt are caused by chemical fixation in the slag forming minerals.

Other mineralogical studies of the slag reported by Jones *et al.* (1996) are consistent with the findings of Imriš and Pirard. Copper in the slag is mainly attributed to the presence of copper rich sulphides. The cobalt oxide, and to a lesser extent, the copper oxide is associated with the silicate/oxide phases.

Free energy diagrams can be used to predict the formation and stability of oxides and sulphides. Formation of cobalt sulphide is possible but less stable than copper sulphide. It can therefore, be said that cobalt can reduce copper oxide/sulphide and get oxidised itself, meaning that some cobalt will always remain in the slag while copper is present.

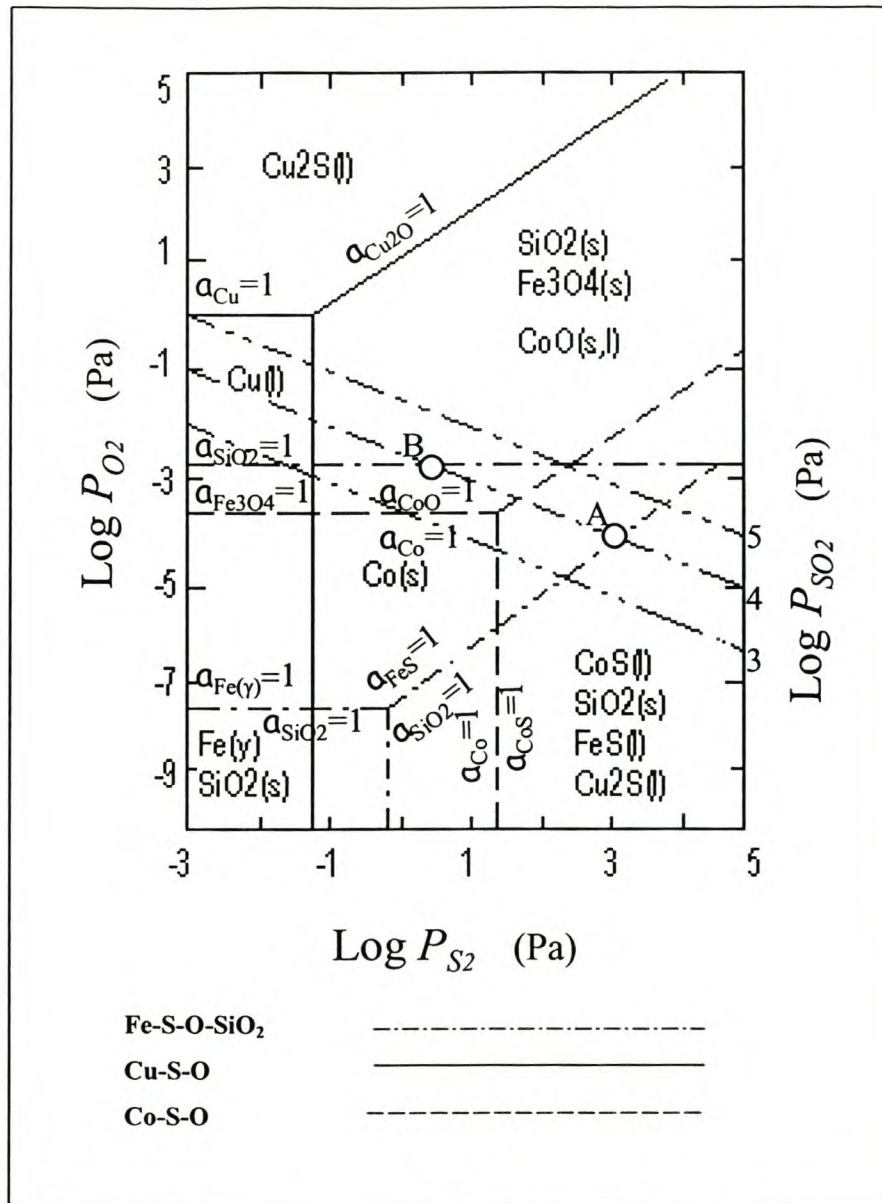


Figure 2.7 Predominance area diagram of system Cu-Co-Fe-S-O-SiO<sub>2</sub> at 1250°C (Imriš, 1982)

### a) Physicochemical Losses

The literature reviewed shows that most of metal losses, cobalt in particular, are lost by physicochemical losses. This form is associated with the chemical dissolution of metal oxide in silicate or ferrite phases in slag. One of the most important parameter that influences the dissolution of metals in slag is oxygen potential of the slag. The slagging of iron is due to the formation of oxides of iron in the slag. Similarly, the loss of cobalt to slag could be said to be due to the formation of oxide of cobalt in slag since its chemical properties are very similar to that of iron. It is for this reason that the cobalt content of



converter slag is higher than that of reverbaratory furnace slag. The association of cobalt oxide with either iron or silica to form ferrites or silicates depends on the affinity of the oxide for iron or silica and the concentration of cobalt oxide in slag. The formation of fayalite seems to dominate, however, due to the higher concentration of iron in the slag compared to cobalt. The temperature could also influence the formation of the silicate compounds. This suggests that cobalt losses to slag may increase with increasing temperature.

### ***b) Mechanical Losses***

Existence of fine droplets or emulsions of metallic phases in slag constitutes mechanical losses of valuable metals in slag during smelting. This form of losses has been reported to contribute to the existence of sulphide phases in the slag of copper iron and cobalt to some extent as described in Chapter 3. These losses are due to the physical state of the slag especially viscosity which, when too high, would inhibit the settling of metal droplets through the slag to the metal bath.

Slag control in pyrometallurgical processes is thus an important part for optimum recovery of metal values from slag.

## **2.5 Recovery of Metals from Slag**

As mentioned earlier, slag cleaning has emerged as a result of recent advancement in technology. But the recovery of metals from slag is an old concept aimed at reducing losses of copper, in most nonferrous smelters, to slag. The other factor encouraging the recovery of such metals is the market price and demand these metals find.

The occurrence of cobalt in slag has been described to be in both oxidic and sulphidic phases according to Floyd and Mackey (1981), Mackey (1982), Imriš (1982), Pirard (1991), and Jones (1997). Its behaviour (cobalt) in slag during smelting of copper minerals is outlined in literature by Reddy and Healy (1981), Grimsey and Toguri (1984, 1988), and most recently by Teague *et al* (2000) who looked at thermodynamics of cobalt iron silicate based slags.



Cobalt recovery from slag is dependant on several factors (temperature, slag chemistry, form and concentration in slag, etc). Recoveries of copper and cobalt are dependant on the initial grades in the converter slags (Whyte *et al.*, about 1975) i.e. the higher the grade the higher the recoveries, which is in agreement with the findings by Harrison and Banks (1975). The metallic iron is the effective reductant for copper and cobalt in the system.

Depending on the levels of concentration of cobalt in slag, and the form in which it is lost, cobalt can be recovered using any of the methods outlined in section 2.5.1.

### 2.5.1 Methods of Metal Recovery from Slags

Different scholars have suggested different methods of recovery either as a part of a process or as a post treatment of discarded slag. The following paragraphs will describe some of the methods that have been suggested by different workers. Some of the methods only apply to high-grade slags though.

**Milling-Flotation:** - This method is suitable for the recovery of copper as pointed out by Ammann (1976) in Imriš' (1975) study. Most of the cobalt is in homogeneous phase with slag matrix, magnetite and fayalite and so the recovery by flotation is not significant as most of it reports to the tailings with the slag.

**Hydrometallurgical:** - This refers mostly to leaching of slag with solution. It requires breaking and grinding of the slag prior to leaching which may be costly in energy requirement to produce a fine grind. The success of this method depends on the leachability of the slag, which could be affected by the amount of sulphur in the slag.

**Pyrometallurgical:** - In this method the slag is brought into contact with carbonaceous reductant. Because slags vary in composition depending on the process conditions, some slag cleaning operations would require other chemical modification of high magnetite before the slags could be processed pyrometallurgically, Ammann *et al.* (1976). Another method is high temperature settling with controlled cooling and washing with sulphides (addition of FeS to molten slag (Ammann, 1976)).



Whyte *et al.* (around 1975) attempted to recover cobalt from converter slag of Rokana smelter (Zambia) using a laboratory muffle furnace at 1500°C and about 12% (by weight of slag) of coal. They recovered about 90% Co and Cu with about 17 to 25% alloy grades. However, further tests on a 50 kg, 50 kVA, single electrode arc furnace was discontinued because of the high conductivity of the slag which did not permit proper generation of heat in the melt. Also the slag had an extra super heat of 300 to 400°C and proved to be highly corrosive to the chrome-magnesite refractory lining.

In turkey, Açma *et al.* (1993) used a 50 kg, 100kVA DC furnace on a pilot scale to recover cobalt and copper from ancient copper slags.

Altudoğan and Tümen (1997) applied a roasting technique on copper converter slags to recover copper (98%), cobalt (38%), nickel (13%) and zinc (59%) The roasting was conducted at 500°C for 120 minutes with ferric sulphate. The slag contained 2.6% Cu, 3600 mg/kg Co, 52% Fe 4.9% S. The calcines obtained were leached with water and sulphuric acid solutions.

### 2.5.2 Process Thermodynamics

In a pyrometallurgical slag cleaning process involving production of a matte or alloy phase, two major operations are carried out either simultaneously or sequentially i.e., reduction of oxidised and dissolved metal by gas-solid-melt contacting, and settling of the entrained metal to form a metal pool beneath the slag. Thermodynamics, in this context, is only concerned with the initial and final state of the slag reduction system. It can be used to predict the chemical composition of the system at equilibrium, provided fundamental data such as free energy and activities are available, but it gives no information on the time to achieve the equilibrium condition. In processes where equilibrium can be established, thermodynamics can play an invaluable role in understanding and optimising chemical metal solubility.



### a) Activity coefficient of CoO in slag

With respect to behaviour of solutions, slag melts are can be referred to as nonideal solutions. A nonideal solution is one in which the activities,  $a$ , of the components are not equal to their mole fractions,  $X$ . To describe the behaviour of compounds with a view of convenience of the concept of activity and Rault's law an addition thermodynamic function is used and referred to as *activity coefficient*, ( $\gamma_i = a_i / X_i$ ). A knowledge of the variation with temperature and composition of the value of  $\gamma_i$  is of vital importance in solution thermodynamics, as the value of  $\gamma_i$  is required for the determination of the value of  $a_i$ , which in turn is required for the determination of the partial molar free energy of solution,  $\Delta \bar{G}_i^M$ , which again in turn is required for the determination of equilibrium state of any chemical reaction involving the component  $i$  in solution. The variation of  $\gamma_i$  with temperature and composition is determined experimentally. Literature is reviewed in this section with regard to the activity coefficient of CoO in slag.

Teague *et al.* (2000) observed that the activity coefficient of CoO was dependent on the silica and lime content in silicate slags. Activity coefficients increased when lime substituted silica in iron silicate slag and decreased with increase in silica addition in lime-free silicate slags. These findings are in agreement with the speculations that the activity coefficient values of FeO and CoO would be concentration dependent.

The activity data for CoO reviewed by Teague *et al.* (2000) shows that there is some inconsistency in the way thermodynamic data has been reported. A typical case is the two values given by Liu and Grimsey (1997) and Grimsey and Toguri (1988) and Katyal and Jeffes (1989). Liu and Grimsey (1997) expressed the activity coefficient of CoO(s) as  $\gamma_{\text{CoO(s)}} = 1.7 - 0.021(\text{SiO}_2 \text{ wt pct})$  at 1573 K and  $p\text{O}_2 = 10^{-10}$ , for silica-unsaturated slag. This expression when extrapolated to silica saturation of approximately 40wt% SiO<sub>2</sub> gave a value of 0.9. On the other hand Grimsey and Toguri, and Katyal and Jeffes gave a value of 2.0. From such differences in values it can be seen that there is still uncertainty on the actual value of activity coefficient of CoO in iron silicate slags.

Grimsey and Toguri (1988) recalculated the activity coefficient of CoO in silica saturated fayalite slags by re-evaluating the solubility of cobalt in silica saturated slags using data



for cobalt activities in Co-Au and Co-Cu alloys. The findings were summarised by a relationship which expressed the activity coefficient of cobalt oxide (relative to solid CoO) as a function of cobalt solubility (wt% Co):  $\gamma_{\text{CoO}} = 1.94 + 0.123 (\text{wt\% Co})$  and, and the solubility of cobalt in slag as a function of activity of cobalt relative to solid to pure solid Co and oxygen pressure in atmospheres:  $\text{wt\% Co} = (0.153(e^{-2.80 \cdot E4/T})pO_2^{1/2} a_{\text{Co}} + 62.2)^{1/2} - 7.89$ . The data re-evaluated was generated from experiments conducted at 1523, 1573 and 1623K and oxygen pressures of  $10^{-10}$ ,  $10^{-9}$ ,  $10^{-8}$ ,  $10^{-7}$  and  $10^{-6}$  in atm. Table 2.3 shows a summary of the original and recalculated values for the activity coefficient of cobalt oxide in slags.

The activity coefficient of CoO,  $\gamma_{\text{CoO}}$ , can be looked at from two points of view. The first is the activity coefficient of cobalt oxide in slag during slagging (matte smelting) and the activity coefficient of cobalt oxide during slag cleaning (reduction smelting). The latter is of fundamental importance to the work studied here. From Table 2.3 it can be seen that the value of the activity coefficient for cobalt oxide in slag varied with temperature and composition of the slag. The above account of activity coefficient calculations is based on matte smelting operations. Some more studies are required to study the behaviour of CoO in highly reductive conditions.

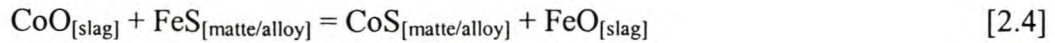
**Table 2.3** The activity of coefficient of CoO in iron silicate slags before and after recalculation. Components in ( ) are part of cobalt alloy (Teague, 2000).

Authors	Temp (K)	Slag(s)	$\gamma_{\text{CoO}}$ original	$\gamma_{\text{CoO(s)}}$ recalculated
Reddy (1985)	1473 1523 1573	Alumina-saturated silicate (Fe/SiO <sub>2</sub> = 1.34)	1.65 1.10 0.61	4.16 (Cu) 2.49 (Cu) 1.25 (Cu)
Grimsey and Toguri (1988)	1523-1623	Silica-saturated iron silicate (up to 43.99wt% SiO <sub>2</sub> , up to 14wt% Co)	1.94 (Au, Cu)	1.9 (Cu) 2.0 (Au)
Katyal and Jeffes (1989)	1523-1623	Silica-unsaturated iron silicate (46-61wt% FeO, 26-35wt% SiO <sub>2</sub> , 7-19wt% Co)	0.93	2.10 (Cu)
Grimsey and Liu (1991)	1573	Silica-saturated iron silicate (50-59wt% FeO, up to 2.9 wt% Fe <sub>2</sub> O <sub>3</sub> , 36-41wt% SiO <sub>2</sub> , up to 8wt% Co)	0.88	0.84 (Au)
Grimsey and Liu (1991)	1573	Alumina-saturated silicate (Fe/SiO <sub>2</sub> = 1.23)	1.20	1.18 (Au)
Grimsey and Liu (1991)	1573	Silica-saturated iron silicate (50-59wt% FeO, up to 2.9 wt% Fe <sub>2</sub> O <sub>3</sub> , 36-41wt% SiO <sub>2</sub> , up to 8wt% Co)	0.91	0.88 (Au)



**b) Distribution of Cobalt in Slag and Metal Alloy**

The distribution of cobalt and iron between slag and matte is determined by the exchange equilibrium of the reactions taking place at the slag-metal (alloy) interface and according to Matusiewicz *et al.* (1998), these could be:



The amount of sulphur in the matte is also a factor in the equilibrium. Soroking *et al.* (1995) presents the distribution of cobalt between matte and slag in terms of mass % as the distribution ratio  $C$  as per

$$C = \{ \% \text{Co}_{[\text{matte}]} \times \% \text{Fe}_{[\text{slag}]} \} / \{ \% \text{Co}_{[\text{slag}]} \times \% \text{Fe}_{[\text{matte}]} \} \quad [2.6]$$

which is linear.

Cobalt behaviour in metallurgical processes is generally analysed using slag/matte distribution coefficients as functions of matte grades or matte iron contents expressed these ratios as (Matousek, 1993),

$$L(s/m) = (\% \text{Co}) / [\% \text{Co}] = f [\% \text{Cu, Ni}] \text{ or } f [\% \text{Fe}] \quad [2.7]$$

or, alternatively,

$$J_s = (\% \text{Co}) / (\% \text{Fe}) \quad [2.8]$$

$$J_m = [\% \text{Co}] / [\% \text{Fe}] \quad [2.9]$$

$$J_s = b + m [J_m] \quad [2.10]$$

Where  $b$  is a constant and  $m$  the slope of the equation of the trend-line representing the plot of the set of data collected from various slag operations. For example, for cobalt and nickel recovery from slags using electric furnace at smelting works in Botswana, the collection of data from this operation was represented as follows for a general trend line.

$$J_s(\%) = 0.111 + 0.035 J_m(\%) \quad [2.11]$$

According to Matousek (1993) cobalt/iron interactions in metallurgical processes can be described as an exchange reaction:



$$K_{2.12} = \{ (\text{Co}^{2+}) [\text{Fe}] \} / \{ [\text{Co}] (\text{Fe}^{2+}) \}, \quad [2.13]$$

where, ( ) represents a slag component and [ ] a matte component;

$K$  = constant of the law of mass action for (Me) and [Me] in concentration units commonly referred to as equilibrium constant and may be rewritten as follows



$$K_{14} = \{(Co)/(Fe)\} / \{[Co]/[Fe]\}, \quad [2.14]$$

thus the symbols “ $J_s$ ” and “ $J_m$ ” are a shorthand presentation of the ratios. Some data from Rokana smelter are summarised below (Matousek, 1993):

- Reverbaratory furnace matte  $J_m(\%) = 5.08$
- Converter slag  $J_s(\%) = 4.94$
- Reverbaratory slag  $J_s(\%) = 2.53$

Mikhail *et al.*, (1992) in a study of the distribution of Cu, Ni, and Co during slag cleaning of nickel smelting slags found that the distribution ratio  $L$  (concentration in matte ÷ concentration in slag), decreased in the order  $L(Cu) > L(Ni) > L(Co)$ . The distribution ratio increased with time of contact between the phases and with temperature but for Ni and Co it decreased with increasing metal/slag ratio.

The distribution coefficient of cobalt in the work by Reddy and Healy (1981) was calculated as a ratio of %Co in slag to %Co in metal for copper silicate slags at 1523 K. This ratio indicates how much cobalt is in slag at equilibrium and can be used to monitor the recovery of cobalt from slags.

### 2.5.3 Process Kinetics

The mass transfer processes occurring between and within phases during the slag cleaning operations have been illustrated by Floyd and Mackey (1981). The illustration in Figure 2.8 shows the processes involving reduction by gases, carbon and sulphides. The method of operation and the type of furnace is important in determining the manner in which slag is contacted by gaseous, liquid and solid reductants and therefore in determining the rate limiting reactions. This, in the context of this study, constitutes what will be referred to as process kinetics.

#### a) Reduction Rates

The reduction of cobalt from the typical levels of the source materials to less than 0.1% requires strongly reducing conditions as indicated by Matuszewicz *et al.* (1998). Under these conditions, cobalt, copper, nickel, and iron are also reduced from the slag. The

major reactions taking place during the reduction stage in an Ausmelt furnace for instance are:

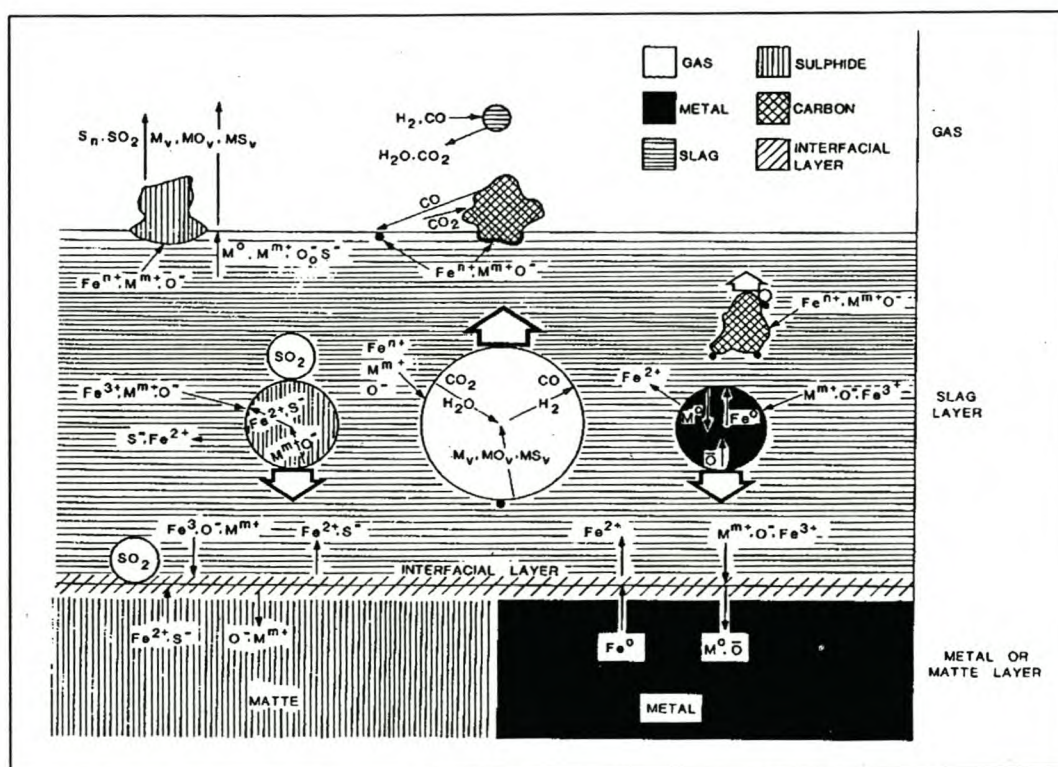
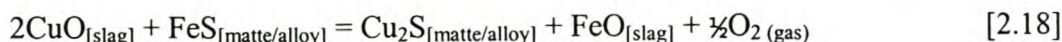
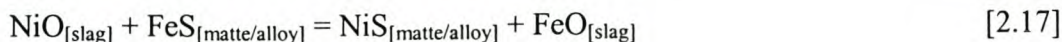
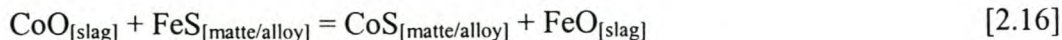


Figure 2.8 A schematic representation of mass transfer processes occurring between and within phases during slag cleaning operations (Floyd and Mackey, 1981).

In cases where the feed materials contain insufficient sulphur to form the relevant sulphides, cobalt metal and iron metal are formed resulting in matte phase and alloy phase as products. Matusiewicz (1998) observed that with a high iron content in the alloy high recoveries of cobalt from the slag were obtainable. Other findings of their work show that the reduction rate of cobalt and other metals from the slag decreases as the metal content in the slag decreases. Typically, a 50-minute reduction period under



strongly reducing conditions (30 kg/h reductant coal) was adequate to leave low levels of metal in the slag during the trials.

In experiments by Jones *et al.* (1996), the addition of carbon the slag was found to reduce various metallic elements in slag to different extents, at a given level of carbon additions as shown in Figure 2.9. This behaviour allows a reasonable degree of separation to take place during smelting of non-ferrous slags to recover valuable metals.

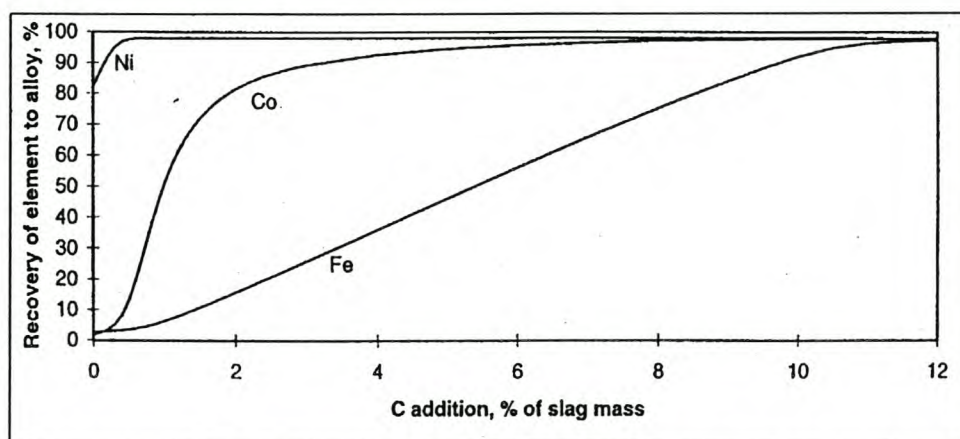


Figure 2.9. Recovery of elements to the alloy as a function of the quantity of carbon added, at 1500°C (Jones *et al.* 1996)

### b) Reaction Mechanisms

Solid carbon in the form of coal or coke is used in many metallurgical processes to control the oxygen potentials of molten slags and to recover metals from solutions. Hayes *et al.* (1995), made observations on the reactions between molten metal oxides and various forms of carbon. The reactions of solid carbon with metal oxides in the slags result in the formation of gaseous carbon monoxide. A number of possible reaction mechanisms have been identified in various reaction systems. The direct reduction mechanism is presented as



where Me is a metal species. However, these reactions require the simultaneous contact of four phases. So it is unlikely that they would proceed in a single reaction step as shown by Equations 2.21 and 2.22. A two-stage gas ferrying mechanism involving carbon dioxide and carbon monoxide may be a possible mechanism (Hayes, 1995).

In the presence of solid carbon, carbon dioxide produced by the reduction reaction forms carbon monoxide through the carbon gasification reaction at the carbon/gas interface,



The carbon monoxide gas produced is then available to react at the slag /gas interface, i.e.



The reaction cycle is completed when the carbon dioxide returns to react once more with solid carbon.

Hayes (1995) concluded that for the reduction of these fayalite slags the reactivity of carbon is an important factor determining reduction rate and the rate limiting reaction in this reduction reaction could be carbon gasification which is in agreement with a review by Warczok and Utigard (1998) who showed that the rate limiting reaction was the Boudouard reaction.

The wetting characteristics of carbon by molten oxides differ depending on the composition of the oxide. When wetting of solid carbon occurs, reduction of the oxides can take place rapidly, even under conditions where the rate of carbon gasification is very low. A good choice of the type of coal to use as reductant is therefore important in process metallurgy. The use of coal has two drawbacks though. It produces a lot of volatile material, which contribute significantly to gas volume, and tar content and it is fairly friable and so affects the burden porosity in the case of furnaces that have a burden (blast furnace). The high ash content also contributes to the slag mass and alloy impurities, particularly sulphur and phosphorus. Aspects that can influence coal reactivity (rate of reaction of a certain mass of coal of a particle size) are:

- i). Particle size.
- ii). Particle porosity.
- iii). Ash levels, ash fusion point and the texture/intergrowth pattern of the original clay minerals.
- iv). Ash composition (influence melting point, viscosity, interfacial tension).
- v). Level of volatiles.
- vi). Level of pyrite (and consequent level of sulphur).



- vii). Moisture levels.
- viii). Coal rank.

An investigation of each of the above would be an important contribution towards the development of a complete understanding of rates and mechanisms of reaction of a system.

## 2.6 The Influence of Fluxing on Slag Properties and Cobalt Recovery

In the study presented here new types of fluxes have been evaluated. Rutile, fluorspar and lime, are tested to investigate the effect on slag chemistry.

Matusiewicz *et al.* (1998), found that the separation of cobalt containing products from slag was improved with the addition of limestone through the improvement of slag fluidity when operating between 1300 and 1400°C. Limestone (like other metal oxides) breaks down the polymeric fayalite melt.

The addition of sulphidising agents such as pyrite in studies by Matusiewicz *et al.* (1998) found

- i. to act as a collector phase to promote removal of the base metals from the slag to the alloy
- ii. to decrease the liquidus temperature of the final cobalt-containing product.
- iii. to allow the collecting phase volume to be increased in cases where the expected metal yields are low. This provides sufficient volume of matte/alloy product to allow separation from the slag.
- iv. to benefit applications where a matte product is desirable for further treatment in existing plant flow sheets.

The typical agent used is pyrite, which may constitute up to 20% of slag material. This amount is large but it has been found that decreasing this amount resulted in more difficult separation of matte from slag and higher operating temps due to the high quantity of alloy with a higher melting temperature.

The effect MgO and Al<sub>2</sub>O<sub>3</sub> on the liquidus of fayalite have been investigated by Zhao, Jak and Hayes (1999). They found that the effect of MgO and combination



(MgO+Al<sub>2</sub>O<sub>3</sub>) were independent of each other. Magnesia expands the fayalite primary phase field toward higher SiO<sub>2</sub> concentration. Addition of the Al<sub>2</sub>O<sub>3</sub> decreases the liquidus temperature of fayalite slags.

The effects of CaO, Al<sub>2</sub>O<sub>3</sub> and MgO addition to silica saturated iron-silicate slags on copper solubility, ferric/ferrous ratio of the slag and the behaviour of minor elements were investigated by Kim and Sohn (1998). The investigations were done under equilibrium conditions at a wide  $pO_2$  range ( $10^{-12}$  to  $10^{-6}$ ) which covers copper smelting, converting and slag cleaning. The solubility of copper in the slag was lowered by the addition of CaO, MgO, and Al<sub>2</sub>O<sub>3</sub> in decreasing order consistent with the basicity of the additives and supporting the acid-base theory of the slags. The Fe<sup>3+</sup>/Fe<sup>2+</sup> ratio in slag was decreased with the additions but was smaller under lower oxygen potential. With regard to this ratio it was observed that SiO<sub>2</sub> in slag increased. SiO<sub>2</sub> in slag is known to affect the Fe<sup>3+</sup>/Fe<sup>2+</sup> ratio in the silica-saturated iron silicate slag and so the effect of additives to reduce the Fe<sup>3+</sup>/Fe<sup>2+</sup> ratio could have been enhanced by the presence of SiO<sub>2</sub> in the slag.

## 2.7 Thermodynamics of Metallic Phase

Cobalt is recovered from the slag in an alloy form consisting of iron, copper, cobalt and sulphur as the major elements. To complete the picture of recovery of cobalt from slag the knowledge of the thermodynamics of Fe-Co-Cu-S is essential. Thermodynamic studies for this system are conducted by equilibrium experiments between slags and alloy systems from which the thermodynamic properties of the specific metals in the system such as activities and activity coefficients could be calculated. Literature on the system Fe-Co-Cu-S which of interest in this study is however, limited but other systems that have been investigated include Co-Fe-Ni-S (Kongoli and Pelton, 1999), Fe-Cu-Ni-Co-Mo (Kor, undated), Fe-Co-S (Soltanieh, Toguri and Sridhar, 1999), and binary systems of Cu, Co, Fe and S. The scope of the study does not cover the thermodynamics of metallic phase but reference is only made to the systems mentioned for discussion purposes only.

Depending on the method used to recover cobalt, the alloy product may contain elements like silicon, carbon, etc. that are soluble in iron. The iron content of the alloy is higher



than the cobalt and copper contents. This is because of amount of iron that is initially contained in the slag. Therefore, it is assumed that the behaviour of cobalt and copper in the alloy follows Henry's law of dilute solutions.

## 2.8 Recovery of Cobalt from Slag by DC Plasma Arc Technology

In this section, the recovery of cobalt from slag by DC arc furnace is described and reviewed. The history and properties of plasmas is reviewed. The problems and operation of the plasma arc furnace are described as well.

### 2.8.1 History of Plasmas

A plasma is an ionised gas consisting of molecules, atoms, ions in their ground or excited states, electrons and photons and is often referred to as a fourth state of matter (Feinman, 1987). Overall, plasma is electrically neutral, a situation known as quasi-neutrality. Reid *et al.* (undated) mentions that plasma is a partially ionised, electrically neutral, high-energy gas with sufficient degree of ionisation to render it electrically conductive.

There are two types of plasmas; the equilibrium or the thermal plasma ("hot" plasma) and the nonequilibrium or nonthermal plasma ("cold" plasma). Thermal plasma has two important features: the electron temperature and heavy particle temperature are equal ( $T_e = T_h$ ) and the existence of chemical equilibrium. In contrast, nonthermal plasmas are characterised by strong deviations from kinetic equilibrium ( $T_e \gg T_h$ ). The plasmas of interest in pyrometallurgical processes are thermal plasmas.

The history of plasma technology is as old as the history of electricity. The transferred arc plasma furnaces have their origin in the early work of Siemens, circa 1878. The application of plasma technology has evolved in several different directions and covers topics such as cutting, welding, surface treatment, spheroidization, etc, as well as the extractive metallurgical applications of melting, smelting and refining. Developments in extractive metallurgy have been influenced by the type of plasma torches available and the particular objective.

### 2.8.2 Principles of Plasma Arcs

Before exploring the heat transfer mode in arc furnaces it is important to first understand what an electric arc is. There is no clear-cut definition of an arc, but there are a number of features, which distinguish an arc from other discharges. The following are some of the features, which characterise steady state arcs (extract from *Plasma Technology in Metallurgical Processing*, *Feinman*, 1987).

- **Relatively high current density** -The current density in an arc column (an arc column represents a true plasma region in which quasi-neutrality prevails) may reach values of  $100 \text{ A/cm}^2$  and higher, whereas the current density in glow discharges is in the order of  $1 \text{ to } 10 \text{ mA/cm}^2$ . The associated heat flux densities are in the range of  $10^6 \text{ to } 10^7 \text{ W/cm}^2$ , which require special precautions to ensure integrity of the electrodes.
- **Low cathode fall** - The potential distribution in an electric arc shows a peculiar behaviour as indicated in Figure 2.10. The potential changes rapidly at the electrodes, forming the so-called cathode and anode falls. The cathode fall assumes values of around  $10 \text{ V}$  in contrast to cathode falls in glow discharges, which usually exceed  $100 \text{ V}$ . Depending on the arc length and the energy balance of the arc column, the overall voltage drop of an arc may be very high.

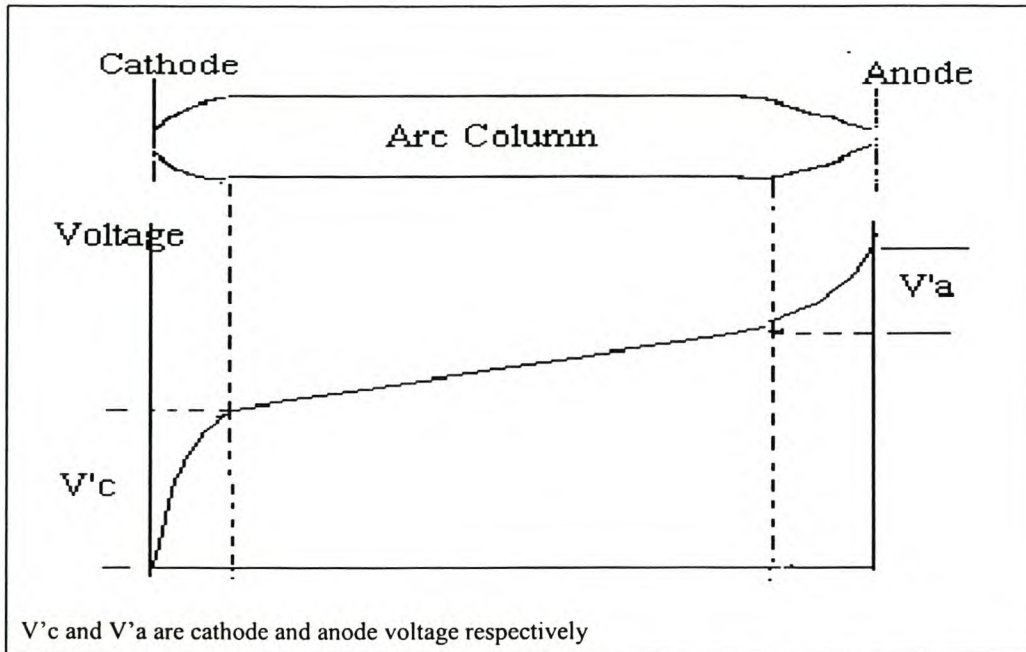
#### a) Heat Transfer Modes

Heat to the molten slag bath is transferred in four modes (Qian *et al.*, 1993):

- i). Convection from the plasma.
- ii). The transport of thermal energy by the electrons.
- iii). Condensation heat flux caused by the electrons crossing the anode fall potential and entering the liquid metal.
- iv). Radiation from the plasma (assumed optically thin, therefore not absorbing any radiation unto itself).



The relative contribution of each of the heat transfer modes to total heat transfer changes with arc length. Detailed description of each of the above modes is discussed in reference Qian *et al.* (1993), concluded that shorter arc length is more efficient for transferring heat to the molten anode. A large amount of energy is needed to maintain the longer arc for the same arc current. This maybe inevitable in a case where the melt is highly conductive.



**Figure 2.10.** Typical Potential distribution along an arc (Jerome Feinman, 1987)

When heating a metal with an arc, the efficiency is almost always higher if the arc is transferred to the metal, rather than heating the gas to get the heat or trying to get the heat from the gas into the metal, thus, most metal melting furnaces use transferred-arc systems. With DC transferred arc, the efficiency of heating in most cases is higher when the metal bath is the anode than when the bath is a cathode. Also the arc orientation in the DC furnace determines the direction of the thrust, flames and splashing, which are important modes of heat transfer.

### ***b) Initiation of the Plasma Arc***

Electric arcs may be initiated in three basically different ways. The choice of the method for striking an arc depends mainly on the arrangement and, and in particular, on the

electrode configuration. The electrode contact method is described here. The other two methods used are:

- i). Pre-ionisation of the discharge gap – this involves making the electrode gap electrically conductive. A high frequency spark within the gap will generate the necessary charge carriers between the electrodes, or stretching a thin wire across the electrodes and applied voltage will lead to wire explosion that supplies the necessary charge carriers for establishing an arc.
- ii). Chemical processes – an arc may be started by holding a burning match below a pair of carbon electrodes.

Now, for the movable electrodes, electrode contact maybe established after an electric potential is applied to the electrodes. The short circuit current flowing over the contact bridge between the electrodes heats the contact point sufficiently for thermionic emission from the cathode. At the same time, electrode material is evaporated and ionised at the contact point, providing the required charge carriers for developing an arc as soon as the electrodes are separated, “drawing of an arc”. There is however a lower current limit for drawing an arc, which is mainly the function of the electrode material. If the discharge circuit allows at least this minimum current to be drawn, the arc will be established in the described way.

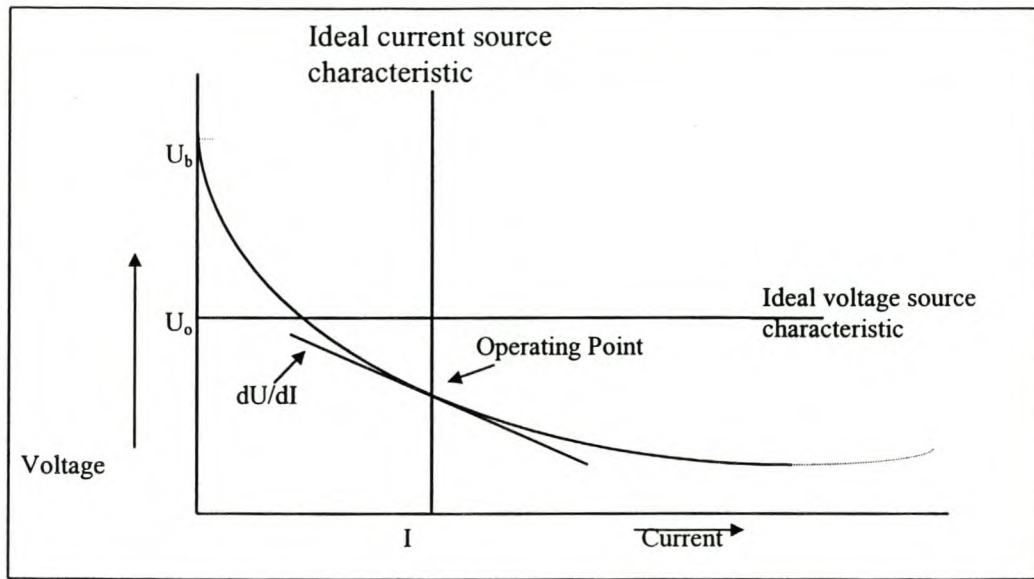
The principles of voltage-current characteristics are shown in Figure 2.11. The actual shape of this arc characteristic depends on the plasma generator geometry, type, gas flow, pressure, etc. After ignition, the arc voltage decreases with increasing current.

The arc resistance,  $R_d = dU/dI$ , is negative. For a plasma generator in the megawatt range,  $R_d$  might be of the order of -0.1 to -1  $\Omega$ . This has an impact on the arc dynamics. It implies using large choke (inductor) in the rectification circuit so that the total circuit still has a positive  $dU/dI$  and therefore have stable operations.

The slope  $dU/dI$  is used to determine the slag resistance (Curr *et al.*, 1983). The slag resistance is a function of the molten bath depth and the slag chemistry. It should be noted that the same current passes through the arc column and the molten bath. Tests carried gave the results in Table 2.4 (Curr *et al.*, 1983) and showed that the recovery of



cobalt and copper varied with change in the bath depth. The bath geometry played a major role in optimising the efficiency of the process. As the bath size increased, it was observed that cobalt extraction improved but iron content was highest. From the results it is speculated that the increased power fluxes could have increased stirring thus resulting in increased recoveries with increasing depth.



**Figure 2.11.** Voltage-current characteristic for an arc and for voltage and current sources, respectively (Jerome Feinman, 1987)

**Table 2.4** Bath resistance as a function of depth (Curr *et al.*, 1983)

Bath Depth, cm	9	18	19	20	29	40
Bath resistance, $\Omega$	0.03	0.04	0.04	0.04	0.05	0.06

### 2.8.3 Application: Specific Technology on Cobalt Extraction

The application of plasma for smelting reactions has not been as successful as in the melting case due mainly to the added requirements of controlling the mass transfer operations associated with the chemical reactions taking place. Smelting cover a wide range of process chemistries, and distribution of energy and the energy transfer modes in a simple transferred arc furnace are not always ideal. The choice of type of a plasma generating device and its integration into the furnace design is important when considering the transfer of energy.

The development under way in the application of plasma arc technology is the recovery of cobalt from copper slag dumps. In South Africa, Mintek (Curr *et al.*, 1983) has carried

out several test work regarding this technology. The following work has been done at Mintek:

- **Copper converter Slag - 100 kVA;** tests have been carried out on converter slag (0.46% Co, 3.25% Cu, 52% Fe, and 0.42% Ni) using a 100 kVA furnace (operating at 20 to 25 kW). In this test a variation of feeding was carried out. In some tests, solid slag and coal were fed together, while in others the slag was first melted and then coal added afterwards. Coal (at 53% fixed carbon) additions were varied between 4, 6, 8, 10, and 12 per cent of the mass of the slag. The mode of addition of the coal, and the reduction periods of the tests were also varied (around 30 minutes). The use of fine coal (less than 1.5 mm) did not seem to have an effect on the degree of reduction. A representative composition of the alloy produced was 6% Co, 32% Cu, 53% Fe, and 6% Ni.
- **Nickel-Copper Converter slag 'A' -100 kVA and 200 kVA;** tests have been conducted on converter slag from a nickel copper plant, on a 100 kVA furnace (operating at 30 kW) and on a 200 kVA furnace (operating at 85 kW), at low additions of reductant (in order to minimise the reduction of iron). The slag composition was 0.45% Co, 3.0% Cu, 47% Fe<sub>total</sub>, 3.5% Ni, and 3.0% S. The objective of this test was to optimise the selective reduction of the slag. The test was conducted using four different methods; smelting of composite pellets of milled slag and coal, adding selected quantities of crushed coal to already molten slag, co-feeding crushed cold slag and coal, and pneumatic injection of pulverised coal into the molten slag. On the 100 kVA furnace the alloy produced had a typical composition of 1.7% Co, 14% Cu, 48% Fe, 16% Ni and 14% S. On the 200 kVA the alloy produced was 2%Co, 15% Cu, 44% Fe, 22% Ni and 10% S in composition. In this test it was found that injection of pulverised coal greatly improved the reduction, and hence the recovery, of cobalt and nickel oxides from the slag. Under good conditions, at 7% carbon addition, on the 100 kVA furnace, calculated recoveries of 81% Co, 78% Cu, and 97% Ni were obtained, while retaining 80% of the iron in the slag.



- **Nickel-copper converter slag 'B' - 200 kVA;** testwork on the slag generated in a plant utilising a conventional six-in-line furnace and Peirce-Smith converter configuration have been carried out. The composition of the bulk slag was 1.25% Co, 1.0% Cu, 49% Fe<sub>total</sub>, 3.6% Ni and 30% SiO<sub>2</sub>. The furnace was operated at power levels of 100 to 170 kW and tapping temperatures of 1400 to 1500°C. The alloys produced comprised 4.5 to 5.5% Co, 5.5 to 8.5% Cu, 35 to 50% Fe, 25 to 35% Ni and 8 to 10% S. Co-feeding of the coal and sequential feeding gave similar recoveries to the alloys of 74 to 80 % respectively. While cobalt recoveries were similar, sequential feeding (the preferred route for industrial plant where molten slag is available) produces a better grade of alloy, with an iron content in the region of 10 to 15 % lower.
- **Nickel-Copper converter slag 'B' - 3.2 MVA;** large scale testwork on converter slag was conducted on the 3.2 MVA DC-arc furnace operating at a power level of 600 kW. The sequential feeding of reductant was used as a preferred mode of feeding. Operating temperatures were in the range 1300 to 1600°C, and neither the temperature of the bath before the reduction period nor the tapping temperature seemed to have a pronounced effect on the cobalt recovery. The alloy produced comprised 7.8% Co, 3.8% Cu, 26.4% Ni, 56.9% Fe, and 2.1% S. the cobalt levels achieved in the discard slag were between 0.15 and 0.33%. A coal addition of 9% was required to achieve cobalt recoveries of at least 80%. Increasing the coal addition did not significantly increase the cobalt recovery of cobalt. Increasing the batch mass of slag from 500 kg to 1000 kg and increasing the reduction period by 75% resulted in an increase in cobalt recovery from 71 to 80%, and from 70 to 82%, for coal additions of 9 and 11%. The main factor affecting cobalt recovery appears to be the time allowed for the reduction to take place. At this scale of operation, duration of two hours was required to achieve cobalt recoveries greater than 80%.
- **Nickel-Copper furnace and converter slag - 200 kVA;** a campaign was conducted on a 200 kVA furnace with the intention of combining the furnace slag with the converter slag previously treated. When treating furnace slag containing 0.22% Co on its own, the maximum cobalt recovery that could be obtained was 66%, with a cobalt value of 0.08% in the discard slag. As in previous testwork, the



cobalt in the discard slag when treating converter slag on its own was still in the region of 0.22%. However, by combining increasing amounts of furnace slag with converter slag, 0.08% Co in the discard slag could still be achieved. This resulted in cobalt recoveries approaching 90% being attained, while the average recoveries were in the region of 85%.

- Copper Reverbaratory Furnace slag - 200 kVA;** a campaign was undertaken on Mintek's 200 kVA furnace to recover cobalt from copper reverbaratory furnace slag (initially containing 0.77% Co and 1.3% Cu). Alloys containing 6-7% Co, 9-11% Cu, 77-78% Fe, and 2-3% S were produced, leaving slags containing 0.08-0.16% Co and 0.18-0.29% Cu. Coal additions of 4% of the mass of the slag fed, and residence times of one to two hours, gave cobalt recoveries ranging from 77 to 91%. Tapping temperature of 1400 to 1560°C was attained. A retention time of 2 hours was required to achieve cobalt recoveries in the region of 90%.

Residence time is seen to have an effect on the Co recovered to the alloy (Curr *et al.*, 1985). Longer residence improves the recovery as shown in Figure 2.12.

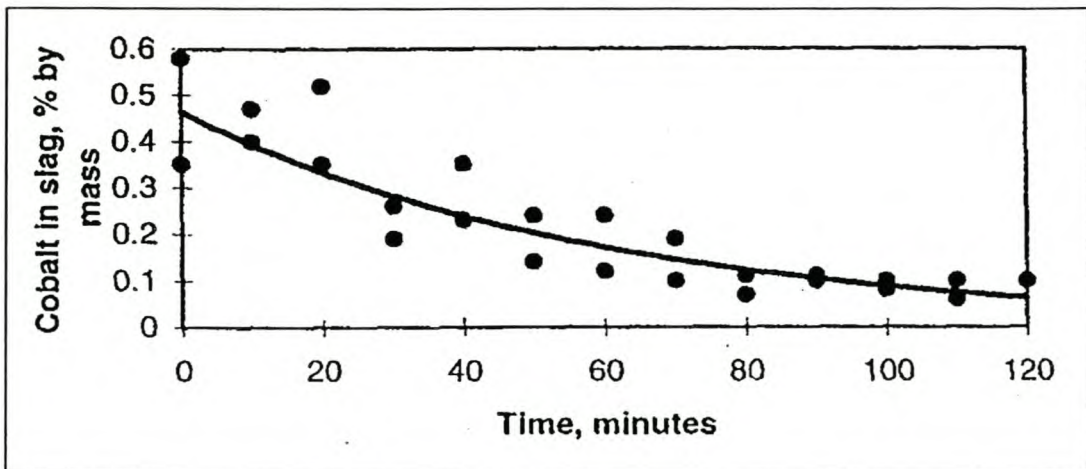


Figure 2.12 Kinetics of slag cleaning (Curr, 1985).

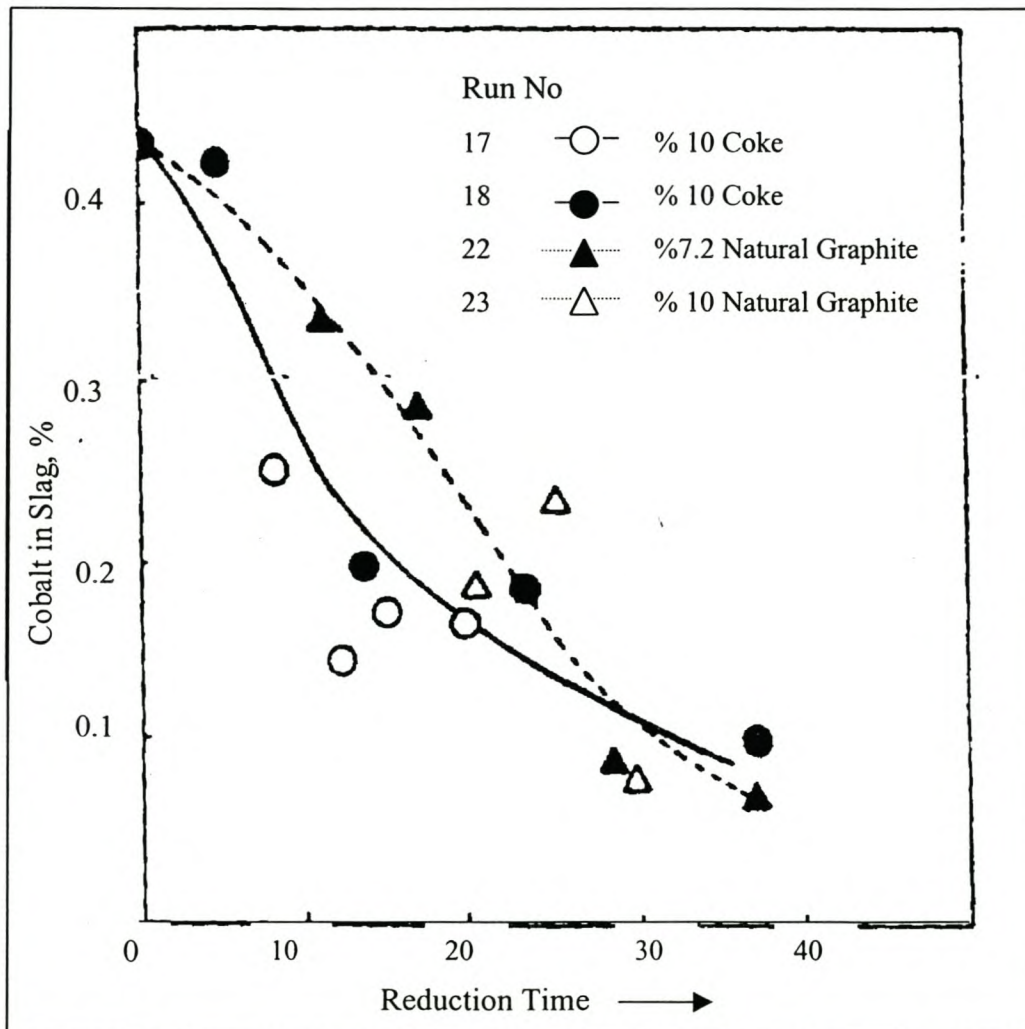
In Turkey, Yucel *et al.* (1992), applied a single phase DC-furnace has recover cobalt from ancient copper slag dumps. The copper slag used was a simple fayalitic slag with little magnetic iron (not shown in the analysis of the slag, Table 2.5.)



**Table 2.5** Analysis of Turkey (Kure) copper slag (Yucel *et al.*, 1992)

Element	Analysis (wt %)	
	Minimum	Maximum
Cu	0.53	1.11
Co	0.35	0.51
Ni	.02	.05
Zn	0.23	0.13
Pb	0.01	0.13
SiO <sub>2</sub>	21.32	26.04
S	1.36	1.72

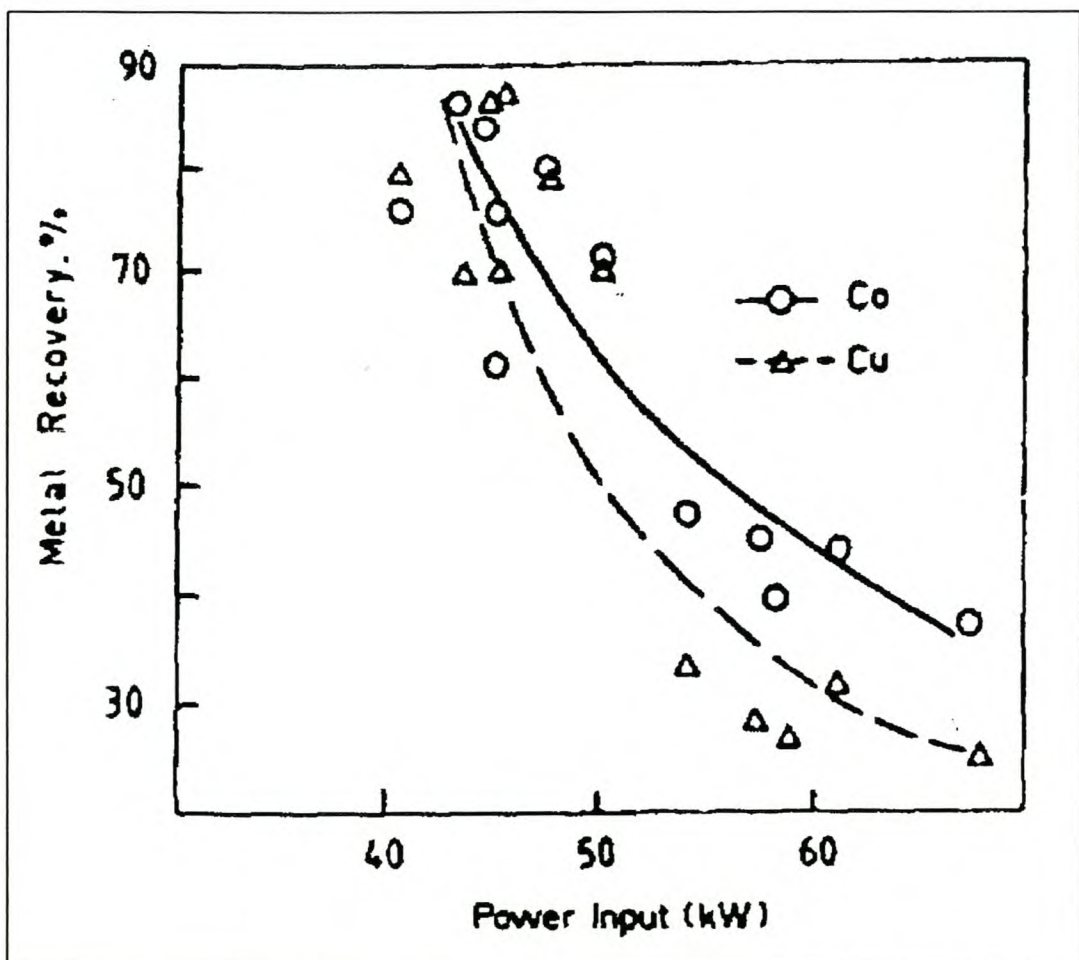
The reductant used in this process was coke and natural graphite. The copper slag was either mixed with carbon/natural graphite and smelted or mixed with carbon/graphite during melting. Results are shown in Figure 2.13.

**Figure 2.13.** Reduction kinetics of the slag by using coke and natural graphite (Yucel *et al.*, 1992)

A pilot scale 100 kVA single phase DC furnace, with a capacity to smelt 50 kg of slag (see Figure 2.15), was used. The cobalt content of the slag decreased down to 0.1% and increased in the alloy to over 3% for a reduction time of half an hour. The extraction efficiencies of Cu and Co decreased rapidly with the increase in power inputs (60 kW), Figure 2.14. However when the power input was in the range of 40 to 43 kW, the cobalt and copper recoveries were over 85 %. At higher temperatures the slag-metal equilibria adversely influences recoveries of Co and Cu into the metallic phase. Açıma *et al.* (1993) indicates that this behaviour could be due to increased entrainment of Co in the slag at high power input. Furnace power features have been provided in Table 2.6.

**Table 2.6** Arc smelting furnace power ratings (Açıma *et al.*, 1993)

Primary			Secondary		
Voltage, V	Current, A	Max. Current, A	kVA	Current, A	Voltage, V
380	154	256	100	300 - 2000	28 – 50



**Figure 2.14** Varying Co and Cu recovery in the metallic matte against various power inputs (Yucel *et al.*, 1992)



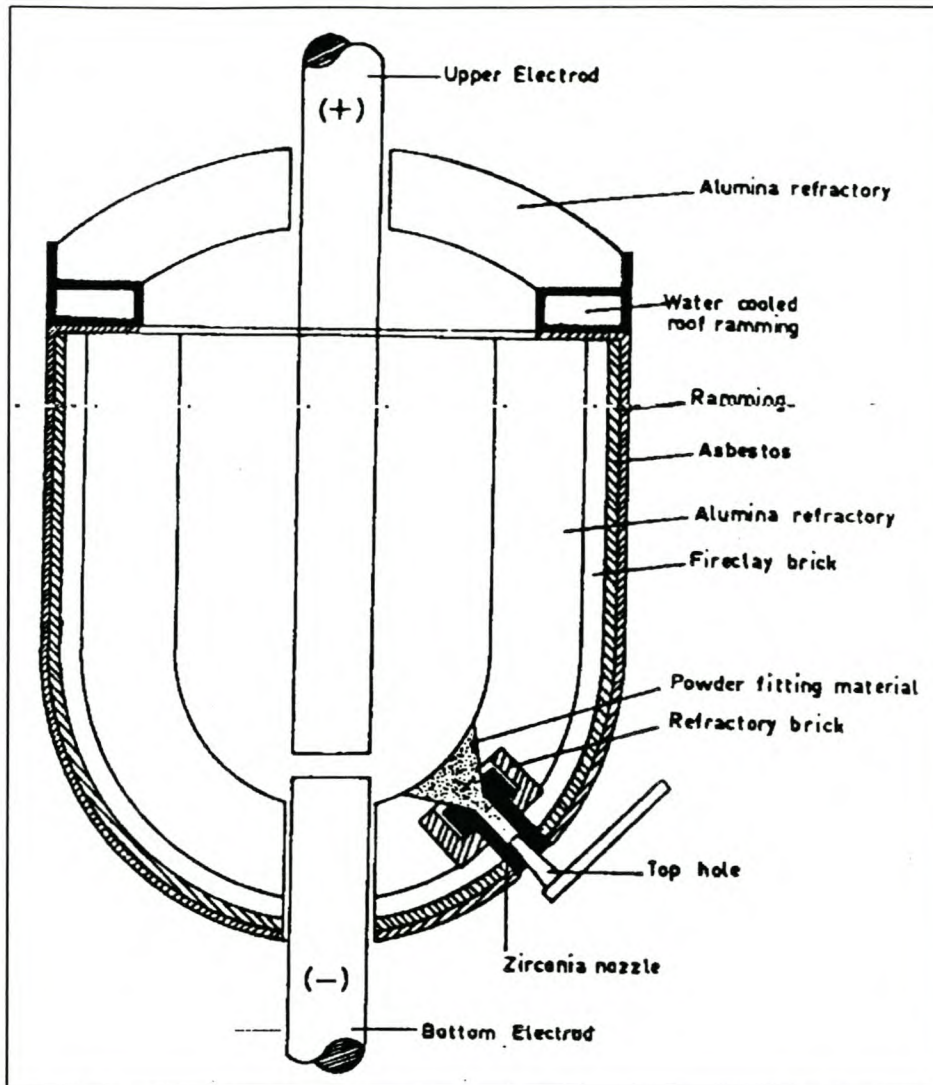


Figure 2.15. Cross section of the furnace with 50 kg slag smelting capacity (Yucel *et al.*, 1992)

#### 2.8.4 Practical Problems Encountered with Plasma arc Furnaces

Curr *et al.* (1983) encountered the problems listed below in their experiments. These problems could be associated with plasma furnace operations in general.

- i). Anode burn-through - it is a rapid event that can occur within 2 minutes leaving the refractory in the anode region almost intact. The correction for this problem could be replacing the central anode electrode with three peripheral anodes and maintaining a 50 to 100 mm metal heel at all times.
- ii). Stray or secondary arching – This is usually manifested by an increase in the arc current without response to upward cathode movement. An extremely irregular event that could occur at any time in the operation but most likely with long (high voltage) arcs, high furnace-roof temperatures, and the absence of feed. The

remedy would be to introduce an additional current path consisting of cathode, carbon roof, steel shell and anodes-earth.

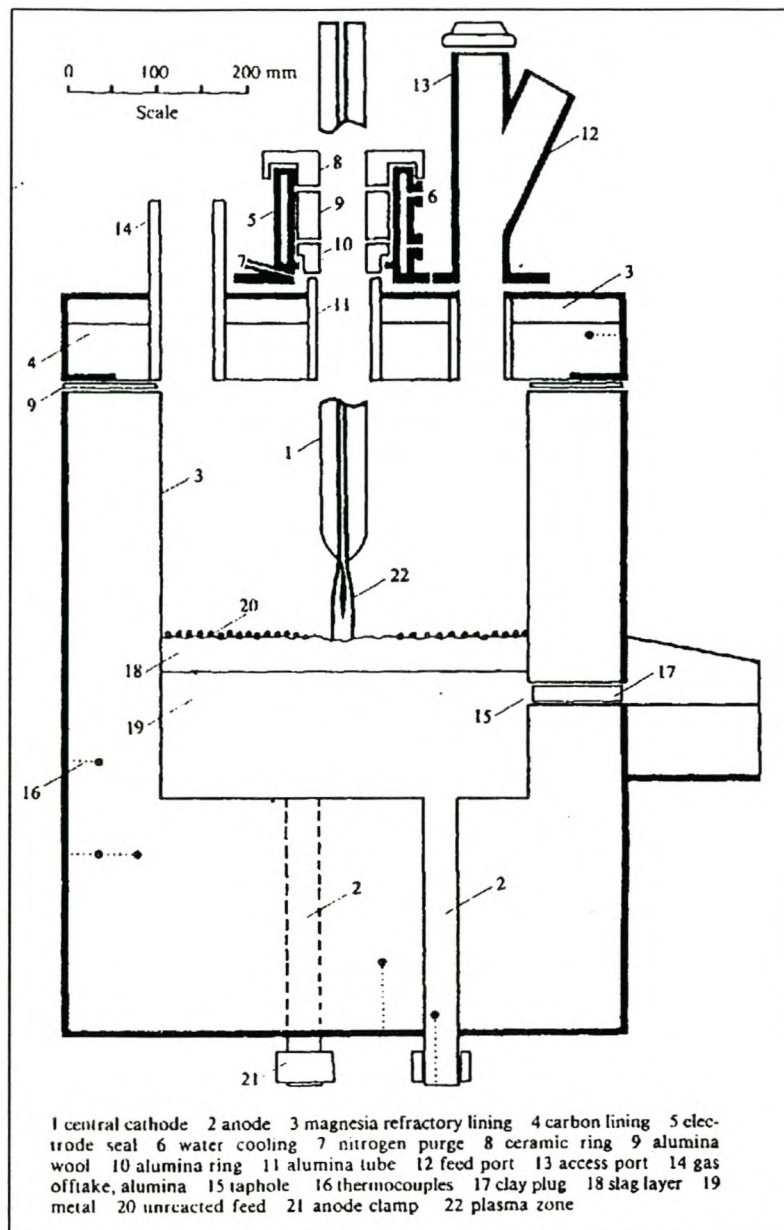


Figure 2.16. A schematic diagram of the DC-arc furnace used at Mintek (Curr *et al.*, 1983).

- iii). Roof damage - overheating and collapse of the roof can occur due to highly reductive conditions maintained in the furnace for the process chemistry. The remedy to this would be to use of carbon (graphite) lining.



- iv). Slag foaming due to carbon monoxide formation - this problem may arise due to high viscosity of the slag/metal mixture in the bath. The foam formed would build up and adversely affect the stability of the furnace reactions.
- v). Heat losses/thermal efficiency - extra heat may be required in furnaces with water-cooling accessories and for heating additives such as fluxes and feed material into the furnace. This in turn will have an effect on the thermal efficiency of the furnace. In DC plasma arc furnace, the biggest problem is that since they have no burden where gas-particle heat exchange should occur, significant amount of heat is lost through radiation to the furnace-roof from the molten slag bath.
- vi). Offgas blockages due to condensation of volatile metals and/or metal oxides such as  $\text{Na}_2\text{O}$ ,  $\text{K}_2\text{O}$ , etc. The offgass port when blocked could lead to increased pressure in the furnace, which could consequently result in structural damage of the furnace.
- vii). Bank formation of feed materials in the furnace and incomplete melting.
- viii). Local loss of freeze-lining leading to slag burn through.
- ix). Blockage of hollow electrodes (in centre fed mechanism) may occur when sticky feed material or in cases where the electrode touches the melt and solidify on cooling.

### **2.8.5 Role of Feed Charge Option: Through Electrode or Through Side Ports**

Feed to the furnace can be either through the electrode or through the side ports. Feeding through the electrodes has the following supposed advantages.

- i). The fines are delivered directly to the hottest areas, the arc plasma it self and the anode spot in the melt. This provides a very close and efficient coupling between the arc power and the process.
- ii). The smelting process is easy to control, with the feed rate being matched with the power input. The charge is consequently reduced as it is being fed, and there is no backlog of unreacted charge material in the furnace.
- iii). The continuous flow of charge material cools and deionises the arc. This leads to an increase in arc resistance, which in turn means that the process can operate with higher arc voltages and lower currents, thereby contributing to lower electrode consumption.

- iv). The arc keeps the slag aside and thus provides an open path for the charge into the bath. Very few fines are lost to the slag in this way.

However, charging material through the electrode reduces the cross section available for the current flow. As at the maximum electrode diameter, one can put more power into the furnace if the electrode is solid and side port feeding is used.

## 2.9 Summary

Below is a summary of the findings from the literature review that are important to the present study.

*Slag composition and structure:* the composition of matte smelting converting slags can be estimated on  $\text{SiO}_2\text{-FeO}_x\text{-CaO-MgO-Al}_2\text{O}_3$ . The present work used a synthetic slag built from the findings in literature.

*Metal losses to slag:* the loss of cobalt to slag is mainly by chemical dissolution and is therefore in the form of cobaltous oxide and associated with iron and silicate compounds. The loss of cobalt to slag can therefore be minimised by fluxing (or modifying) the slag to give it optimum operational window. The present study looks at the influence of  $\text{CaO}$ ,  $\text{CaF}_2$ , and  $\text{TiO}_2$ .

*Recovery of metals from slag:* a carbothermic reduction of cobalt from slag at high temperatures has been shown and chosen as the appropriate method to recover cobalt from the old slag dumps from reverbaratory furnaces.

*Activity coefficient of  $\text{CoO}$  in slag:* even though there seem to be no distinct value for the activity coefficient of cobalt oxide in slag, the recovery of cobalt from slag could be influenced by controlling this value in the slag during a smelting operation. The actual value of activity coefficient of cobalt oxide relevant to the reductive smelting conditions and higher temperatures need to be established for a clearer understanding of cobalt behaviour during slag cleaning.



*Reduction rates and mechanism:* the rate of reduction of iron-silicate slags by solid carbon has been shown to depend on the type, amount and the ability of the slag to wet carbon. The mechanism of reduction is has been found to be a gas ferrying mechanism with iron metal playing the role of an intermediate reducing agent for cobalt oxide and copper oxide.

*Application of plasma furnace to recovery of cobalt:* the DC plasma-arc furnace has been applied successfully at pilot-plant scale to recover cobalt from slags. In the present study the recovery of cobalt from slag was performed on a laboratory scale DC plasma-arc furnace.

DC-arc furnace has been applied at pilot scale to recover cobalt, nickel, and copper from non-ferrous furnace and converter slags at Mintek (Jones et al., 1998) and has demonstrated recoveries of 98% for nickel and over 80% for cobalt, at power levels of up to 600 kW. In Turkey a DC furnace has been used at laboratory scale to extract copper and cobalt from ancient copper smelter slags (Açma et al., 1993). This process is under development and coke and graphite additions have been used to reduce fayalitic slag containing 1%Cu and 0.43%Co. A metallic alloy, consisting of 3.8%Cu, 3.3%Co, 2.1%S, and the rest being Fe, was produced.

## CHAPTER THREE

### *Experimental*

This chapter describes the experimental techniques and procedures used to study the recovery of cobalt from old reverbaratory furnace slag to a Co-Cu-Fe-S alloy. The experiments were conducted in duplicate and are categorized as synthetic slag experiments and actual slag experiments. On the actual slag further experiments were conducted using a laboratory scale DC plasma-arc furnace. The first section of this chapter describes the materials, equipment and methods used to prepare the synthetic slag and to characterize the actual slag. The procedures followed to conduct the experiments are also described in this section. The next section describes the analytical methods used to analyse the materials prepared and the samples arising from the experiments. Finally, a description of the preliminary experiments conducted prior to final experiments is given in the last section.

### 3.1 Materials and Equipment

#### 3.1.1 Materials

All the reagents used in the experiments were of chemically pure (CP) grade and analytical reagent grade as shown in Table 3.1. A muffle furnace was used to prepare magnesium oxide (MgO) from magnesium hydroxide carbonate (pure MgO could not be sourced). The powder was weighed to about 500g and placed in the muffle furnace at 600°C for 5 hours after which the sample was removed and stored in a desiccator for use when making the master slag. Magnesium oxide tends to revert to a more stable hydroxide when exposed to the atmosphere.

#### *a) Preparation of Slags: Synthetic Slag*

The base slag used in the synthetic-slag experiments was synthesized in an induction furnace, described in 3.1.2, using a graphite crucible. This base slag was a quaternary system of  $\text{SiO}_2\text{-CaO-Al}_2\text{O}_3\text{-MgO}$  (Appendix A) with a composition for a liquidus



temperature range of 1300 to 1400°C (Verein Deutscher Eistenthüttenleute, 1995). The amount of  $\text{Al}_2\text{O}_3$  in the ternary system adopted was 20% although the slag intended needed to have only 10 to 15%  $\text{Al}_2\text{O}_3$ . This system was selected because of the certainty of the presence of only one phase (anorthite) and thus ensuring homogeneity in the final product. Another reason was to reduce anticipated corrosion of the crucibles used in the experiments, which were of re-crystallized alumina material. The composition shown in Table 3.2 was corrected to suit the final slag composition used in the experiments (refer to section 3.2.1) so as to simulate the actual slag composition and physical properties (e.g. viscosity). The method of preparation of the slag was adopted from the work by Wright *et al.*, (2000) and is described below.

Table 3.1 Reagents used and their purity

Reagent	Purity (grade)	Form
$\text{SiO}_2$	CP	Powder
$\text{CaO}$	CP (95%)	Powder
$\text{Al}_2\text{O}_3$	CP (98%)	Powder
Magnesium Hydroxide Carbonate	CP	Powder
Iron metal	99%	Powder
Ferric Oxide (chiefly $\text{Fe}_2\text{O}_3$ )	99%	Powder
$\text{CoO}$	99.5%	Powder
Copper Oxide ( $\text{CuO}$ - $\text{Cu}_2\text{O}$ mixture)	CP%	Wire
Cupric Sulphide (chiefly $\text{CuS}$ )	TG%	Granules
Rutile ( $\text{TiO}_2$ )	99%	Powder
Fluorspar ( $\text{CaF}_2$ )	99%	Powder
Graphite	99%	Powder
Ultra High Purity Argon	99.999%	Gas

A graphite crucible containing about 100g of powder mixture ( $\text{SiO}_2$ ,  $\text{CaO}$ ,  $\text{Al}_2\text{O}_3$ , and  $\text{MgO}$ ) was placed in the induction furnace and the furnace switched on. When the mixture was molten, about 50g was added until 800g of powder was added and melted. The molten slag was quenched in water and the crystalline granules that formed were dried in a muffle furnace set at 100°C and then milled in a ring mill to  $-75\mu\text{m}$  powder. The powder was placed in the muffle furnace for 8 hours at 700°C to remove the carbon contamination that came from the graphite crucible. The procedure was repeated to ensure homogeneity of the powder. The slag powder was stored for use in the experiments.



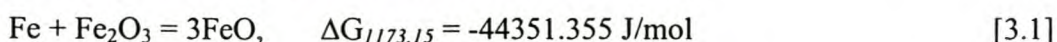
The composition of the slag prepared was analysed by X-ray fluorescent spectrometry (XRFS) technique. Table 3.2 shows the initial and final chemical composition of the master slag. The minimal discrepancies in the compositions between the initial and final compositions could be attributed to the accuracy of the analytical method, which had a detection limit of 0.01% as well as to the loss of bonded compounds (impurities), which could have evaporated during melting.

**Table 3.2** Composition of base slag

Slag Component	Composition (wt%)		
	Initial	Final	Normalized
SiO <sub>2</sub>	56.1	55.6	56.39
CaO	20.4	19.4	19.67
Al <sub>2</sub> O <sub>3</sub>	18.4	19.0	19.27
MgO	5.1	4.6	4.67

### ***b) Preparation of Wüstite***

The intended slag for the experiments was silica saturated iron-silicate slag and to achieve this, wüstite (“FeO”) was added to the pre-melted base slag described previously. The iron oxide preparation method was adopted from Nzotta *et al.* (1999) who mixed stoichiometric amounts of ferric iron (Fe<sub>2</sub>O<sub>3</sub>) and reduced iron powder (pure Fe) as expressed in Equation 3.1. The mixture was pressed with a 5 metric ton load using a hydraulic press to produce a pellet that was then sintered in a tube furnace at 900°C for 12 hours in an argon atmosphere in the tube furnace.



The final product was a dark metallic gray pellet. In order to avoid re-oxidation of the ferrous oxide to ferric oxide (a reddish colour), the sintered pellet was ground into a powder in a ring mill and stored under absolute alcohol in a desiccator (Hayes, personal communication, 2000). The moisture content of the wüstite was less than 2% by dry mass. A sample from the powder was analysed by X-ray diffraction (XRD) technique using a Philips PW 1130/00 apparatus with a detection limit of 5%. The composition of the product was a mixture of wüstite and magnetite (FeO· Fe<sub>2</sub>O<sub>3</sub>) as shown in Figure 3.1 and not as suggested by the stoichiometric reaction in Equation 3.1. Some re-oxidation of “FeO” was inevitable due to the labile nature of “FeO” at room temperature. The ferric/ferrous ratio of the compound was 0.314.



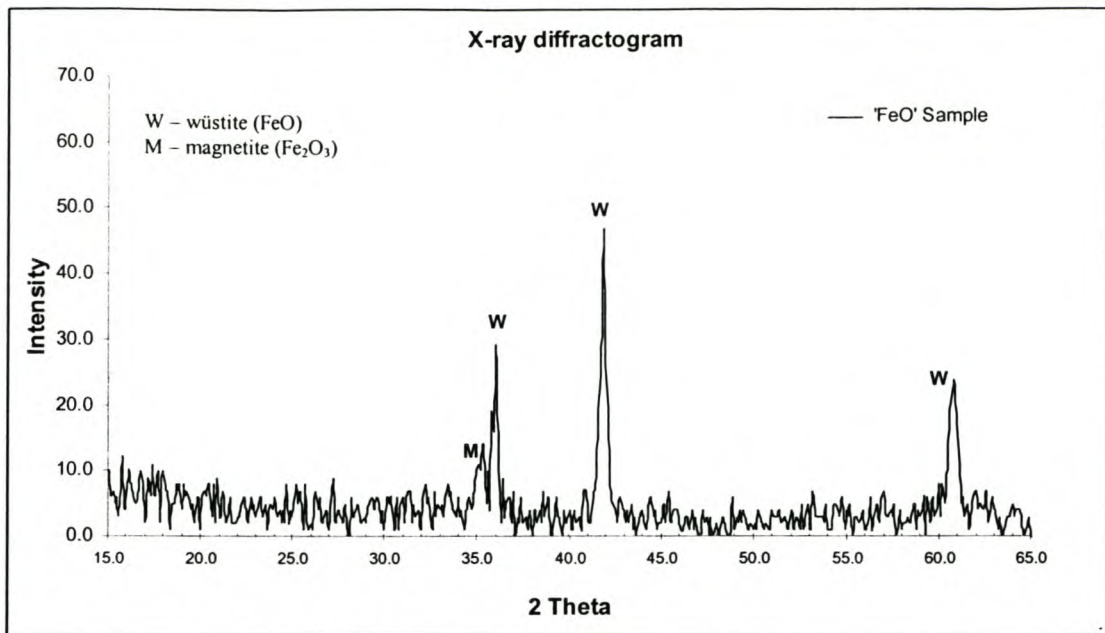


Figure 3.1 X-ray diffractogram of the "FeO" compound

### ***b) Preparation of slags: Actual Slag***

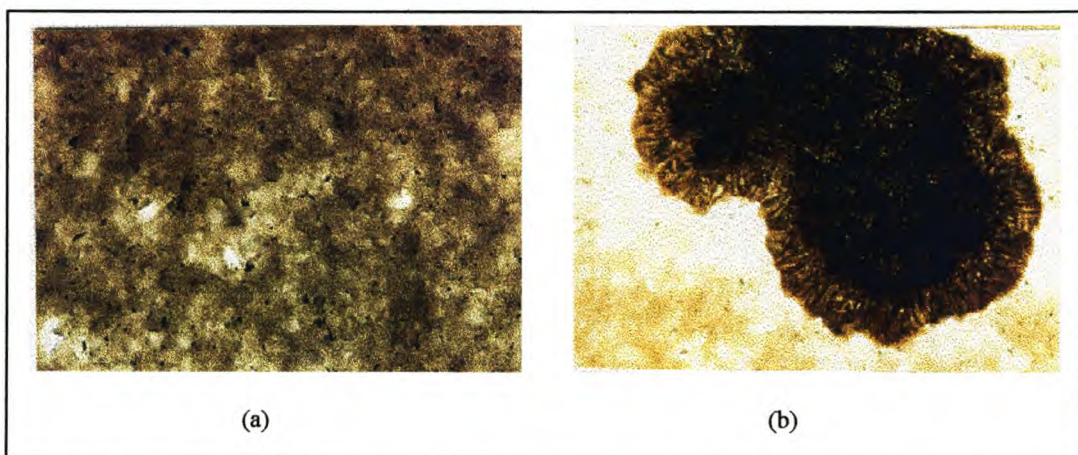
The actual slag was obtained from an old slag dump of a Zambian copper mine of formerly Zambia Consolidated Copper Mines (ZCCM) limited. This slag was discarded from a reverbaratory furnace in the early years (since 1952) of operation and then from the converter furnace during the later years. The dump therefore represents a mixture of reverbaratory and converter furnace slags. From the samples supplied (of twenty-one samples) three random bags were picked and blended and prepared for the experiments. The blended slag was divided into three portions for the following purposes:

*i) Tube furnace experiments Slag:* Slag for tube furnace experiments was pulverized in a ring mill to  $-100\mu\text{m}$  and stored. The analysis of the slag is given section 3.2.1.

*ii) DC arc furnace experiments Slag:* The slag for the plasma furnace experiments was crushed in a cone crusher and screened to particle size range of between 2 and 4mm. A coarser feed was necessary for this part of experiments because of the nature of the plasma reactor, which tend to blow out fine particles due to pressure build up within the furnace.

iii) *Characterization and analysis of actual Slag*: Characterization of the slag was conducted by means of microscopic techniques, namely transmitted and reflected light microscopes and scanning electron microscope. About 12g of slag (particle size of 2mm) was placed in the 20ml alumina crucible and placed in a tube furnace for an hour. The furnace was heated from 1000°C to 1300°C with UHP argon gas flowing at 40cc/s through the reaction zone. This setup temperature and inert atmosphere was intended to melt the slag without initiating any reactions within the slag. After one hour, the crucible was lowered to the bottom of the tube where it was cooled slowly in argon gas atmosphere. The cooled crucible with the slag was cut in a disk measuring 5mm thick and 20mm in diameter. This represented most of the slag and was assumed to be of homogeneous mixture.

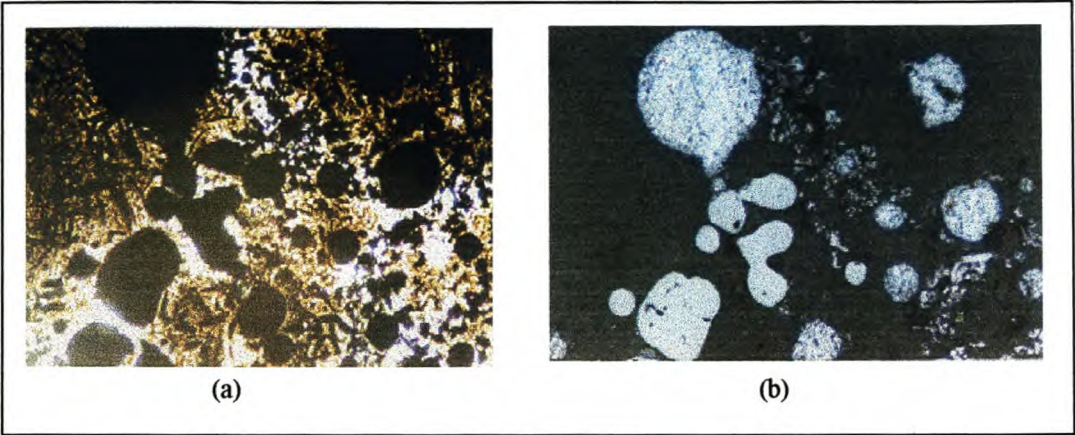
A thin section from the disk was mounted on a glass slide for microscopy analysis. The piece was examined for slag composition and metallic composition. The slag matrix in Figure 3.2a shows the presence of material entrained in the slag which, at higher magnifications were observed to be cumulates (the composition of these cumulates was not determined) as shown in Figure 3.2b and metallic particles as shown in Figure 3.3.



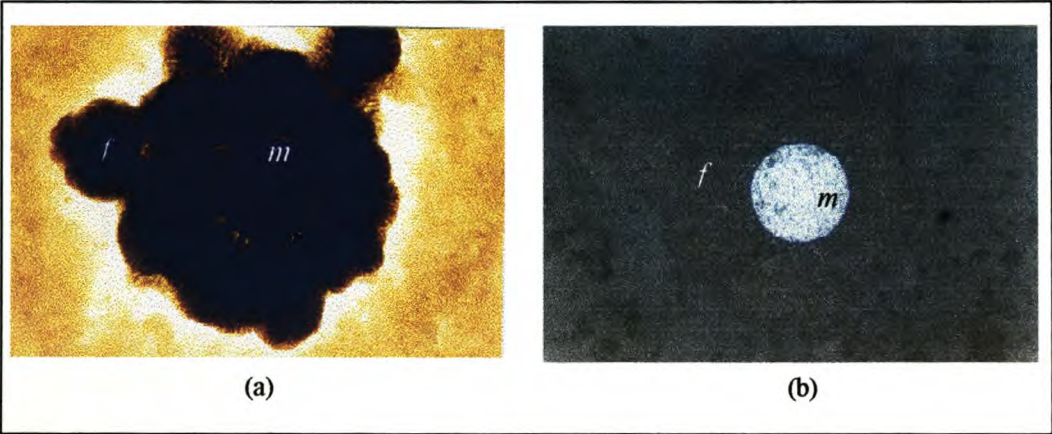
**Figure 3.2** Slag matrix with entrained phases (a) and (b) cumulates at x200 magnification

The metallic phase in the slag matrix shown in Figure 3.4 is surrounded by a phase rich in iron that was assumed to be a ferrite phase. Examination of the metallic phase revealed the presence of subphases appearing as light and gray spots as shown in Figure 3.5.

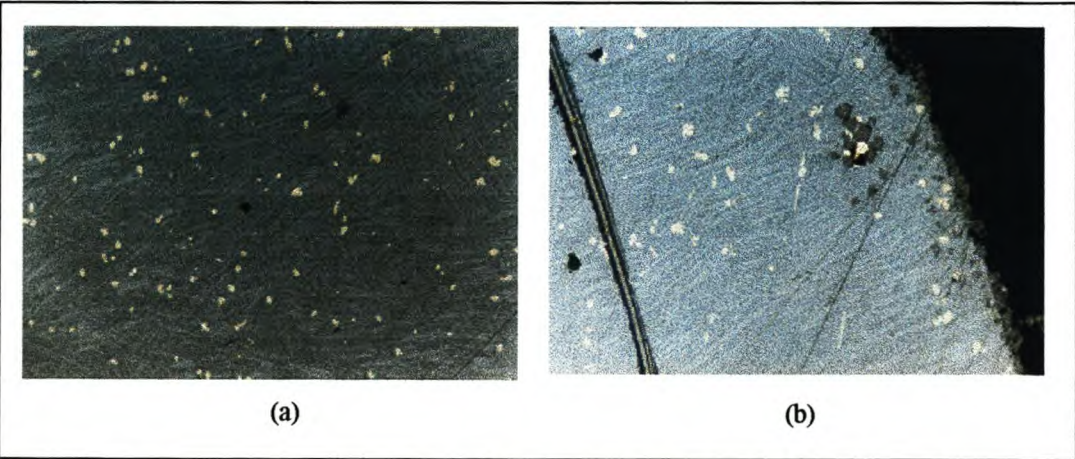




**Figure 3.3** Metallic phase within the slag matrix, (a) transmitted light microscope image, (b) reflected light microscope image.



**Figure 3.4** A ferrite subphase, *f*, around metallic phase, *m*. (a) transmitted light microscope image, (b) reflected light microscope image.



**Figure 3.5** Metallic phase within the metal phase appearing as light spots in (a) and some gray spots in (b).

The composition of the slag matrix and the metallic phase were determined by electron microprobe analysis. The electron microscope image for the slag matrix is shown in Figure 3.6. It was not possible to identify some phases such as silicates with the method used in the present study.

The electron microprobe analyser revealed that the metallic phases entrained in the slag are a combination of Cu-Fe-S, Cu-S, and Co-Cu-Fe-S phase systems as shown in Figures 3.6 to 3.9. This is in agreement with the findings by Imriš (1982).



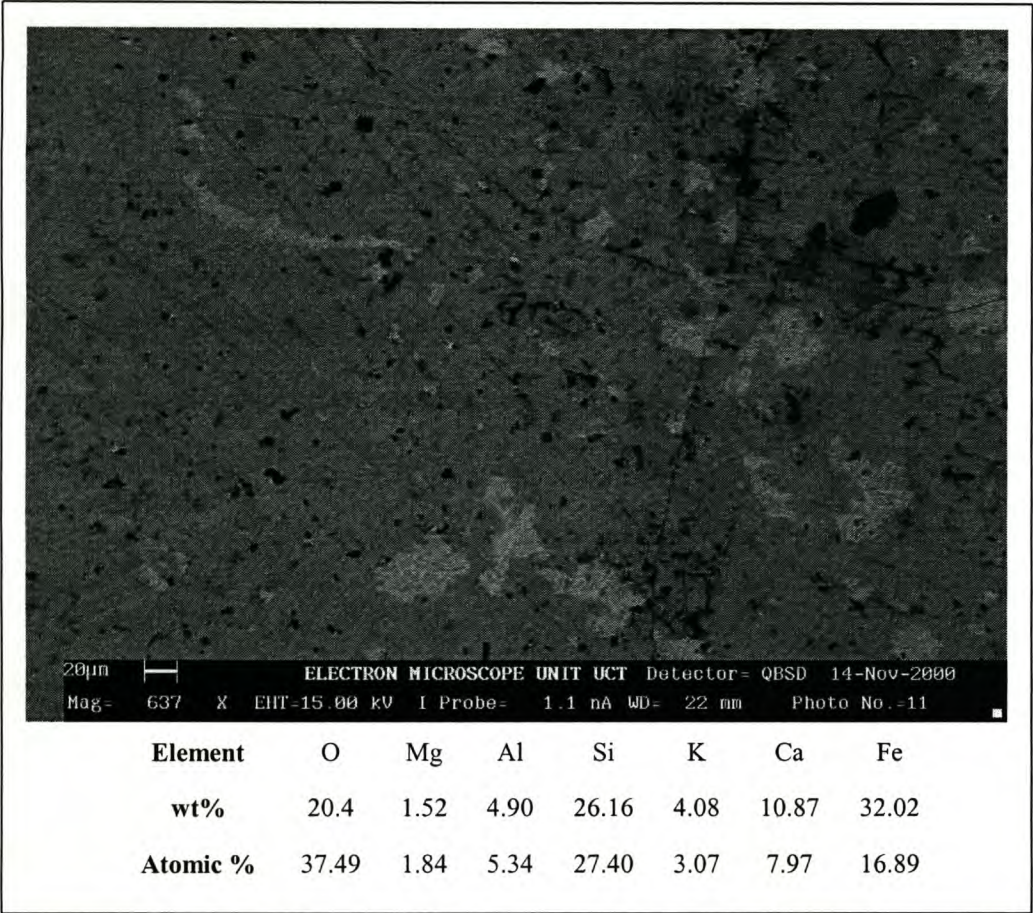


Figure 3.6 Composition and microscopic image of the slag matrix

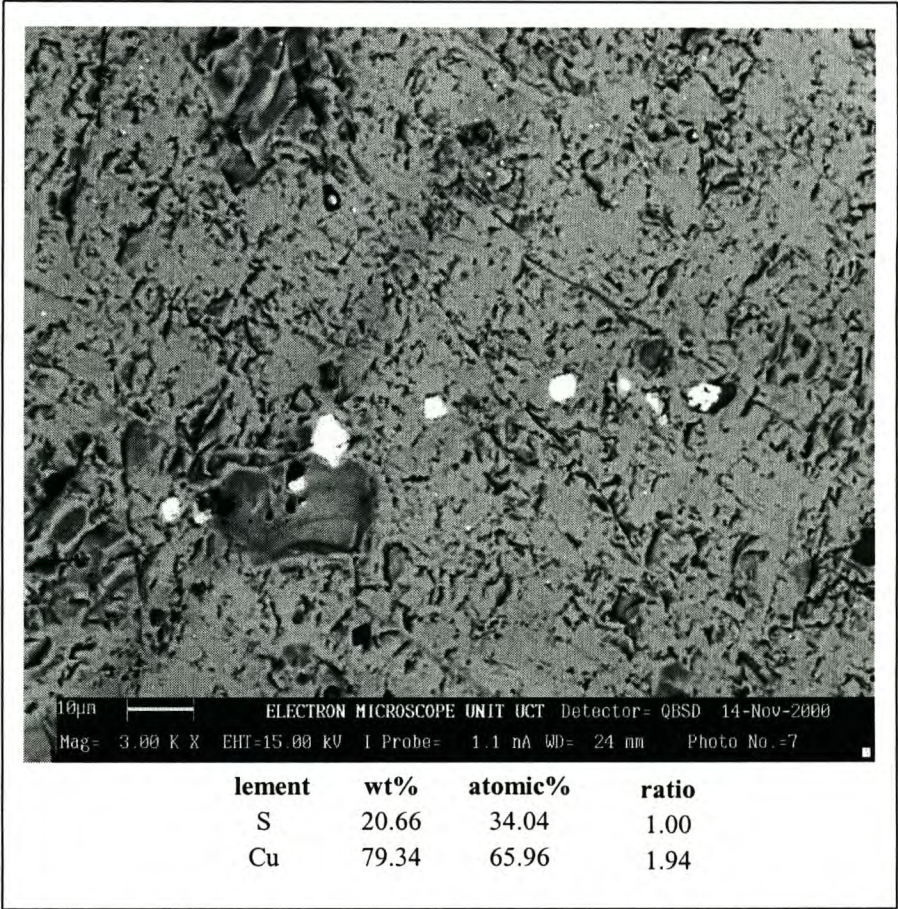


Figure 3.7 Image of the copper sulphide phase (white dots) within metallic phase



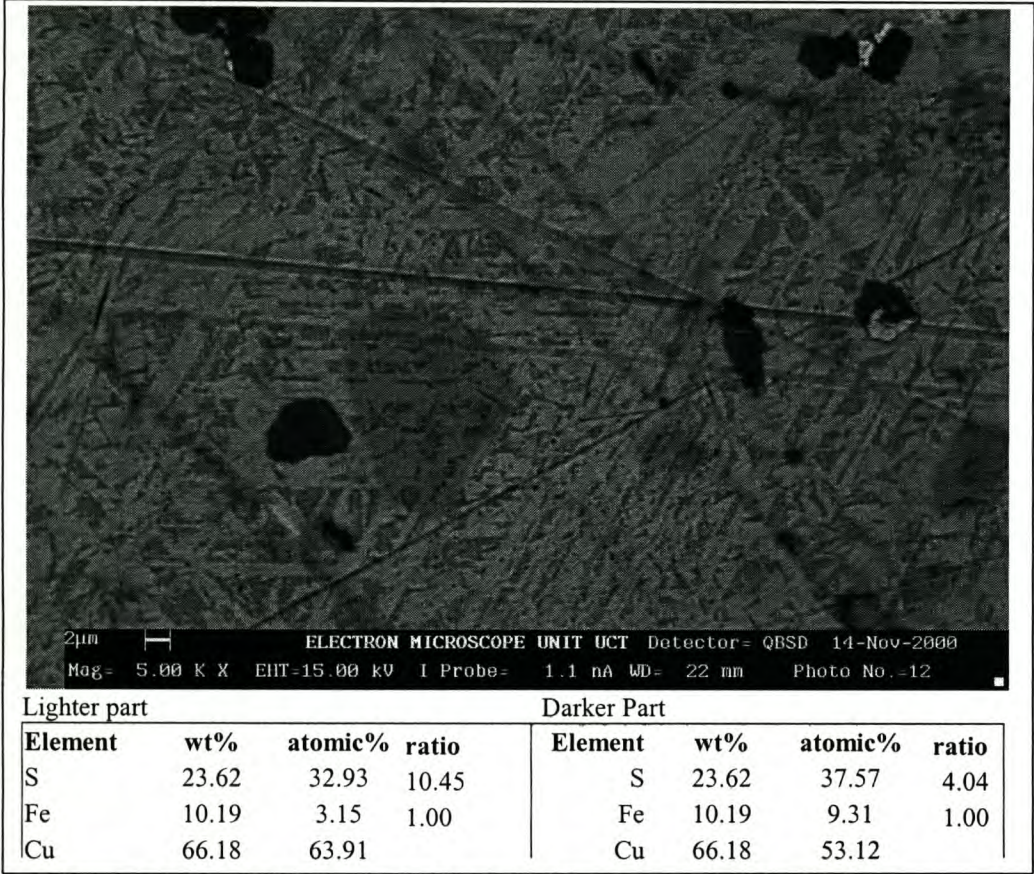


Figure 3.8 Image and composition of Cu-Fe-S system within the metallic phase

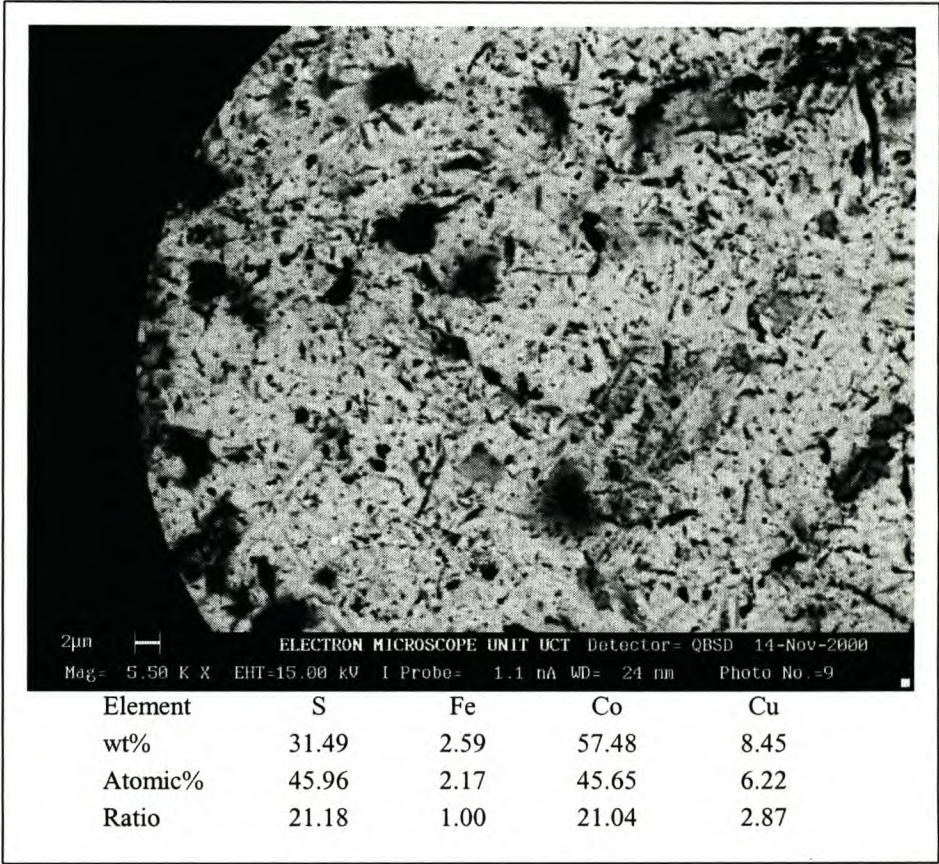


Figure 3.9 Image and composition of the phase containing cobalt, Co-S-Cu-Fe phase within the metallic phase.

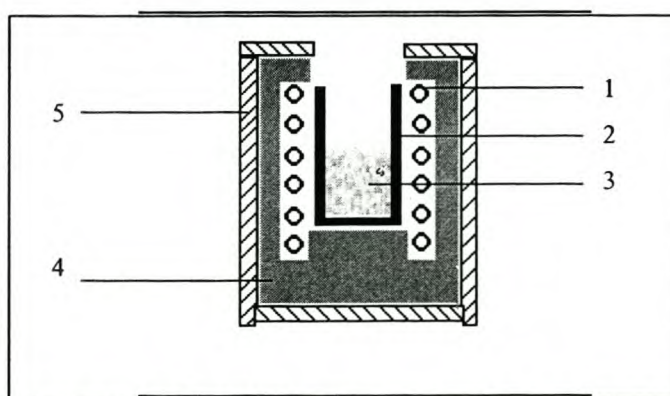


### 3.1.2 Equipment

This section describes the apparatus used in the study to carry out experiments and the preparation of the material (base slag and wüstite). Photographs of the apparatus are shown in Appendix B.

#### *a) Induction furnace*

The Pillar Hand induction furnace (440V, 15kW, and 10kHz) with a capacity to handle 3lb of molten steel was used to prepare the base slag for the experiment (refer to section 3.1.1a). The copper induction coil was water-cooled and the space between the furnace wall and the coil was filled with ceramic fibre material. The setup for the equipment is illustrated in Figure 3.10.



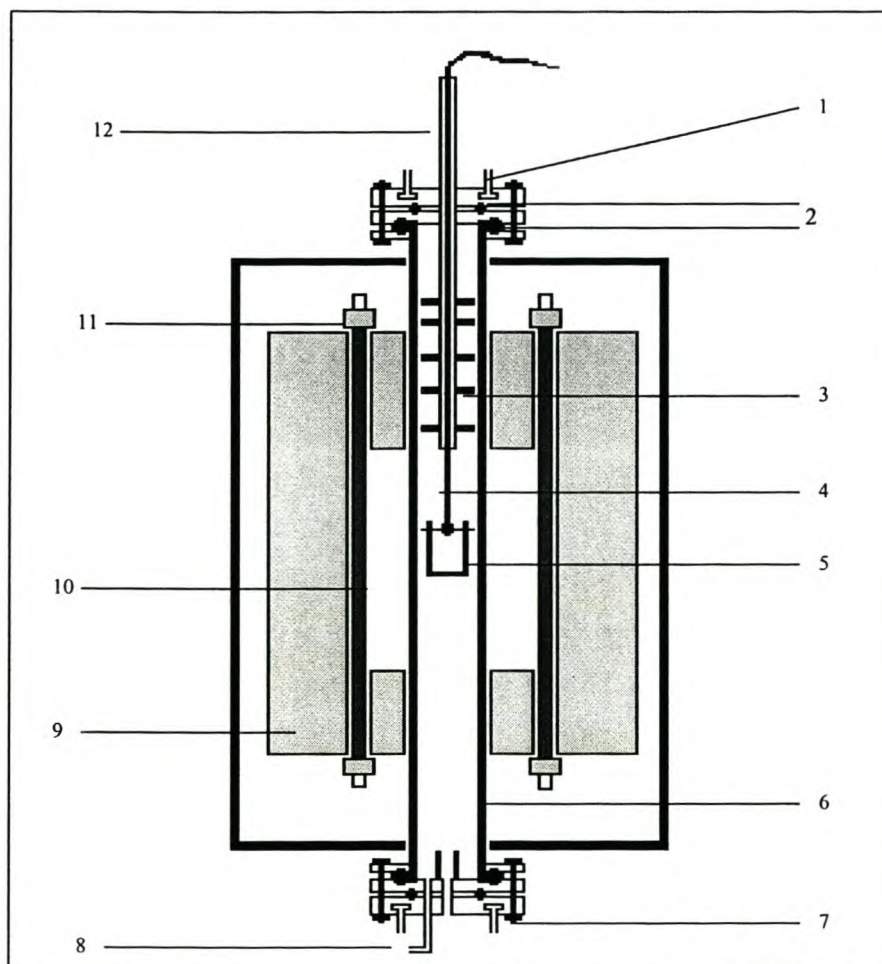
**Figure 3.10** A schematic diagram of the Induction furnace setup for the preparation of master slag ( $\text{SiO}_2$ ,  $\text{CaO}$ ,  $\text{Al}_2\text{O}_3$  and  $\text{MgO}$ ). 1. Induction Coil, 2. Graphite Crucible, 3. Slag Mixture, 4. Insulating Material, 5. Furnace Shell.

#### *b) Tube Furnace*

The main furnace used in the study was a Carbolite Vertical Tube Furnace with a maximum operating temperature of  $1800^\circ\text{C}$  fitted with a programmable Eurotherm 2416CC temperature controller and a 2132 overtemperature controller. The furnace was heated with six vertical lanthanum chromate elements that are secured around the furnace work tube. The work tube is made of recrystallised alumina. Both ends of the tube were fitted with airtight metal plate assemblies that were water-cooled with a provision for gas inlet and outlet. The top end of the tube was fitted with a radiation shield for efficient heating of the reaction zone. Figure 3.11 shows the schematic drawing of the furnace

setup. Gas flow to the furnace was controlled and kept at 40 cc/s of UHP Argon (reading 3 lpm of air) by a flowmeter situated between the furnace and the gas supply cylinder.

The crucible was suspended in the centre of the hot zone by a platinum wire (0.25mm thick, and 2m long). The crucible was connected to the wire by strip of recrystallised alumina passing through the slits on the sides of the crucible and then through a ring of recrystallised alumina tied to the wire. The setup of crucibles is shown in Appendix B.



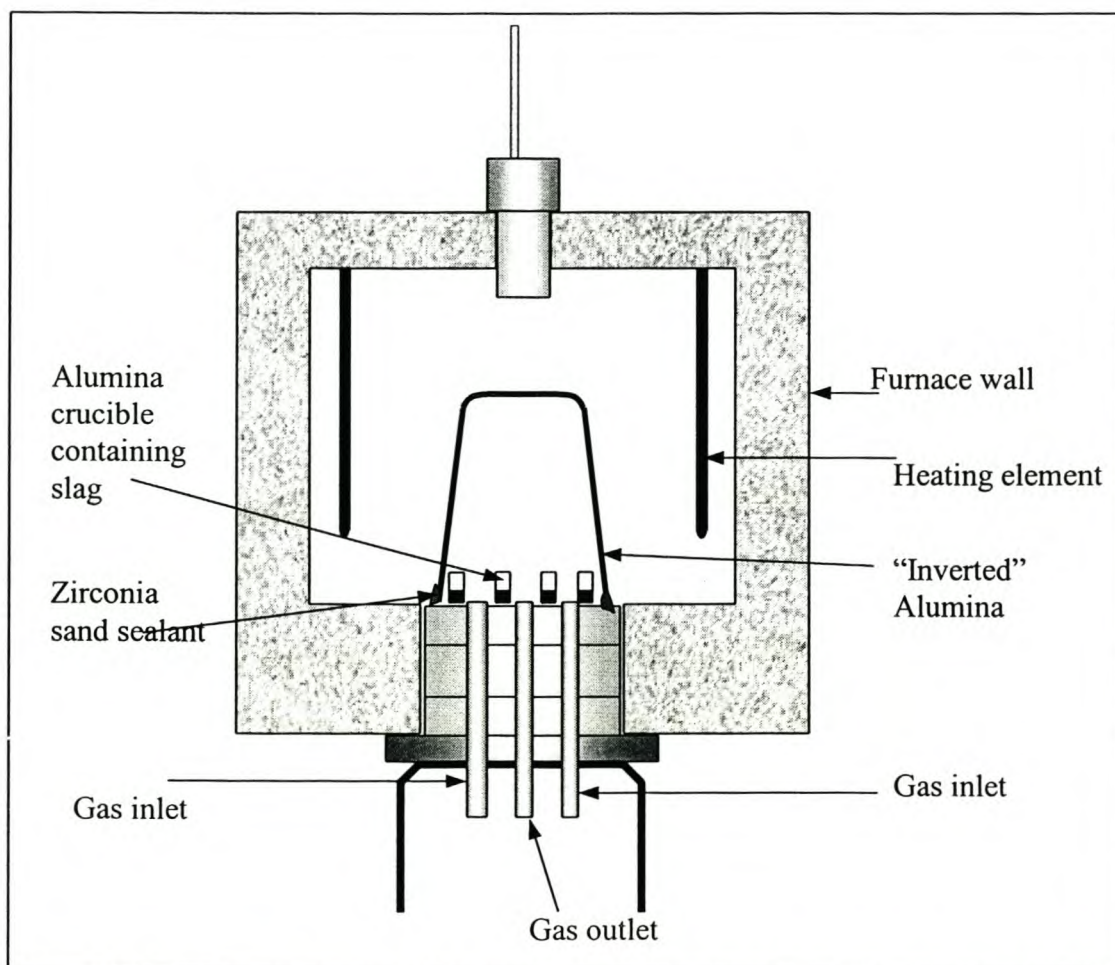
**Figure 3.11** A schematic diagram of the set-up of the tube furnace used in the experiments. 1. Cooling Water channel, 2. Rubber Seals, 3. Radiation Shield, 4. Platinum Wire, 5. Recrystallized Alumina Crucible, 6. Recrystallized Alumina Work Tube, 7. Bolt and Nut, 8. Gas Inlet, 9. Insulation Material, 10. Lanathanum Chromate Element, 11. Element Support Collar, 12. Gas Outlet

### *c) Bottom - Loading Furnace*

A Carbolite Bottom-Loading Furnace was used in experiments conducted in parallel to this study to determine the mechanism and rates of reaction during carbothermic reduction of silica saturated iron-silicate slags. The setup of equipment for this set of



experiments is shown in Figure 3.12. The furnace had a maximum attainable temperature of  $1800^{\circ}\text{C}$ , which was controlled with a Eurotherm 2416CC controller, and a Eurotherm 2132 overtemperature controller. The upward or downward movement of the furnace hearth was motorized and was controlled by a switch located on the control panel of the furnace. The gas to the reaction chamber was supplied through two points in the hearth (base), and the off-gas from the furnace passed through a separate third point and burnt off by a burner located at the top of the furnace. For this experimental setup one inlet was used for UHP argon gas and the other for pure carbon monoxide gas.



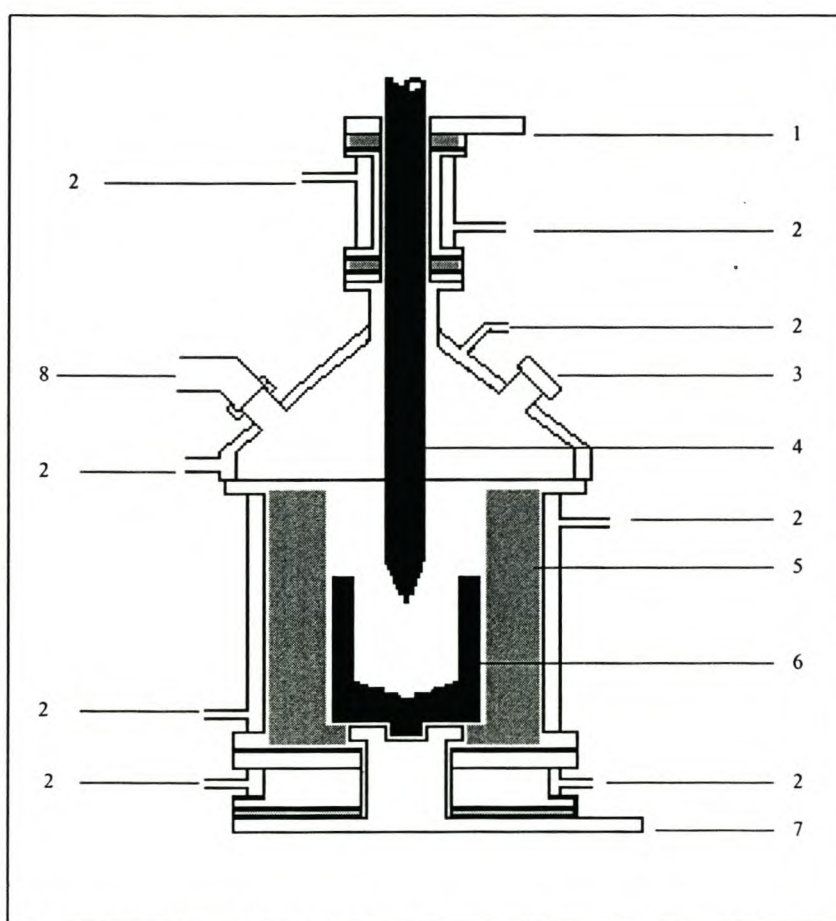
**Figure 3.12** A schematic drawing of the setup for the determination of mechanisms and rates of reaction experiments

#### **d) Plasma Furnace**

A 44V/1100A rated Direct Current (DC) Plasma Arc Furnace was used in the experiments. The equipment worked on the theory of transferred plasma arc technology (described in section 2.8) with a single movable electrode as the cathode. The graphite

crucible in the setup formed part of the anode that was located at the base of the furnace. The equipment was designed and constructed in the workshop at Chemical Engineering Department of the University of Stellenbosch. Figure 3.13 shows a schematic drawing of the furnace assembly. The off gas was extracted via a scrubber, which had metal plates to trap and retain solid particles.

The furnace walls and the roof were water-cooled. A piece of refractory fibre blanket was placed between the inner wall of the furnace and the crucible to reduce heat loss. The electrode was threaded to allow upward and downward movement.



**Figure 3.13** Schematic diagram of the DC plasma furnace used in extraction of cobalt from slag. 1. Cathode Terminal, 2. Cooling Water Channel, 3. Feed Port, 4. Graphite Electrode, 5 Refractory Material, 6. Graphite Crucible, 7. Anode Terminal, 8. Offgas Outlet,

#### *d) Crucibles*

The crucibles used for the main experiments in the tube furnace were cylindrical recrystallised alumina crucibles with a volume of 20ml, 20mm wide, and 50mm high. In



order to secure the crucible to the wire, two slits on opposite sides were cut at about 2mm from the open side of the crucible.

Graphite crucibles used in the plasma experiments measured 130mm high and 120mm wide with a capacity of about 750ml. The bottom inside of the crucibles was tapered at 120° to enhance easy settling and collection of molten metal. The crucibles were made in the workshop of the Department of Chemical Engineering of the University of Stellenbosch. Smaller (250ml) graphite crucibles were used in the induction furnace for the preparation of base slag.

## 3.2 Method

### 3.2.1 Tube Furnace Experiments

#### *a) Synthetic Slag Experiments*

The feed slag was prepared by adding the reducible slag components, namely, CuO, CoO, CuS, and “FeO” to the master slag in proportions as shown in Table 3.3. For each experiment a mass of 6g feed slag was prepared. This composition of the slag was prepared to reproduce the composition of the actual slag that was also used in this study. Graphite (99.9% carbon) and a particular flux (CaO, CaF<sub>2</sub> or TiO<sub>2</sub>) were then added in required proportions, thoroughly mixed in a mortar and pestle, reweighed and placed in crucibles which were in turn placed in the desiccator prior to experiments.

**Table 3.3** Composition of the synthetic slag

Component	SiO <sub>2</sub>	Al <sub>2</sub> O <sub>3</sub>	FeO	MgO	CaO	CuS	CuO	CoO	Total
wt%	40.74	13.33	22.22	3.70	14.82	1.48	1.85	1.85	100.00

The grade of cobalt in the above slag composition was 1.46 wt%, iron was 17.8 wt%, and copper 2.47wt%. Cupric sulphide was used to provide sulphur in the system since the composition of the actual slag contained sulphur that originated from matte smelting (reverbaratory furnace). The steps for calculation of feed are given in Appendix C.

The procedure by which the crucible, with its contents, was loaded in the hot part of the furnace was as follows:

- the crucible was secured to one end of the platinum wire from the bottom of the furnace's work tube, while the other end was secured from the top of the tube,
- the crucible was then pulled to a position just below the reaction zone and was held in that position for about, 5 to 10 minutes, at the same time, the bottom metal piece was fitted and closed tightly, and the gas turned on,
- finally, the crucible was pulled up until it was in the centre of the hot zone. The time for the experiment was then started.

The temperature at which the crucible was pulled and located into the hot zone was noted and observed in all the experiments. This temperature was between 1390°C and 1400°C and, within 10 to 15 minutes, the experiment temperature (1500°C) was attained. The temperature at the bottom portion of the tube was observed to be between 600°C and 700°C when the furnace temperature controller was reading 1450°C. So holding the crucible and its contents for a few minutes below the hot zone was assumed not to cause any gasification reaction of carbon to CO if oxygen was present in the atmosphere of the reaction chamber. On the other hand holding the crucible in this place seemed to have served the following purposes:

- to drive out any moisture that could have been present in the sample, arising from the wüstite which was kept under absolute alcohol (the presence of moisture in the system could encourage slag foaming), and
- to raise the temperature of the crucible and its contents steadily to avoid thermal shock, that caused crucibles to develop cracks and drop during the course of experiments

The time to reach equilibrium was determined in separate experiments described in section 3.2.3. It was observed that the reduction time of the slag was within 60 minutes with high recoveries occurring in the first 15 minutes.

### ***b) Actual Slag Experiments***

Experiments on the actual slag were conducted in the same manner as in the previous section. Only graphite and the particular slag modifier needed (CaO, CaF<sub>2</sub> or TiO<sub>2</sub>) were



added to the slag in required proportions. About 6g of slag was used. The composition of the slag used in the experiment is shown in Table 3.4.

Table 3.4 Composition of the actual slag

Component	SiO <sub>2</sub>	TiO <sub>2</sub>	Al <sub>2</sub> O <sub>3</sub>	FeO	MnO	MgO	CaO	K <sub>2</sub> O	P <sub>2</sub> O <sub>5</sub>	CuO	CoO
wt%	41.72	0.52	7.96	30.75	0.12	2.77	9.19	3.48	0.22	1.63	1.75

### 3.2.2 Plasma Furnace Experiments

About 500g of actual slag, with composition given in Table 3.5, was reduced in a plasma furnace in graphite crucibles. Anthracite coal (74% fixed carbon) with composition, given in Table 4.6, was used as reductant. To facilitate startup of the furnace (ignition of the plasma arc), about 5.6g of copper metal clippings (99% Cu) were arranged at the centre of the bottom of the crucible with about 100g of slag placed around the copper metal. The copper clippings were arranged such that there was contact between the electrode and the copper. Once the plasma arc was stable, about 100g of slag and coal mixture was added every five minutes. The DC voltage reading was noted prior to feeding and after feeding. After about 25 minutes and all the feed completed, the electricity supply to the furnace was switched off and the flux (CaO, CaF<sub>2</sub> or TiO<sub>2</sub>) added in required proportions and the power supply restored. The experiment was run for 60 minutes after which the crucible was slowly cooled. The slag and the metal were removed from the crucible using a chisel and hammer. The alloy was ground in a ring mill to about 100 µm and analysed for Co Cu, Fe, S, Si, and C. The analysis for the slag at the end of the experiment was not carried out.

Calculations for the charge requirements for plasma furnace experiments are given in Appendix C.

Table 3.5 Composition of the actual slag used in plasma furnace experiments

Component	SiO <sub>2</sub>	TiO <sub>2</sub>	Al <sub>2</sub> O <sub>3</sub>	FeO	MnO	MgO	CaO	K <sub>2</sub> O	P <sub>2</sub> O <sub>5</sub>	CuO	CoO
Wt%	42.25	0.49	7.94	33.74	0.10	3.20	6.96	3.46	0.25	1.06	1.83



Table 3.6 Analysis of anthracite used in the plasma furnace experiments

Proximate analysis	%	Ultimate analysis	%
Moisture	2.45	Moisture	2.45
Ash	13.62	Ash	13.62
Volatile Combustible Matter	8.46	Sulphur	0.65
Fixed Carbon	74.47	Carbon	73.8
		Hydrogen	3.02
		Nitrogen	1.82
		Oxygen	4.64
	<b>99.00</b>		<b>100.00</b>

### 3.2.3 Determination of Reaction Mechanisms and Reduction Rates

A separate set of experiments was conducted along side this study (M. Pelsers, 2000) to determine the reduction rates and to predict the reaction mechanisms during the carbothermic reduction of the copper smelter slags. Six 5ml alumina crucibles containing about 3g slag mixture were placed on the furnace hearth of the muffle furnace and introduced into the reaction zone by the motorized lifting of the hearth (activated by a switch on the control panel of the furnace). A larger alumina crucible was placed top-side-bottom to cover the smaller crucibles and create a unique atmosphere (Ar + CO) for the experiment and to protect the furnace elements from the CO gas attack. This crucible was held in place by filling the groove in which the crucible was placed with zircon powder. The experiments were conducted at 1500°C.

During heating up of the furnace argon was flushed through the reaction chamber to prevent the oxidation of carbon by atmospheric oxygen. Upon reaching 1500°C, one crucible was removed from the furnace and the rest at time intervals of 15, 30, 60, and 120 minutes. The furnace takes some time to reach the set-point temperature and during this heating period reduction of the slag by carbon could start and so to check this the first crucible was removed to determine the extent of reduction, if any, that could have taken place during heating up period.

An alternative reductant used was carbon monoxide (CO) gas. A number of crucibles with different slag compositions were heated in an argon atmosphere and after attaining the operating temperature (1500°C) the gas supply was switched from argon to carbon monoxide to initiate a reducing atmosphere for a specific time (i.e., for 15 or 30 minutes) after which the furnace was flushed with argon gas to restore the inert atmosphere in the



reaction chamber. The crucibles were cooled slowly in argon atmosphere within the reaction chamber.

### 3.2.4 Analytical Procedures

Several methods were used to analyse the samples. Analysis for cobalt, copper, and iron in the alloy from the experiments was analysed by ICP (inductively coupled plasma). Slag analysis for cobalt, copper, iron and total composition was carried out by XRD (X-ray diffraction) and XRFS (X-ray fluorescence spectrometry).

#### *a) ICP*

Each alloy sample was separated from the slag and weighed. The analysis was conducted at an external private laboratory. The alloys were dissolved in aqua regia (mixture of 1 part  $\text{HNO}_3$  and 3 parts  $\text{HCl}$ ) to digest cobalt, copper, iron and sulphur in the alloy. The resulting solution was then analysed for the four elements (Co, Cu, Fe, and S) by ICP (inductively coupled plasma)

#### *b) XRFS*

Samples were analysed for major elements on a Philips PW 1410 wavelength dispersive X-ray fluorescence spectrometer using a Rh-tube at the University of Stellenbosch. Major elements were analysed on fusion discs using the Norrish and Hutton (1969) fusion technique.

#### *c) XRD*

Crushed and milled samples were analysed by means of X-ray diffraction techniques. Powder preparations were produced and subjected to  $\text{Co}(K_\alpha)$  radiation. Semiquantitative mineral proportions were determined from the peak heights of X-ray diffraction patterns and peak identification was done in correspondence with the JCPDS database.

#### ***d) Titrametric Analysis***

Analysis for ferrous and ferric oxides in the slag from experiments was carried out by titrametric analysis. About 0.5g of powder sample was heated and dissolved with boiling HF and H<sub>2</sub>SO<sub>4</sub>. A “dissolving solution” (boric acid and phosphoric acid) was added and titrated against 0.06262N – K<sub>2</sub>Cr<sub>2</sub>O<sub>7</sub> with 0.2% sodium diphenylamine as indicator.

### **3.3 Preliminary Experiment**

Trial experiments were conducted to establish two important factors for the experimental work and setup, namely, the amount of feed (mixture of slag, graphite powder and flux) to be reduced and the reaction time. These experiments led to the build up of the experiments described previously.

#### **3.3.1 Determination of Graphite and Flux Amount**

Initially 12g of slag was used in the experiments but slag overflow or creeping was observed and then 6g was used and no overflow was observed. To this slag quantity, various amounts of the reductant and slag modifiers were added. The amounts of graphite and flux required for the experiments needed to be determined too. Therefore, an amount of carbon equivalent to that required to reduce all the cobalt oxide in the slag was calculated and used initially (calculations are given in Appendix C). This amount reduced the slag yielding an alloy in most of the experiments, which were then analysed for cobalt, copper, iron and sulphur. However, the results from these experiments were not satisfactory, with very low recovery of Co and Cu and so a different approach was sought.

A third trial of experiments was then conducted in which graphite was added up to an excess of the amount of carbon required to reduce all the reducible metal oxides. The results of the metal yield against the amount of graphite added revealed that despite an improvement in the mass of metal recovered there was a constant mass of metal recovered after a certain amount of graphite was added (about 0.3g per 6g of slag). This amount was adopted as the amount to give a sufficient recovery of metal. In subsequent experiments fluxes were added from 2wt% to 14wt% of slag feed.



### 3.3.2 Setup of Slag Reduction Experiments

The choice of holding the crucible in the reaction zone by platinum wire was made when the initial setup of an alumina pedestal presented difficult challenges when loading the crucible in the furnace. The system was unstable and could not keep the crucible in the centre of the reaction chamber affecting the heat distribution to the crucible.

The inert atmosphere was necessary to eliminate the oxygen potential that could arise from the atmospheric air in the reaction chamber. This ensured that all the reduction of the slag was entirely by the graphite added.

The results obtained from the experiments are presented and discussed in Chapter four.

---

## CHAPTER FOUR

### *Results and Discussion*

In this chapter, the results from the experiments conducted in the present study are presented and discussed. The results from the three sets of experiments, including those generated from preliminary experiments, are presented and discussed under appropriate subheadings for convenience and easy understanding of the relationship between the three experiments i.e. the effect of the slag modifiers and the reductant on synthetic and actual slag experiments in tube and DC plasma-arc furnaces.

Different fluxes were used with the aim of modifying the slag so as to improve the selective recovery of cobalt against the recovery of iron to the alloy. These fluxes ( $\text{CaF}_2$ ,  $\text{CaO}$ , and  $\text{TiO}_2$ ) were chosen based on the different thermodynamic properties they exhibit when in solution in silicate slags (as described in section 1.2.2). They were added individually to modify the slag at fixed amount of reductant added to the slag.

All the experiments conducted in the tube furnace were conducted at  $1500^\circ\text{C}$  in an argon atmosphere for 90 minutes. The temperature attained in the plasma experiments were measured using an optical pyrometer and ranged between  $1550$  and  $1750^\circ\text{C}$ . However, these temperatures are not considered in the discussion due to the difficulties experienced when taking temperature readings resulting in inaccuracies. Therefore, the temperatures only serve as an indication of the type of temperatures generated in this Plasma furnace.

#### 4.1 Preliminary Experiments

##### 4.1.1 Determination of Carbon Requirement

One of the unknowns at the onset of the study was the amount of carbon reductant that would reduce the slag to recover cobalt, along with copper and iron. The amount of reducible components in the slag were determined by chemical analysis and from which the stoichiometric amount of carbon required to deoxidise these compounds was calculated. However, because of the adverse conditions in the furnace, the actual amount



of carbon required was in excess of this stoichiometric amount. Therefore, an experiment was conducted to determine the actual amount required to effectively reduce the slag.

The total mass of reducible oxides in the slag was 1.555g and the equations considered for this calculation were



The moles for the metal oxides were determined by dividing the oxide mass by their molecular weight. Since one mole of metal oxide reacts with one mole of CO in the reactions of Equations 4.1 to 4.3, the total moles obtained can be related directly to the moles for CO and subsequently to the carbon moles required. The mass of carbon was then calculated by multiplying the moles by the atomic mass of carbon. The results from the calculation (given in Appendix C) are shown in Table 4.1.

**Table 4.1** Calculation of carbon requirement

Mass of metal oxide, g			Moles of metal oxide			Total moles	Moles of CO reqd	Moles of C reqd	Mass of C, g
FeO	CoO	CuO	$N_{\text{FeO}}$	$N_{\text{CoO}}$	$N_{\text{CuO}}$				
1.333	0.111	0.111	0.019	0.0015	0.0014	0.0214	0.0214	0.0214	0.2568

#### 4.1.2 Effect of Amount of Reductant on the Recovery of Cobalt

The data from the preliminary experiments is shown in Table 4.2. The amount of graphite that gave “enough” carbon for the “complete” reduction of all the reducible oxides in the slag was determined to be 0.3g as shown in Figure 4.1, the trend of recovery in metal mass as the amount of reductant is increased. In the experiments where only cobalt oxide in the slag was targeted for reduction, very low recoveries of cobalt were observed (below 1 wt% Co in alloy) but higher recoveries of copper were observed (over 40 wt% Cu in alloy). In terms of metal alloy mass recovered, the highest amount of metal alloy recovered was 0.151g at 0.031g of graphite and the lowest was 0.039g of



alloy at 0.018g of graphite. However, when the amount of reductant was increased, cobalt recoveries were noticed to increase to 51% Co at 0.20g of graphite, and 68% at 0.50g of graphite. When the amount of graphite added was 0.3g, 62% Co was recovered, above this amount of graphite the recovery remained steady, about 68% Co recovery (in the absence of slag modifiers). In terms of metal alloy mass recovered, the highest amount of metal alloy recovered was 0.822g at 0.50g of graphite and the lowest was 0.521g of alloy at 0.20g of graphite.

**Table 4.2** Data from the initial experiments conducted at 1500°C

Expt.#	Slag mass g	Mass of Graphite, g	Flux		Metallic alloy analysis				
			Type	Mass, g	Co, mg/kg	Cu wt%	Fe wt%	S wt%	Mass, g
1	6.0	0.031	nf	-	0.353	65.94	3.11	12.8	0.151
2	6.0	0.022	nf	-	0.088	72.17	1.13	12.08	0.116
3	6.0	0.018	nf	-	0.039	75.44	0.69	12.15	0.071
4	6.0	0.009	CaO	0.25	0.02	83.49	0.45	12.43	0.038
5	6.0	0.009	CaF <sub>2</sub>	0.25	0.004	89.47	0.31	13.29	0.011
6	6.0	0.009	TiO <sub>2</sub>	0.25	0.008	88.44	0.47	15.99	0.015
7	6.0	0.009	TiO <sub>2</sub>	0.75	0.015	79.55	0.37	12.05	0.058
8	6.0	0.009	CaF <sub>2</sub>	0.75	0.003	86.91	0.17	13.17	0.022
10	6.0	0.018	CaO	0.25	0.128	62.51	3.59	13.62	0.129
11	6.0	0.018	CaF <sub>2</sub>	0.25	0.112	70.11	1.26	12.93	0.125
12	6.0	0.018	TiO <sub>2</sub>	0.25	0.123	72.71	1.47	11.31	0.122
13	6.0	0.018	CaO	0.50	0.104	73.31	1.18	11.20	0.136
14	6.0	0.018	CaF <sub>2</sub>	0.50	0.143	72.13	1.79	12.74	0.126
15	6.0	0.018	TiO <sub>2</sub>	0.50	0.114	71.82	1.50	13.59	0.126

*nf stands for no flux*

The recovery of cobalt from the slag with carbon is dependent on the quantity of graphite (reductant) added up to a point when the recoveries were static. The recoveries did not represent a complete recovery of cobalt as can be seen from the analysis of the slag that showed high cobalt levels in the slag. Two observations could be made from the initial experiments: Firstly the grade of copper in the alloy was high in both instances of low graphite additions and high graphite additions whereas those of cobalt and iron were low (with cobalt lower than iron) in lower graphite additions and high at high levels of graphite. This behaviour of copper shows that most of the copper is entrained as matte and its recovery does not directly depend on the amount of reductant added but rather on the liquidus state of the slag. Secondly, the insignificant recoveries of cobalt at lower



levels of graphite would suggest that the amount of reductant added plays a major role in the reaction mechanisms of the reduction process. This is in agreement with Reddy (1981): the reduction time increased with increasing addition of carbon. The addition of carbon improves the recoveries of all the metals.

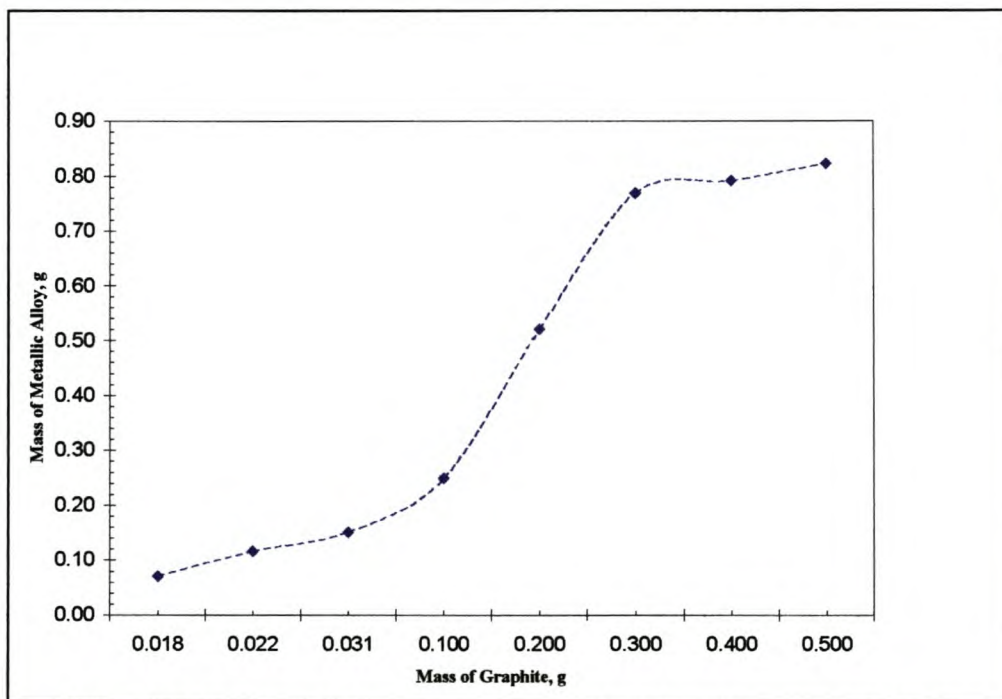


Figure 4.1 The effect of reductat on the amount of metal alloy recovered at 1500°C.

The cobalt and iron grades in the alloy were affected by the introduction of fluxes ( $\text{CaF}_2$ ,  $\text{CaO}$ , and  $\text{TiO}_2$ ) that were intended to modify the slag and improve the recoveries. This improvement in grade indicates that the existence of cobalt and iron in slag is in the form of dissolved species as suggested by Imriš (1982) and Pirard (1995) who investigated the distribution of cobalt and its association with iron in the copper slags.

#### 4.1.3 Reduction Rates and Reaction Mechanisms

Solid carbon is used to control the oxygen potential of the molten slags and to recover metal values from solutions. Despite the widespread utilization of the reaction, some uncertainties remain as to the factors influencing the interactions between the phases. Whilst overall reactions of solid carbon with metal oxides in slags result in the formation of gaseous carbon monoxide and carbon dioxide, a number of possible reaction mechanisms such as direct reduction reaction, a two-stage gas ferrying mechanism, and

electrochemical reactions (in cases where slags contain iron or other species which can exist in more than one oxidation state) have been identified (Hayes *et al.*, 1995).

The time required to recover the metal from the slag to the alloy was determined from experiments conducted alongside this study in which the slag containing cobalt oxide and copper oxide was equilibrated with pure iron at 1500°C in a muffle furnace. The results from the analysis showed that the metal oxide reduced within 60 minutes as shown in Figure 4.2. The reduction rate was observed to be a function of the amount of reducible oxide (cobalt oxide) in the slag. This was in agreement with findings by Jones *et al.* (1996).

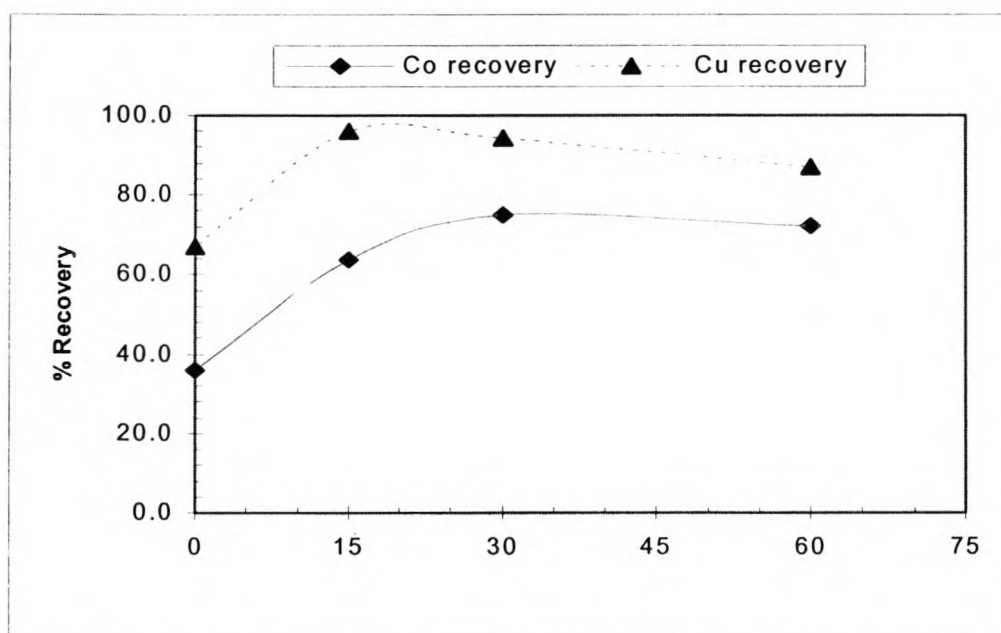


Figure 4.2 Determination of reduction rate of metal oxide in slag at 1500°C.

The other property that would affect the reduction rate of slag is the wettability of the solid carbon by slag. From the studies on the reactions of molten oxides in slags with coke by Hayes (1996), it was found that fayalite slags did not wet the coke and that the reduction rates were dependant on the gasification of coke. From these findings Hayes *et al.* (1996) concluded that the gas ferrying mechanism with carbon gasification was rate limiting.



## 4.2 Final Experiments

As described in section 3.2, the experiments were conducted on two types of slags, a synthetic slag, and an actual slag. The first set of experiments was conducted in a tube furnace and consisted of synthetic slag experiments and actual slag experiments. The second set of experiments was conducted in a DC plasma-arc furnace on actual slag only. In the second part of experiments, anthracite coal (about 2mm particle size) was used as a reductant instead of graphite.

At the end of the tube furnace experiments, the metallic alloy recovered (which was in a form of a bead) was separated from the slag and weighed. The slag was removed from the crucibles. The removal of the slag from the crucible was found to be difficult. The slag was stuck to the crucible walls, and so the mass of the slag at the end of experiments was not recorded. Both the metallic alloy and the slag were analysed as described in section 3.2.4. The metallic alloy from the DC plasma-arc furnace experiments was separated from the slag and submitted for analysis. The slag was not analysed. The results from the experiments are presented and discussed in the following sections.

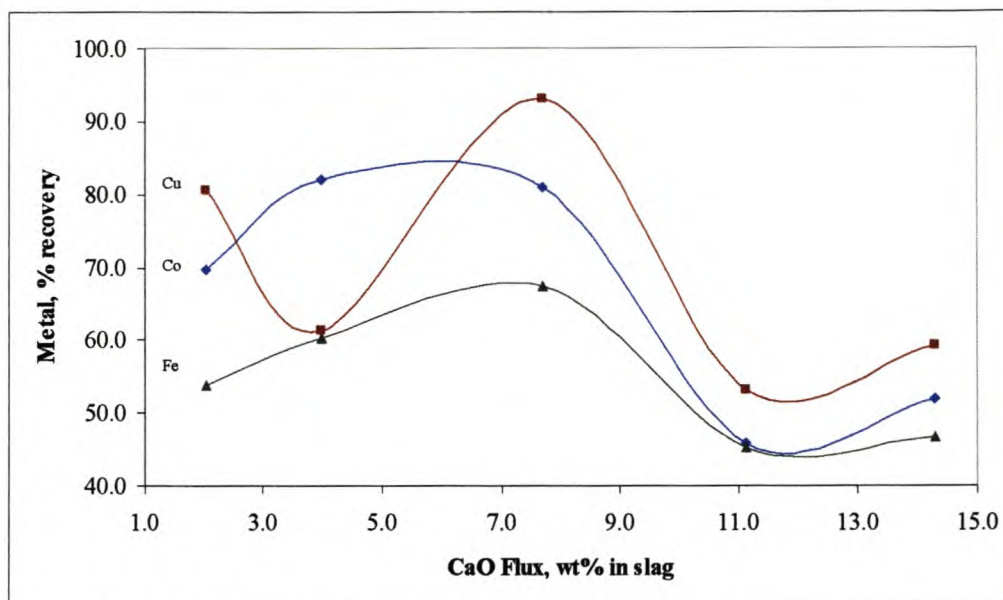
### 4.2.1 Synthetic slag experiments

#### *a) Effect of CaO on the Recovery of Co, Cu and Fe Metals from Slag*

The results of the alloy and slag analyses are shown in Table 4.3. The plot in Figure 4.3 shows the effect of CaO on the recovery of cobalt, copper, and iron. It can be seen that the addition of CaO to the slag increased the recovery of cobalt and iron metals up to about 7wt% of flux added to the slag. On the other hand, copper recovery decreased during the initial addition of flux (from 80 %Cu at 2 wt% CaO to 61 %Cu at 4wt% CaO) then increased to a high of 93% at 7wt% CaO before following a decreasing trend exhibited by all the three metals after the 7wt% CaO level. The highest recovery of Co was 82% at 4wt% CaO and the lowest was 45% at 11wt% CaO. Iron recovery was highest at 7wt% CaO (67% Fe) and the lowest at 11wt% CaO (45% Fe). This drop could simply imply the formation of other phases at the expense of metal recovery due to the changes in the slag chemistry and thermodynamic properties discussed in section 4.3. Table 4.3 shows the analysis of the slag and the calculated basicity. It is apparent that in



all cases of CaO addition, an optimum recovery exists and that excess lime may lead to significant decrease in metal recovery.



**Figure 4.3** The effect of CaO on cobalt, iron and copper recoveries

#### ***b) Effect of $\text{CaF}_2$ on the Recovery of Co, Cu and Fe Metals from Slag***

The recovery of cobalt, copper, and iron is affected by the addition of fluorspar ( $\text{CaF}_2$ ). Figure 4.4 shows that the addition of  $\text{CaF}_2$  in small amounts increased the recovery of cobalt and copper. A decrease in the recovery of both metals is observed beyond 4wt%  $\text{CaF}_2$  addition to the slag. The recovery of iron, on the other hand decreases in the same range of fluxing and then increases slightly beyond 4wt%  $\text{CaF}_2$  and then remains the same (about 67%) for the rest of the experiments. The recovery of cobalt and copper was the highest (76% Co and 97% Cu) at 4wt% of  $\text{CaF}_2$  in slag. And for iron the highest recovery was 69% at 2wt% of flux. It was observed that the lowest for all the three metals was at 11wt%  $\text{CaF}_2$ .

The influence of this flux on the recovery of cobalt copper and iron could be its ability to lower the liquidus temperature of the slag and less on the slag chemistry as is discussed in section 4.3. It has been suggested that the addition of  $\text{CaF}_2$  to silicate melts makes them less viscous by breaking the network (Sano *et al.*, 1997). Generally the effect of fluorides on the slag is not well understood. It may increase the ionic character of the slag without actual depolymerisation.



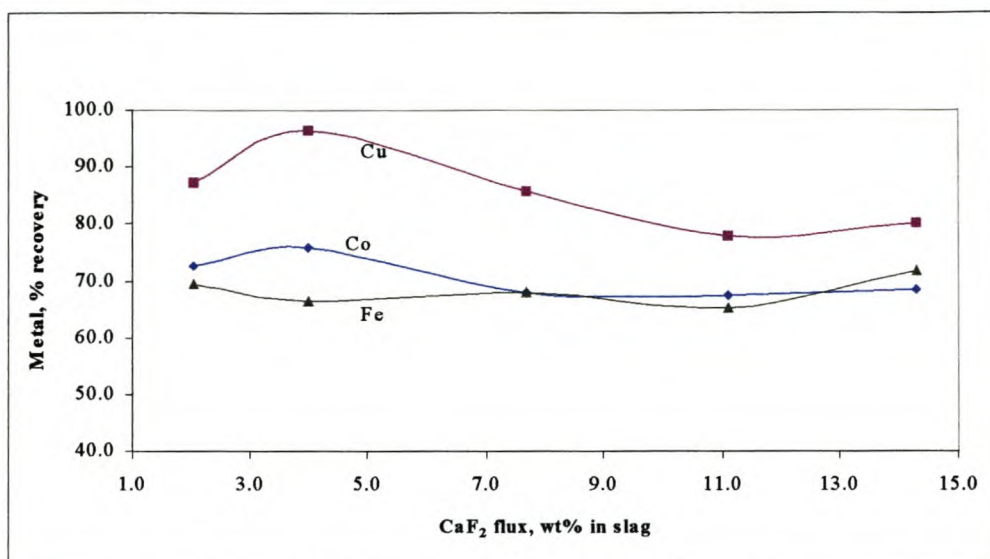
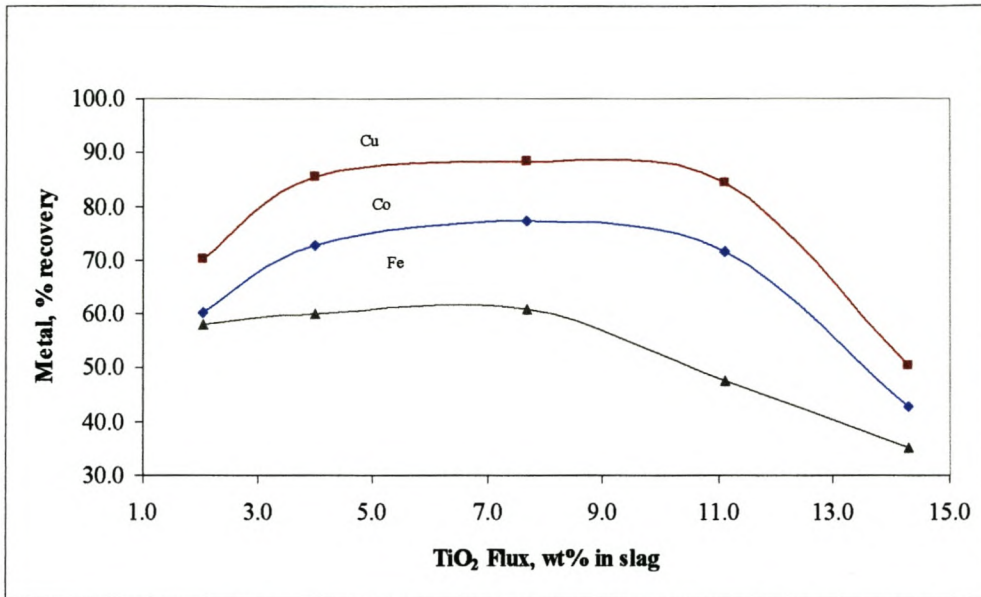


Figure 4.4 The effect of CaF<sub>2</sub> on cobalt, iron and copper recoveries.

#### c) Effect of TiO<sub>2</sub> on the Recovery of Co, Cu and Fe Metals from slag

The effect of TiO<sub>2</sub> on the recovery of the three metals to Co-Cu-Fe-S alloy is shown in Figure 4.5. From 2wt% to about 7wt% of TiO<sub>2</sub> in the slag, the recovery of cobalt copper and iron increases. At this amount, TiO<sub>2</sub> is known to exist as a network former (Mills, 1995) allowing it to form titanates with iron as discussed in section 4.3. The increment in the recovery between flux additions is very small though, resulting in a constant level of iron in alloy up to 7wt% TiO<sub>2</sub> in slag and then decreased sharply beyond this point. Cobalt and copper recoveries decreased steadily up to 11wt% and then decreased steeply beyond this amount. The recovery of cobalt, copper, and iron was highest (77% Co, 88% Cu, and 61% Fe) at about 7wt% of TiO<sub>2</sub> in slag and lowest (43% Co, 50% Cu, and 35% Fe) at 11wt% TiO<sub>2</sub> in slag.

From these results, it can be seen that all the three fluxes affect the recovery of cobalt, copper, and iron in a positive way but only up to certain proportions. It is also apparent from all the results mentioned above that the addition of slag modifiers is effective at lower weight percentage addition. Higher weight percentage additions lead to either no additional recoveries or a sharp decrease in recoveries.



**Figure 4.5** The effect of TiO<sub>2</sub> on cobalt, iron and copper recoveries

The decrease in recoveries in all three cases can be attributed to the fact that the recovery of metals does not depend on the quantity of the flux only but on the chemistry and composition of the slag, and the physical properties of the slag as well. The effects of the fluxes on the slag basicity and recovery ratios are discussed in section 4.2.4.



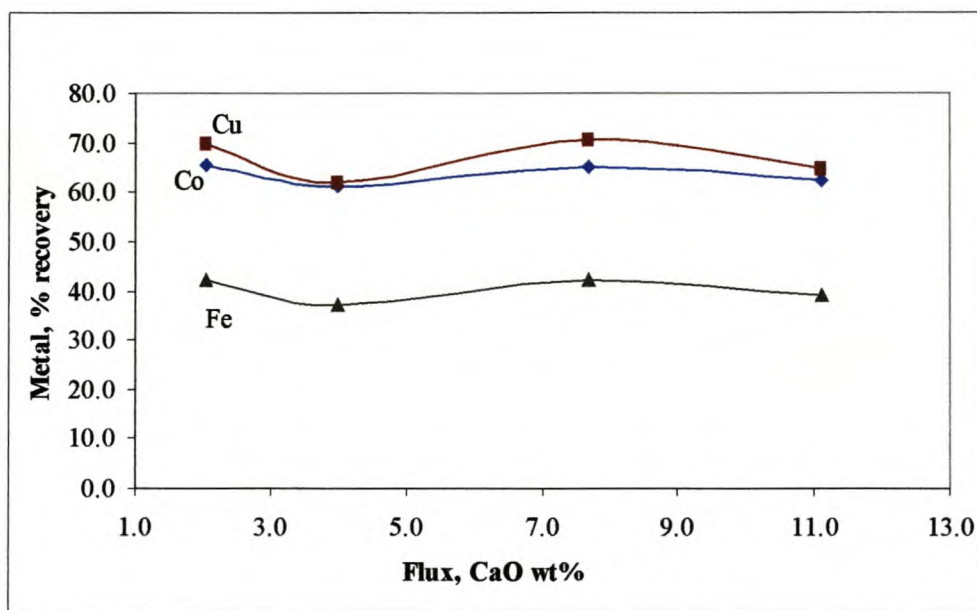
**Table 4.3** Analysis of Metal contents of slag and alloy at the end of experiments-synthetic slag experiments

Expt#	Graphite, g	Flux		Metal alloy, g	Metal Analysis of alloy, wt%				Smoothing Factor 100/total wt% in alloy	Metal Recovered, %				Recovery ratio Co/Fe	Metal content of slag, wt%			
		Type	wt% in Feed slag		Co	Cu	Fe	S		Co	Cu	Fe	S		Fe	Co	Cu	Fe/SiO <sub>2</sub>
25	0.30	CaF <sub>2</sub>	2.04	0.942	6.74	13.75	78.22	1.29	0.98	72.53	87.43	69.30	40.38	1.05	4.72	0.82	32.26	15.72
8	0.30	CaF <sub>2</sub>	4.00	0.930	7.15	15.40	75.80	1.65	0.98	75.88	96.63	66.30	51.27	1.14	5.00	0.90	40.96	16.66
11	0.30	CaF <sub>2</sub>	7.69	0.920	6.46	13.83	78.40	1.31	0.98	67.80	85.87	67.84	44.06	1.00	4.52	0.79	35.20	15.05
20	0.30	CaF <sub>2</sub>	11.11	0.878	6.73	13.15	78.95	1.17	0.99	67.44	77.90	65.20	34.32	1.03	4.71	0.81	27.42	15.69
22	0.30	CaF <sub>2</sub>	14.29	0.950	6.30	12.47	80.15	1.08	0.99	68.28	79.96	71.62	37.11	0.95	4.40	0.75	29.64	14.68
26	0.30	CaO	2.04	0.766	7.96	15.58	74.80	1.65	0.95	69.64	80.55	53.89	42.18	1.29	5.57	1.02	33.70	18.57
7	0.30	CaO	4.00	0.840	8.83	11.33	78.33	1.30	0.98	82.02	61.24	60.26	0.00	1.36	6.18	1.07	0.00	20.59
10	0.30	CaO	7.69	0.937	7.56	14.72	76.41	1.30	0.96	80.90	93.08	67.34	40.63	1.20	5.29	0.94	32.45	17.63
13	0.30	CaO	11.11	0.607	6.62	13.00	79.22	1.17	1.01	45.84	53.24	45.23	23.57	1.01	4.63	0.80	18.83	15.42
21	0.30	CaO	14.29	0.638	7.13	13.78	77.84	1.25	0.98	51.90	59.33	46.71	26.68	1.11	4.98	0.87	21.32	16.61
1	0.20	No Flux	0.00	0.521	8.58	16.25	73.52	1.64	0.97	51.03	57.14	36.97	28.55	1.38	6.00	1.09	22.81	30.00
2	0.30	No Flux	0.00	0.769	7.09	14.16	77.37	1.38	1.00	62.21	73.50	55.96	35.25	1.11	4.96	0.87	28.16	16.52
3	0.40	No Flux	0.00	0.792	7.58	15.71	75.15	1.56	0.97	68.54	83.94	55.98	41.31	1.22	5.30	0.96	33.00	13.26
4	0.50	No Flux	0.00	0.822	7.21	15.04	76.59	1.16	0.96	67.66	83.40	59.21	31.92	1.14	5.04	0.90	25.50	10.09
24	0.30	TiO <sub>2</sub>	2.04	0.782	6.77	13.33	78.74	1.15	0.95	60.45	70.36	57.92	30.04	1.04	4.74	0.82	24.00	15.79
9	0.30	TiO <sub>2</sub>	4.00	0.840	7.59	15.11	75.88	1.42	0.97	72.80	85.63	59.95	39.64	1.21	5.31	0.96	31.67	17.70
17	0.30	TiO <sub>2</sub>	7.69	0.886	7.88	15.21	75.44	1.47	1.01	77.35	88.28	61.02	43.50	1.27	5.51	1.00	34.75	18.37
15	0.30	TiO <sub>2</sub>	11.11	0.705	8.91	17.76	71.61	1.72	0.99	71.73	84.47	47.49	40.40	1.51	6.23	1.19	32.27	20.78
23	0.30	TiO <sub>2</sub>	14.29	0.493	7.61	15.11	75.73	1.54	0.97	42.83	50.28	35.12	25.33	1.22	5.32	0.96	20.24	17.74

### 4.2.2 Actual Slag Experiments

#### a) Effect of CaO on the Recovery of Co, Cu and Fe Metals from Slag

The results of the alloy and slag analyses are shown in Table 4.4. The plot in Figure 4.6 shows the effect of CaO on the recovery of cobalt, copper, and iron. It can be seen from the results that the addition of CaO to the slag decreased the recovery of cobalt, copper, and iron metals up to about 4wt% CaO and then the recovery of all the metals increased but only slightly when about 7wt% of CaO was added to the slag. At 11 wt% the recoveries dropped slightly again. The highest recovery of Co was 65% at 2wt% and 7wt% CaO and the lowest was 61% at 4wt% of CaO flux added to the slag. The highest recovery of Cu was 70% at 2wt% and 7wt% CaO and the lowest was 62% at 4wt% of CaO flux added to the slag. Iron recovery to the alloy was highest (42% Fe) at 2wt% and 7wt% CaO and the lowest (37% Fe) at 4wt% of CaO flux added to slag.



**Figure 4.6** The effect of CaO on the reductive recovery of Co, Cu, and Fe from slag at 1500°C.

#### b) Effect of CaF<sub>2</sub> on the Recovery of Co, Cu and Fe Metals from Slag

The recovery of cobalt, copper, and iron was affected by the addition of fluorspar (CaF<sub>2</sub>). Figure 4.7 shows the effect of this flux on the carbothermic recovery of Co, Cu, and Fe recovery to the alloy. An increase in the recovery of all the three metals was observed



during the initial flux additions. When 11wt% of flux was added to the slag, the recoveries decreased. The recovery of cobalt was highest (83% Co) at 4wt% of  $\text{CaF}_2$ . Copper was highest (91% Cu) at 7wt% of  $\text{CaF}_2$  in slag, and iron recovery was highest 64% Fe at 7wt%  $\text{CaF}_2$  flux added to slag. It was observed that the lowest recovery for all the three metals was at 11wt%  $\text{CaF}_2$  (49% Co, 58% Cu, and 51% Fe).

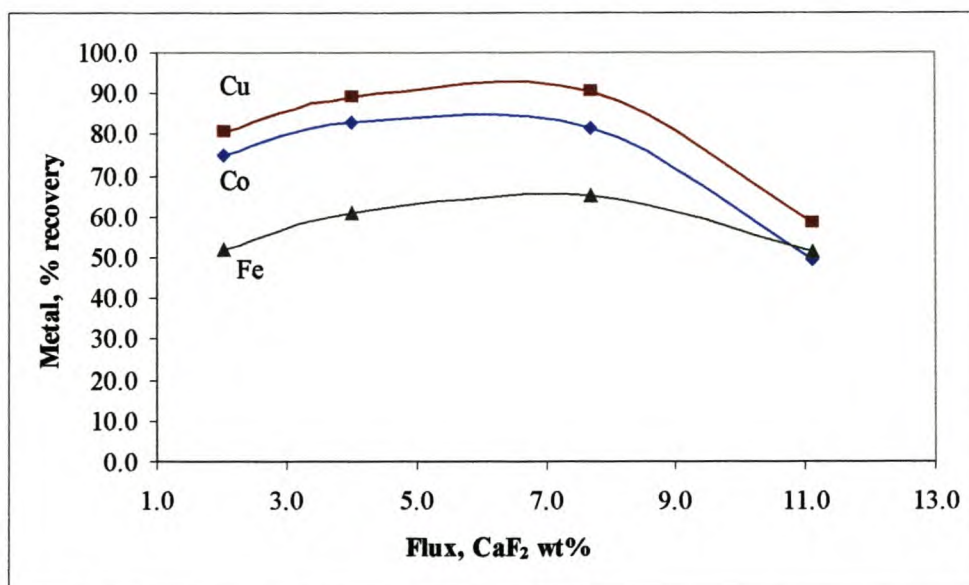


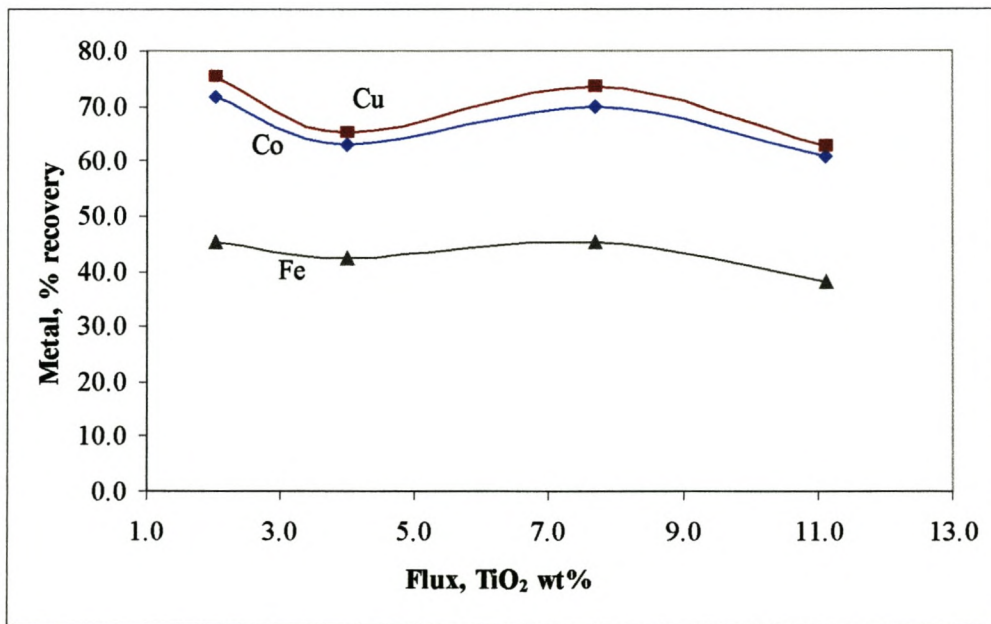
Figure 4.7 The effect of  $\text{CaF}_2$  on the reductive recovery of Co, Cu, and Fe from slag at 1500°C.

### c) Effect of $\text{TiO}_2$ on the Recovery of Co, Cu and Fe Metals from Slag

The effect of  $\text{TiO}_2$  on the recovery of the three metals to Co-Cu-Fe-S alloy is shown in Figure 4.8. When 4wt%  $\text{TiO}_2$  equivalent of flux was added the recovery of all the metals decreased slightly, and then increased when about 7wt% was added. The increment in the recovery of metals between flux additions was very small though. The recovery of cobalt, copper, and iron was the highest (72% Co, 75% Cu, and 45% Fe) when 2wt%  $\text{TiO}_2$  flux was added to slag and the lowest recoveries (43% Co, 50% Cu, and 35% Fe) occurred at 11wt%  $\text{TiO}_2$  addition to slag.

From the results presented in the sections above it is evident that the carbothermic recovery of cobalt, copper, and iron from slag is influenced by flux addition. At constant carbon reductant addition the recoveries were increased by about 10% Co (by difference) with reference to the maximum recoveries, about 3% Cu, and about 3 to 7% Fe in all the three cases of fluxing, for both types of slags, compared to a situation of similar

conditions where no flux was added. In general, the effects of  $\text{CaF}_2$  are more pronounced than the effect of  $\text{CaO}$ . The effect of  $\text{CaF}_2$  addition on the slag chemistry and thermodynamic properties is discussed in section 4.3



**Figure 4.8** The effect of  $\text{TiO}_2$  on the reductive recovery of Co, Cu, and Fe from slag at  $1500^\circ\text{C}$ .



**Table 4.4** Analysis of Metal content of alloy and slag at the end of Experiments-Actual slag experiments

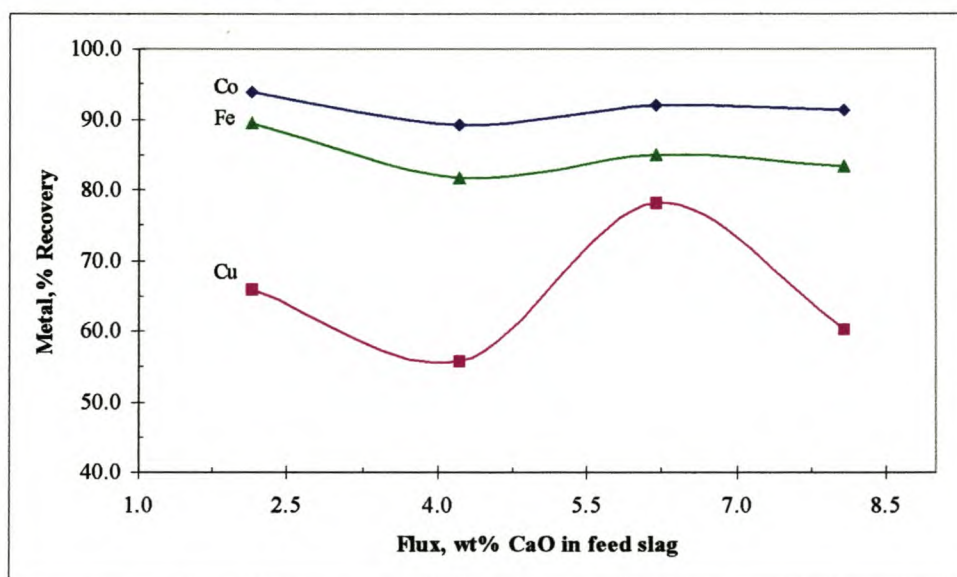
Expt#	Graphite, g	Flux		Metal alloy, g	Metal Analysis, wt%				Smoothing Factor 100/ $\Sigma$ original total	Metal Recovered, %			Recovery ratio Co/Fe	Metal content of slag, wt%			
		Type	wt% in Feed slag		Co	Cu	Fe	S		Co	Cu	Fe		Fe	Co	Cu	Fe/SiO <sub>2</sub>
2	0.30	CaF <sub>2</sub>	2.04	0.851	7.050	7.174	84.662	1.113	0.951	75.18	80.86	51.77	1.452	7.06	0.05	0.00	0.14
5	0.30	CaF <sub>2</sub>	4.00	0.990	6.686	6.795	85.737	0.782	0.990	82.94	89.10	60.99	1.360	4.69	0.03	0.07	0.10
8	0.30	CaF <sub>2</sub>	7.69	1.050	6.187	6.526	86.016	1.271	0.942	81.40	90.76	64.90	1.254	8.24	0.05	0.07	0.16
11	0.30	CaF <sub>2</sub>	11.11	0.810	4.857	5.456	88.490	1.197	0.997	49.30	58.53	51.50	0.957	2.49	0.02	0.04	0.06
1	0.30	CaO	2.04	0.703	7.422	7.511	83.532	1.536	0.991	65.38	69.94	42.20	1.549	3.15	0.03	0.04	0.07
4	0.30	CaO	4.00	0.620	7.899	7.536	83.110	1.455	1.039	61.37	61.88	37.03	1.657	9.68	0.06	0.10	0.19
7	0.30	CaO	7.69	0.700	7.443	7.638	83.491	1.428	0.978	65.28	70.82	42.00	1.554	7.39	0.03	0.07	0.16
10	0.30	CaO	11.11	0.650	7.671	7.545	83.419	1.366	0.969	62.48	64.96	38.96	1.604	7.64	0.02	0.02	0.17
16	0.50	Non	0.00	0.930	6.270	7.090	85.721	0.918	0.987	73.07	87.33	57.28	1.276	4.82	0.07	0.12	0.09
18	0.20	Non	0.00	0.520	10.149	9.929	78.106	1.816	0.956	66.13	68.39	29.18	2.266	12.75	0.10	0.13	0.27
19	0.30	Non	0.00	0.560	7.298	7.549	83.764	1.388	0.964	51.21	55.99	33.71	1.519	9.43	0.09	0.11	0.19
3	0.30	TiO <sub>2</sub>	2.04	0.757	7.561	7.499	83.440	1.500	1.034	71.72	75.19	45.39	1.580	8.44	0.04	0.08	0.16
6	0.30	TiO <sub>2</sub>	4.00	0.700	7.196	7.027	84.240	1.537	0.998	63.12	65.15	42.37	1.490	8.52	0.04	0.09	0.17
9	0.30	TiO <sub>2</sub>	7.69	0.750	7.452	7.380	83.833	1.335	1.019	70.03	73.31	45.18	1.550	8.08	0.04	0.10	0.16
12	0.30	TiO <sub>2</sub>	11.11	0.630	7.708	7.512	83.741	1.038	0.979	60.85	62.69	37.91	1.605	7.04	0.04	0.08	0.16

### 4.2.3 DC Plasma-arc Furnace Experiments

The results of metal analysis and calculated values of recoveries are shown in Table 4.5 and all the subsequent figures are based on it. As stated earlier in section 3.2.4, the chemical analysis of the slag from the DC plasma arc furnace experiments was not performed. A mass balance could determine the composition of the slag at the end of experiments. Therefore, the results presented in this section only takes into account the chemical analysis of the metallic part of the furnace product.

#### *a) Effect of CaO on recovery of Co, Cu and Fe Metals from Slag*

The plot in Figure 4.9 shows the effect of CaO on the recovery of cobalt, copper, and iron. It was observed that the first proportion of CaO (2.15wt%CaO in feed slag) produced the highest recoveries of Co and Fe (94%Co and 89%Fe). The highest recovery of copper was 78% at 6wt% CaO in slag. The second addition (4wt% CaO) produced lowest recoveries of all the metals but the recoveries were higher in the next stage. This pattern of decreased and then increased recovery at different proportions of flux was observed throughout the experiment.

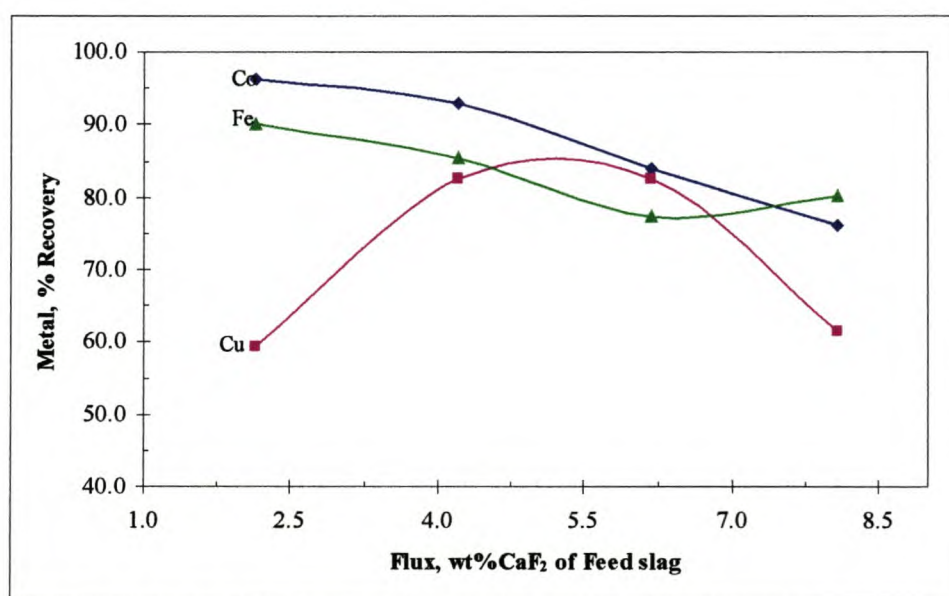


**Figure 4.9** The effect of CaO on the reductive recovery of Co, Cu, and Fe from slag using a DC Plasma arc Furnace.



### ***b) Effect of $\text{CaF}_2$ on recovery of Co, Cu and Fe Metals from Slag***

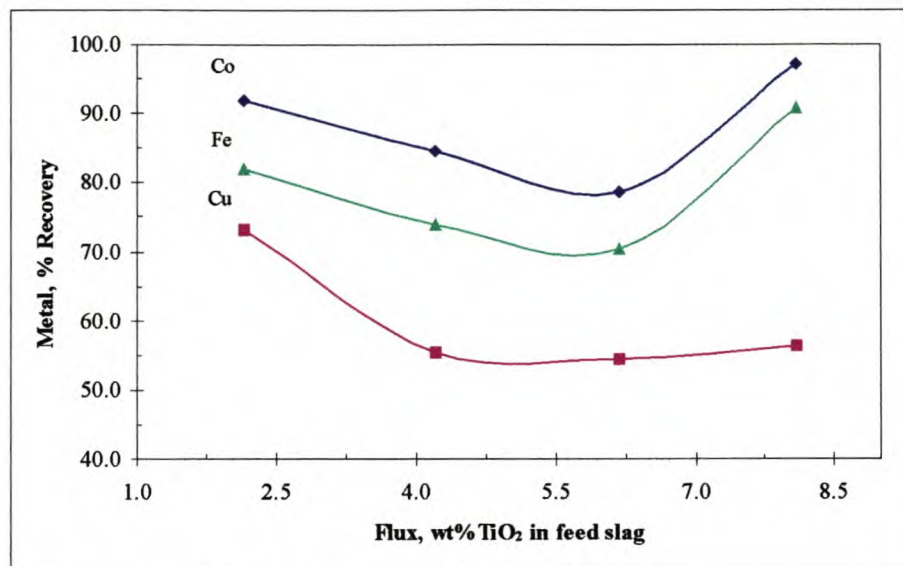
The recovery of cobalt, copper, and iron was affected by the addition of fluorspar ( $\text{CaF}_2$ ) as shown in Figure 4.10. Like in the case of  $\text{CaO}$  flux, the recoveries of cobalt and iron were highest (96% Co and 90% Fe) when about 2.15wt%  $\text{CaF}_2$  of slag was added. At the same proportion of flux, copper recovery was 59% and the lowest. When about 4wt%  $\text{CaF}_2$  was added to the slag the recovery of copper was highest (82% Cu) and remained the same at the next stage before decreasing to 62% at 8wt%  $\text{CaF}_2$ . The recovery of cobalt continued to decrease throughout the experiment whereas that of iron increased to 80% at 8wt%  $\text{CaF}_2$  in the slag.



**Figure 4.10** The effect of  $\text{CaF}_2$  on the reductive recovery of Co, Cu, and Fe from slag using a DC Plasma arc Furnace.

### ***c) Effect of $\text{TiO}_2$ on the Recovery of Co, Cu and Fe Metals from Slag***

The effect of  $\text{TiO}_2$  on the recovery of the three metals (Co, Cu, and Fe) to the metal alloy is shown in Figure 4.11. From 2wt% to about 6wt%  $\text{TiO}_2$  in slag the recovery of cobalt and iron decreased from 92% Co and 82% Fe to 79% Co and 70% Fe. The recoveries increased to 97% Co and 91% Fe when about 8wt%  $\text{TiO}_2$  was added to the slag. Copper recovery also decreased but only when 4wt%  $\text{TiO}_2$  was added. The increment in the recovery of copper between flux additions was very small though, yielding about 55% Cu for the rest of the experiments.



**Figure 4.11** The effect of TiO<sub>2</sub> on the reductive recovery of Co, Cu, and Fe from slag using a DC Plasma arc Furnace.

The experiments conducted in the DC plasma-arc furnace show that recoveries of cobalt and iron are higher than that of copper, and when flux proportions added to the slag was above 2.15wt% of flux in slag, the metal yield decreased with successive additions of flux. Copper on the other hand had the opposite trend to that of the cobalt and iron. In the case of rutile flux, the recoveries increased when 8.09wt% TiO<sub>2</sub> was added unlike when the same amount of either CaO or CaF<sub>2</sub> was added.

The chemical analysis of the metal alloys showed the presence of dissolved silicon. In general, high amounts of silicon reported to the metallic alloy. The presence of silicon and carbon in the metallic alloy could be attributed to either of the following.

- **Effect of Reductant:** the amount of reductant added, coupled with the fact that the crucible was acting as a reductant at the interface between molten slag and crucible wall, could have been in excess of the required amount. When this is the case, the formation of carbon compounds (at high temperatures) such as carbides of iron and silicon is possible.
- **Effect of Temperature:** the formation of SiO gas is promoted by high temperature, high SiO partial pressure, high carbon content in metal droplets, high reducing potential (low partial pressure of CO) and the activity of silica in the slag (Steiler, 1997). These conditions prevail in DC plasma arc and therefore, the following reaction could occur:





$$p_{\text{SiO}} = K \cdot a_{\text{SiO}_2} \cdot a_{\text{C}} \cdot \frac{1}{p_{\text{CO}}} \quad [4.8]$$

with  $K$  = equilibrium constant of the reaction;  $a$  = activity of C or  $\text{SiO}_2$ ; ( $x_{\text{CO}}$  = concentration of CO in gas;  $P$  = total pressure).

### 4.3 Effect of Slag Modifiers on Slag Composition and Recovery of Metals

In general the role of slag modifiers (flux) on slag can be considered in two ways: a physical effect and a physicochemical effect. The physical effects on the slag include the influence on the viscosity and surface and interfacial energy between different phases (especially metals, mattes and slags) in the slag. The physicochemical effects include the behaviour of slags with respect to the activities and activity coefficients of major slag components like  $\text{SiO}_2$ ,  $\text{CaO}$  as well as  $\text{FeO}$  and other metallic oxides in the slag, and their energies of formation.

The results from the analyses on slags from experiments conducted in the tube furnace for synthetic slag and actual slag experiments are given in Tables 4.6 and 4.7. From the results on the analysis of the slag, the basicity index was calculated with respect to  $\text{CaO}$ ,  $\text{MgO}$ ,  $\text{SiO}_2$ , and  $\text{Al}_2\text{O}_3$  in the slag at the end of experiments. From the values of the metal content (Co, Cu, and Fe) of the slag after experiments the recovery ratio of cobalt to iron (Co/Fe) and distribution of cobalt between slag and metallic alloy were determined and plotted. Analysis on slag from the DC plasma-arc furnace experiments was not conducted. A thermodynamic interpretation of the effect of slag modifiers on the slag will be discussed in section 4.4.

#### 4.3.1 Effect of Slag Modifiers on the Basicity of Slag

The basicity of the slag,  $B$ , was calculated using the index given in Equation 4.8, which is a modification of the common “V ratio” expression (i.e.  $\% \text{CaO} / \% \text{SiO}_2$ ) (Mills, 1997). The change in basicity with the addition of different fluxes in increasing proportions is shown in Table 4.6 for synthetic slag and Table 4.7 for actual slag experiments. The values of  $B$  show that the addition of different fluxes have influence on the composition

of the slag that in turn affects the recovery of cobalt and iron from the slag. The actual effects could be on the structure and so viscosity of the melt and, a probable effect on the partitioning coefficient of the elements in the melt (Mills, 1997). The basicity value of the slag before reduction was 0.342, for the synthetic slag and 0.241 for the actual slag.

$$B = \frac{\%CaO + \%MgO}{\%Al_2O_3 + \%SiO_2}, \quad [4.8]$$

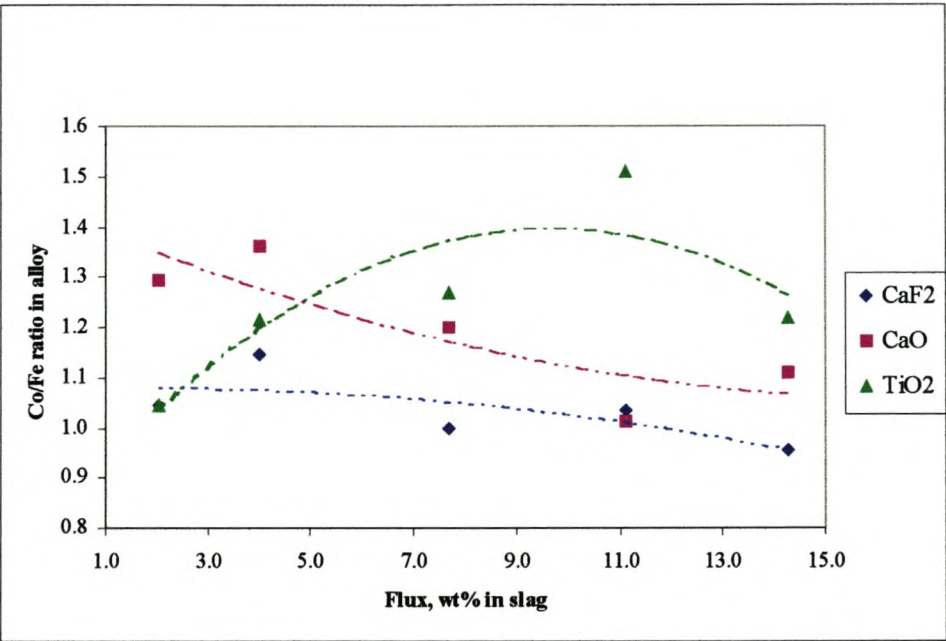
#### 4.3.2 Effect of Slag Modifiers on Recovery Ratio of Co to Fe in Metal Alloy

One of the challenges of recovering cobalt from iron-silicate slags of the type arising from a copper smelter (e.g. reverbaratory furnace) is how to control the levels of iron reporting to the metal alloy. The compositions of both the synthetic slags and actual slag, described in section 3.1.1 show that cobalt (and copper) is low in concentration and so can be said to be dilute in solution in molten slag. Despite this fact, cobalt recovery from such slags under carbothermic conditions is accompanied by iron, which is present in larger quantities in the slag.

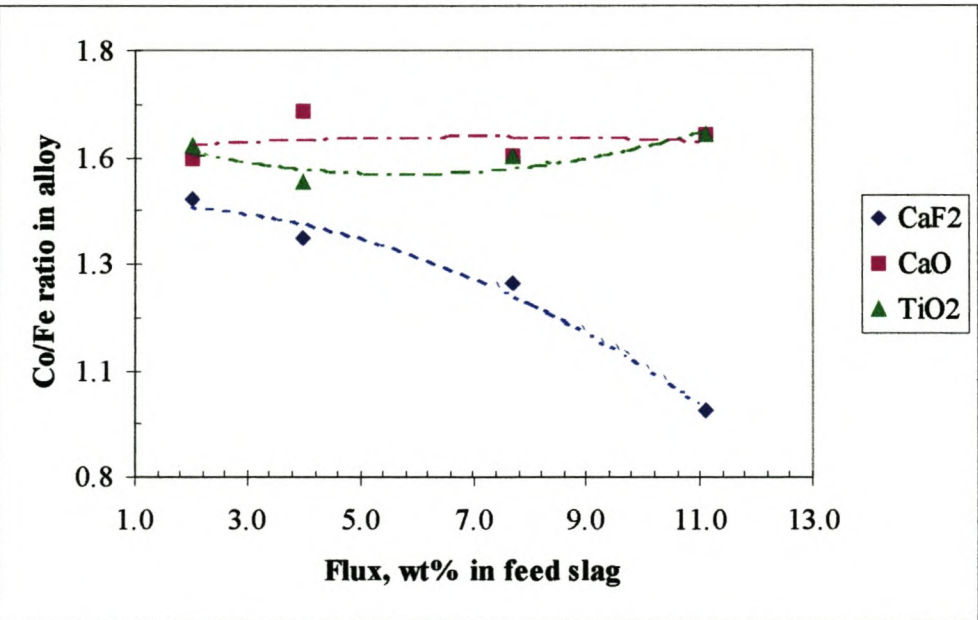
From the recoveries calculated in Tables 4.3 to 4.5 the ratios between cobalt and iron in the alloy were determined. The graphs of recovery ratio against flux show that the ratio tends to increase with the addition of rutile ( $TiO_2$ ). Figures 4.12 to 4.14 show the effect of fluxing on the recovery ratio. The lines on the Figures represent the fitted polynomial trend lines from MSExcel. A thermodynamic explanation to this effect will be discussed in section 4.4.

It is therefore, apparent that rutile additions led to the highest selectivity with regard to cobalt/iron recovery ratio and fluorspar on the hand led to the lowest cobalt/iron ratio recovery. However, in terms of absolute recovery, fluorspar gave the highest recovery of all the metals in all three cases.

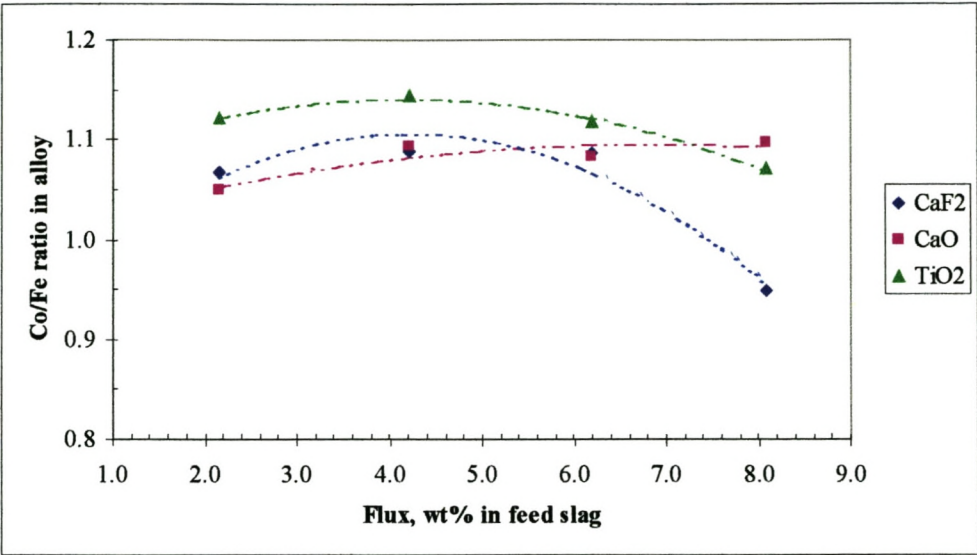




**Figure 4.12** The effect of flux addition on the Co/Fe ratio in metal alloy during the carbothermic reduction of synthetic slag in a tube furnace at 1500°C.



**Figure 4.13** The effect of flux addition on the Co/Fe ratio in metal alloy during the carbothermic reduction of actual slag in a tube furnace at 1500°C.



**Figure 4.14** The effect of flux addition on the Co/Fe ratio in metal alloy during the carbothermic reduction of actual slag in a DC plasma-arc furnace.



**Table 4.5** Analysis of Metal content of alloy at end of experiment and feed slag – Actual slag experiments in DC Plasma arc Furnace

Expt#	Flux		Metal content analysis of alloy, wt%							Smoothing Factor 100/ $\Sigma$ original total	Mass of alloy grams	Metal content in alloy, grams			Metal content in feed slag, grams			Metal recovery, %			
	Type	wt% in feed slag	Co	Cu	Fe	Si	Ti	C	S			Co	Cu	Fe	Co	Cu	Fe	Co	Cu	Fe	Co/Fe ratio
10	CaF <sub>2</sub>	2.15	4.46	4.13	75.94	14.58	0.45	0.25	0.20	0.99	140.06	6.25	5.78	106.36	6.49	9.75	117.98	96.26	59.27	90.16	1.07
1	CaF <sub>2</sub>	4.21	4.34	5.79	72.45	16.47	0.34	0.32	0.31	0.99	139.07	6.03	8.05	100.75				92.93	82.55	85.40	1.09
4	CaF <sub>2</sub>	6.19	4.40	6.50	73.60	14.09	0.47	0.83	0.11	0.98	123.88	5.45	8.05	91.18				83.97	82.56	77.28	1.09
7	CaF <sub>2</sub>	8.09	3.92	4.76	75.07	15.35	0.44	0.30	0.16	0.96	126.15	4.94	6.00	94.70				76.16	61.55	80.27	0.95
11	CaO	2.15	4.24	4.47	73.43	16.57	0.36	0.34	0.58	1.01	143.66	6.09	6.42	105.50				93.83	65.89	89.42	1.05
2	CaO	4.21	4.35	4.09	72.38	18.02	0.36	0.63	0.16	1.01	133.09	5.79	5.45	96.34				89.25	55.86	81.66	1.09
5	CaO	6.19	4.37	5.57	73.34	15.59	0.33	0.56	0.24	1.02	136.72	5.98	7.61	100.27				92.08	78.12	84.99	1.08
8	CaO	8.09	4.42	4.38	73.35	16.60	0.23	0.89	0.13	1.00	133.95	5.93	5.87	98.25				91.28	60.24	83.28	1.10
12	TiO <sub>2</sub>	2.15	4.44	5.32	71.96	16.98	0.43	0.38	0.50	0.98	134.36	5.96	7.14	96.68				91.82	73.27	81.95	1.12
3	TiO <sub>2</sub>	4.21	4.58	4.52	72.75	16.59	0.44	0.92	0.20	1.01	119.73	5.48	5.41	87.10				84.47	55.50	73.83	1.14
6	TiO <sub>2</sub>	6.19	4.49	4.66	72.99	16.02	0.70	0.75	0.40	1.01	113.63	5.10	5.30	82.93				78.61	54.35	70.30	1.12
9	TiO <sub>2</sub>	8.09	4.35	3.80	73.90	16.29	0.69	0.74	0.24	1.02	144.79	6.30	5.50	107.00				97.06	56.42	90.70	1.07

**Table 4.6** Analysis of slag at the end of experiment – Synthetic Slag Experiments in the tube Furnace

Expt#	Graphite g	Flux		Smoothing Factor 100/total wt% in slag	Slag Analysis, wt%								Basicity = (%CaO + %MgO) ÷ (%SiO <sub>2</sub> + %Al <sub>2</sub> O <sub>3</sub> )
		Type	wt% in Feed slag		SiO <sub>2</sub>	TiO <sub>2</sub>	Al <sub>2</sub> O <sub>3</sub>	FeO	MgO	CaO	CuO	CoO	
25	0.30	CaF <sub>2</sub>	2.04	0.989	48.184	0.110	22.849	3.278	3.880	18.480	0.117	0.033	0.315
8	0.30	CaF <sub>2</sub>	4.00	0.994	47.354	0.038	21.908	3.878	3.723	19.914	0.074	0.043	0.341
11	0.30	CaF <sub>2</sub>	7.69	1.015	43.822	0.068	25.382	2.304	3.451	21.732	0.052	0.019	0.364
20	0.30	CaF <sub>2</sub>	11.11	0.973	40.021	0.080	21.722	4.741	2.739	27.644	0.062	0.040	0.492
22	0.30	CaF <sub>2</sub>	14.29	1.023	37.310	0.040	30.495	1.565	2.858	24.519	0.045	0.012	0.404
26	0.30	CaO	2.04	0.981	48.133	0.057	18.105	6.891	3.950	19.806	0.075	0.048	0.359
7	0.30	CaO	4.00	0.983	47.401	0.039	20.618	4.297	3.648	20.648	0.115	0.049	0.357
10	0.30	CaO	7.69	0.991	45.440	0.129	20.928	3.033	3.473	23.818	0.063	0.035	0.411
13	0.30	CaO	11.11	0.987	42.871	0.141	21.410	3.141	3.118	26.136	0.078	0.027	0.455
21	0.30	CaO	14.29	0.980	48.036	0.069	18.477	3.858	2.369	24.169	0.056	0.030	0.399
1	0.20	No Flux	0.00	0.974	47.535	0.043	20.050	8.952	3.815	16.392	0.143	0.050	0.299
2	0.30	No Flux	0.00	0.971	49.375	0.042	21.214	5.103	3.979	17.069	0.166	0.100	0.298
3	0.40	No Flux	0.00	0.977	49.959	0.044	21.078	4.145	4.090	17.484	0.135	0.064	0.304
4	0.50	No Flux	0.00	0.984	48.665	0.041	22.578	4.178	3.916	17.200	0.328	0.080	0.296
24	0.30	TiO <sub>2</sub>	2.04	0.981	47.187	2.696	21.596	4.922	3.808	16.452	0.242	0.070	0.295
9	0.30	TiO <sub>2</sub>	4.00	0.970	46.924	4.551	21.558	3.789	3.694	16.338	0.138	0.061	0.293
17	0.30	TiO <sub>2</sub>	7.69	0.980	48.980	0.863	19.927	5.499	3.999	17.487	0.148	0.050	0.312
15	0.30	TiO <sub>2</sub>	11.11	0.978	39.838	11.850	19.520	7.957	3.360	14.321	0.154	0.047	0.298
23	0.30	TiO <sub>2</sub>	14.29	0.983	48.358	12.699	17.323	4.818	2.540	11.198	0.092	0.029	0.209



Table 4.7 Analysis of slag at the end of Experiments-Actual slag experiments

Expt#	Graphite g	Flux		Smoothing Factor 100/ $\Sigma$ original total	Slag Analysis, wt%														Basicity = $(\% \text{CaO} + \% \text{MgO}) \div$ $(\% \text{SiO}_2 + \% \text{Al}_2\text{O}_3)$
		Type	wt% of Feed		SiO <sub>2</sub>	TiO <sub>2</sub>	Al <sub>2</sub> O <sub>3</sub>	Cr <sub>2</sub> O <sub>3</sub>	FeO	MnO	NiO	MgO	CaO	Na <sub>2</sub> O	K <sub>2</sub> O	P <sub>2</sub> O <sub>5</sub>	CuO	CoO	
2	0.3	CaF <sub>2</sub>	2.04	1.00	51.07	0.62	17.37	0.15	10.09	0.13	0.01	3.19	12.38	0.71	4.06	0.01	0.14	0.06	0.183
5	0.3	CaF <sub>2</sub>	4.00	0.97	48.87	0.62	21.74	0.14	6.71	0.15	0.01	3.28	14.44	0.00	3.92	0.00	0.09	0.04	0.207
8	0.3	CaF <sub>2</sub>	7.69	1.00	51.43	0.63	15.29	0.14	11.78	0.14	0.01	3.13	12.73	0.32	4.21	0.03	0.09	0.07	0.193
11	0.3	CaF <sub>2</sub>	11.11	0.99	44.83	0.61	27.38	0.12	3.56	0.11	0.01	2.52	17.15	0.96	2.68	0.00	0.05	0.02	0.239
1	0.3	CaO	2.04	1.04	45.99	0.60	24.91	0.12	4.51	0.12	0.01	2.96	16.47	0.88	3.34	0.00	0.05	0.04	0.234
4	0.3	CaO	4.00	0.99	49.76	0.67	17.31	0.13	13.83	0.15	0.01	3.23	10.34	0.00	4.35	0.02	0.13	0.07	0.156
7	0.3	CaO	7.69	1.00	46.60	0.60	17.49	0.13	10.57	0.13	0.01	2.74	17.27	0.52	3.79	0.02	0.09	0.04	0.271
10	0.3	CaO	11.11	0.97	44.21	0.62	21.47	0.11	10.92	0.13	0.01	2.46	16.45	0.00	3.55	0.02	0.03	0.03	0.252
16	0.5	Non	0.00	0.98	55.58	0.68	16.29	0.10	6.90	0.14	0.01	3.46	11.43	0.59	4.58	0.03	0.15	0.08	0.161
18	0.2	Non	0.00	1.00	47.63	0.59	16.19	0.13	18.23	0.13	0.01	2.93	9.72	0.15	3.96	0.05	0.16	0.12	0.154
19	0.3	Non	0.00	1.00	49.69	0.62	16.88	0.15	13.48	0.15	0.01	3.14	10.50	0.98	4.12	0.03	0.14	0.11	0.160
3	0.3	TiO <sub>2</sub>	2.04	1.02	51.47	0.95	16.62	0.14	12.06	0.13	0.01	3.28	10.70	0.26	4.21	0.01	0.10	0.05	0.159
6	0.3	TiO <sub>2</sub>	4.00	0.99	50.49	0.95	17.93	0.14	12.18	0.14	0.01	3.23	10.61	0.00	4.14	0.02	0.11	0.05	0.157
9	0.3	TiO <sub>2</sub>	7.69	0.98	50.78	0.58	18.36	0.14	11.56	0.14	0.01	3.28	10.76	0.00	4.21	0.00	0.13	0.05	0.158
12	0.3	TiO <sub>2</sub>	11.11	0.98	44.41	0.84	18.31	0.14	10.06	0.12	0.01	2.91	19.32	0.00	3.73	0.00	0.11	0.05	0.310

#### 4.4 Thermodynamic Considerations

It has been shown that cobalt oxide dissolution in slag is associated with the complex compounds of silicates and ferrites (Pirard, 1991 and Imriš, 1982). Cobalt oxide like iron has the ability to form silicate, ferrite or titanate compounds with silica, iron oxide or titanium oxide, respectively depending on temperature, oxygen potential and composition of the slag. If the slag contains CoO, FeO, and SiO<sub>2</sub> the existence of cobalt orthosilicate is as likely to be possible like iron orthosilicate (fayalite) is possible. The slag studied in this work consisted of low concentration of cobalt (1.24 to 1.46wt% Co) compared to iron (17 to 22wt% total Fe). From such concentrations the dominating orthosilicate will be the fayalite. The existence of compounds such as Fe<sub>2</sub>SiO<sub>4</sub>, FeTiO<sub>3</sub>, CaSiO<sub>3</sub>, Al<sub>2</sub>TiO<sub>5</sub>, etc., show that these compounds interact with each other in molten slags. The formation of complex compounds of silicates, ferrites or even titanates slag depends on the affinity of oxides towards each other.

The recovery of metals from slag depends on the composition of the slag apart from temperature and the oxygen potential. Going by the reaction mechanism assumed in section 1.2.4, the equilibrium reactions taking place at the slag/metal/gas interface would be



where, ( ) is a compound in slag phase and [ ] is an element in the metal alloy phase. These reactions can only explain the reduction of “free” metal oxides in the slag matrix or entrained in the slag. In order to account for all the cobalt in the slag, and explain the influence of fluxing the changes in the slag composition in terms of activities and activity coefficients of “FeO” and CoO in the slag must be considered.

Thermodynamic calculations for equilibrium amounts of complex compounds were performed with the help of HSC package that utilises the Gibbs Energy Minimisation



concept to calculated equilibrium compositions. The proportions of the slag components and flux amount in moles were the same as those used in the experiments.

It should be noted that the effect of the presence of CuO (or Cu<sub>2</sub>O) in the slag and other compounds such as K<sub>2</sub>O, Cr<sub>2</sub>O<sub>3</sub>, P<sub>2</sub>O<sub>5</sub>, etc. that are present in the actual slag, have not been considered in this discussion.

#### ***a) Effect of CaO on Slag Composition***

The effect of CaO on slag has been said to decrease the viscosity of the slag by breaking down the silicate network. The addition of CaO or lime to the slag will tend to increase the recovery of cobalt along with high levels of undesired iron as can be seen in Figures 4.12, 4.13 and 4.14 of section 4.3.2. This effect is explained by the fact that the addition of CaO simply replaces the FeO in the silicate leading to an increase in the activity of “free” FeO in the slag. On the other hand the rate of reduction of Co<sub>2</sub>SiO<sub>4</sub> is very low. Figure 4.15 is a plot of values generated from HSC and it shows that the formation of Ca<sub>2</sub>SiO<sub>4</sub> in the slag is possible and form preferentially to Fe<sub>2</sub>SiO<sub>4</sub>.

From the physical properties point of view, the effect of the addition of CaO to the slag has been studied and is generally accepted that the presence of CaO in silicate melts decreases the viscosity. Kongoli *et al.* (2000) have suggested that the addition of CaO, at constant Fe/SiO<sub>2</sub> ratio, decreases the liquidus temperature in reductive conditions (olivine precipitation surface) but it increases it in an oxidative conditions (spinel saturation surface). This reveals that there is a fundamental difference between the effect of CaO in oxidative smelting ( $10^{-6} < pO_2 < 10^{-8}$ ) and under reductive smelting ( $pO_2 > 10^{-9}$ ) (Kongoli *et al.*, 2000).

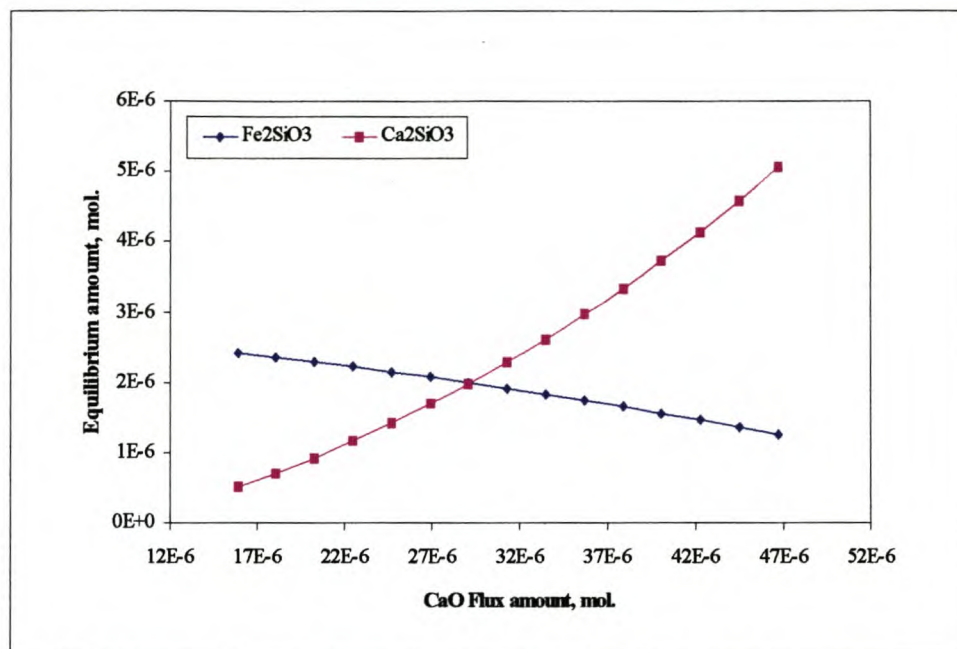


Figure 4.15 Influence of CaO on iron-silicate slag. Calculated from HSC thermodynamic package

#### ***b) Effect of CaF<sub>2</sub> on Slag Composition***

The influence of CaF<sub>2</sub> on slag composition can be explained on the basis of its effect on fluidity of slags. It has been suggested that the addition of CaF<sub>2</sub> to silicate melts makes them less viscous by breaking the network (Sano *et al.*, 1997). Generally, the effect of fluorides on the slag is not well understood especially in slag cleaning of nonferrous metallurgy. The high recoveries of cobalt and iron can only be explained, in this study, on the change in physical properties of the slag. The addition of fluorspar to the slag has the character of a diluent, and does not seem to affect much the activities of other components (Rosenqvist, 1983).

#### ***c) Effect of TiO<sub>2</sub> on Slag Composition***

The effect of TiO<sub>2</sub> on the iron-silicate slag of composition similar to the slag used in the study is shown in Figure 4.16. The plot was generated from HSC thermodynamic package. The addition of TiO<sub>2</sub> to the slag displaces SiO<sub>2</sub> in silicate compounds (Fe<sub>2</sub>SiO<sub>4</sub>, Ca<sub>2</sub>SiO<sub>4</sub>, Co<sub>2</sub>SiO<sub>4</sub>) resulting in the formation of more stable titanate compounds. As described in Chapter 3, TiO<sub>2</sub> in molten slag exists as Ti<sup>3+</sup> and Ti<sup>4+</sup> depending on the conditions of the system. The latter behaves as an amphoteric oxide and thus as a



network former. The behaviour of rutile in this case could be postulated that because of a ready reaction between  $\text{TiO}_4^{4-}$  and  $\text{FeO}_2^-$  in molten slag activity of FeO in the slag is decreased leading to reduced iron in metal allow. However the free,  $\text{SiO}_4^{4-}$  in the slag may form cobalt orthosilicate with  $\text{Co}^{2+}$  ions leading to increased losses of cobalt in slag.

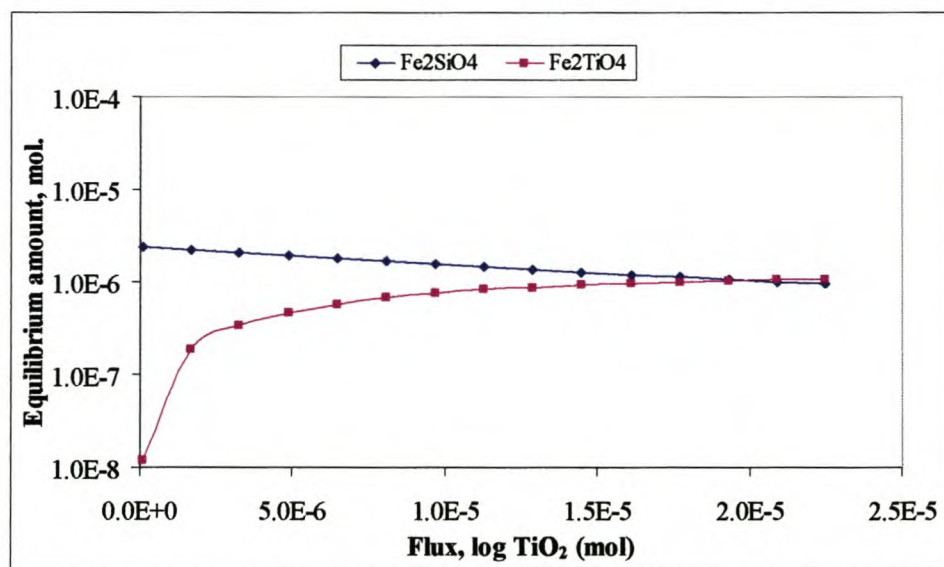


Figure 4.16 Influence of  $\text{TiO}_2$  on iron-silicate slag. Calculated from HSC thermodynamic Package

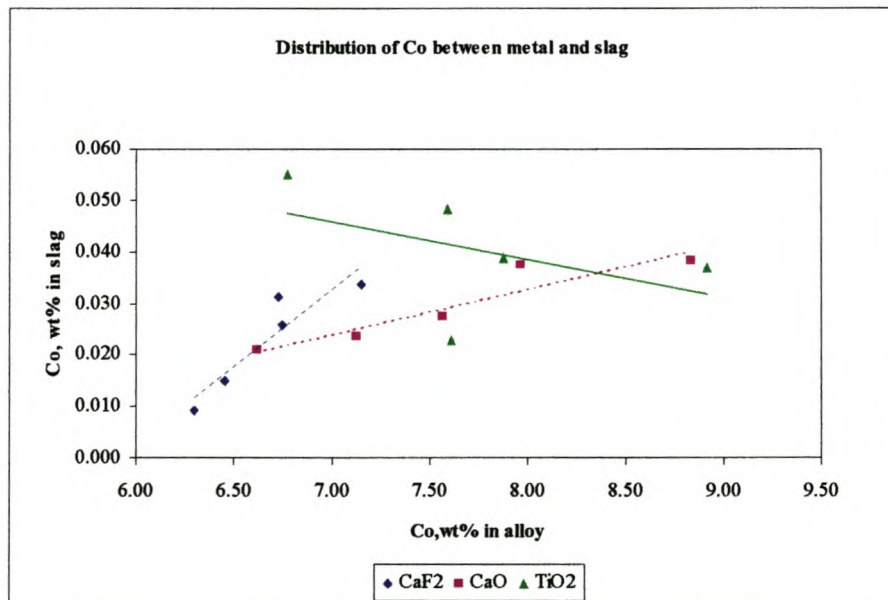
The addition of  $\text{TiO}_2$  to slag high in silica containing CaO is said to decrease the melting point and increases the activity of  $\text{SiO}_2$ .  $\text{TiO}_2$  is partially immiscible with  $\text{SiO}_2$ . The viscosity of the slag is decreased by the addition of  $\text{TiO}_2$  to silica-saturated slags (Rosenqvist, 1983).

The presence of  $\text{Al}_2\text{O}_3$  in the slag helps to retain some of the  $\text{TiO}_2$  and thus reducing its activity in the slag and in turn minimise the recovery of Ti in the alloy, which seems to be the case in electrical reduction of slag in a DC-arc furnace.

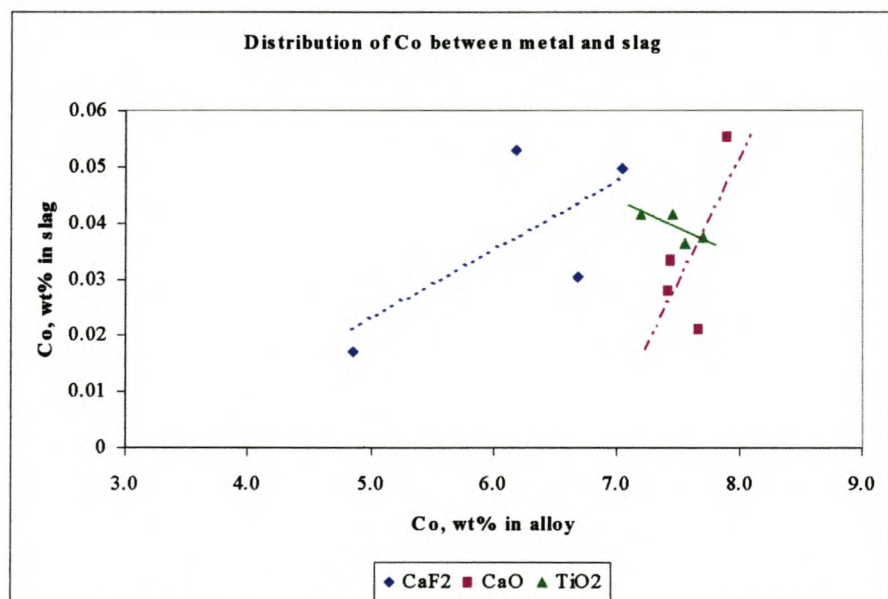
#### 4.4.1 Effect of Slag Modifier on Cobalt in Slag

The amount of cobalt retained in slag after the experiments was compared to that in the metal alloy and plotted as shown in Figures 4.17 and 4.18. The slopes of this data represent the distribution coefficient,  $L_{\text{Co}} = (\% \text{Co in slag}) / (\% \text{Co in metal})$  of cobalt at different levels of fluxing. It is observed that out of the three fluxes used rutile had an opposite effect on the modification of the slag. The amount of cobalt in the slag

decreased with increased amount in metal alloy. Generally, the comparison of the values of entrained cobalt in slag after experiments showed that  $\text{TiO}_2$  addition led to slightly higher losses of cobalt to slag, than when  $\text{CaO}$  or  $\text{CaF}_2$  were added. This effect was observed in both synthetic and actual slag experiments conducted in the tube furnace.



**Figure 4.17** Effect of slag modifiers on the Co distribution between slag and metal in synthetic slag at 1500°C.



**Figure 4.18** Effect of slag modifiers on the Co distribution between slag and metal in synthetic slag at 1500°C.



The study of the effect of fluxes on the carbothermic recovery of base metals from nonferrous slags at 1500°C showed that  $\text{TiO}_2$  had lower overall recovery of cobalt at various levels of addition than in cases where  $\text{CaF}_2$  and  $\text{CaO}$  fluxes were used. On the other hand  $\text{TiO}_2$  significantly improved the selective recovery of cobalt over iron. From this work it can be shown that modification of the slag would play a major role to improve the recovery of base metals from slag.

## CHAPTER FIVE

### *Conclusions and Recommendations*

The findings from the experiments presented and discussed in Chapter 4 show that cobalt can be recovered from slag by reduction with solid carbon at 1500°C. The recovery of cobalt increases when slag modifiers “fluxes” are added in certain proportions. The following are the main findings of the present study.

1. Cobalt recovery is dependant on the amount of reductant added. However, there is an optimum amount of reductant that is required. In this study this amount was found to be about 5% of the total slag feed in the absence of any slag modifier.
2. The recovery of cobalt from slag depends on the composition of the slag apart from other conditions like oxygen partial pressure and temperature of the system. In this study, the composition of the slag was influenced by the addition of lime (CaO), fluorspar (CaF<sub>2</sub>), and rutile (TiO<sub>2</sub>) that showed that the recoveries of cobalt improved. At a fixed amount of carbon added to slag, the recoveries were increased by about 10% Co (by difference of maximum recoveries), about 3% Cu, and 3-7% Fe in all the three cases of fluxing, compared to a situation of similar conditions where no flux was added. Below is a summary of the recoveries achieved:
  - Recoveries attained in synthetic slag experiments were
    - 51-68% Co, 57-84% Cu; 36-59% Fe in the absence of flux
    - 67-75% Co, 77-96% Cu, 65-71% Fe in the presence of CaF<sub>2</sub>
    - 45-82% Co, 53-93% Cu, 45-67% Fe in the presence of CaO
    - 42-77% Co, 50-88% Cu, 35-61% Fe in the presence of TiO<sub>2</sub>
  - Recoveries attained from actual slag experiments were
    - 51-73% Co, 55-87% Cu; 29-52% Fe in the absence of flux
    - 49-82% Co, 58-90% Cu, 52-60% Fe in the presence of CaF<sub>2</sub>
    - 61-65% Co, 61-70% Cu, 37-42% Fe in the presence of CaO
    - 60-71% Co, 62-75% Cu, 38-45% Fe in the presence of TiO<sub>2</sub>
  - Recoveries attained from actual slag experiments in the DC plasma furnace were



- 
- 76-96% Co, 59-62% Cu, 80-90% Fe in the presence of  $\text{CaF}_2$
  - 89-93% Co, 55-78% Cu, 81-89% Fe in the presence of  $\text{CaO}$
  - 78-97% Co, 55-73% Cu, 70-90% Fe in the presence of  $\text{TiO}_2$
3. As part of the recovery process of cobalt, the alloy from of the smelter is further processed by a hydrometallurgical operation. At this stage it is desired that the iron content of the loaded electrolyte is minimal for an efficient recovery to take place. In the present study it has been found that rutile ( $\text{TiO}_2$ ) has a more selective effect on cobalt recovery than lime ( $\text{CaO}$ ) and fluorspar ( $\text{CaF}_2$ ), but led to lower overall recoveries of cobalt at various levels of addition than in cases where  $\text{CaF}_2$  and  $\text{CaO}$  fluxes were used. The effect of  $\text{TiO}_2$  on the slag chemistry leads to the formation of iron titanate compounds in the slag unlike  $\text{CaO}$ , which displaces  $\text{FeO}$  from iron silicate compounds and thus increases the activity of  $\text{FeO}$  in slag, which in turn affects the iron recoveries to the alloy product.
- The ratio of cobalt recovered to iron recovered ( $\text{Co/Fe}$ ) was increased when rutile was added. This effect was not observed with the other two fluxes.
4. The alloys obtained from the plasma furnace yielded higher recoveries of cobalt accompanied by high iron recoveries as well as the dissolved silicon and carbon in slag. It was also found that the recoveries decreased with increased addition of fluxes. This decrease in recovery needs to be investigated further.

Arising from 4 above, the following are recommended regarding the DC plasma furnace experiments.

- Temperature calibration. This would enable the calculation of the necessary thermodynamic properties associated with slag/metal equilibrium calculations.
- Power input to the slag per square unit (power flux) need to be calibrated. This would enable the establishment of a relationship between the power input, slag composition and the slag conductivity.

- Since the laboratory scale furnace is batch operated, it is necessary that a different feeding mechanism be devised to avoid material losses that occur and affect the overall material balance.

It is further recommended that a value for the activity coefficient of CoO in the slag should be re-evaluated and calculated to make its use relevant to reductive conditions and higher temperatures (above 1400°C), and slag composition of the plasma furnace found in the recovery of cobalt from reverbaratory slags practices. If this value were established then a relationship between the effects of fluxes on CoO (and FeO to some extent) would be established and used to maximise the recovery of cobalt from slag.

The following studies would be important to improve the knowledge on the behaviour of cobalt during reductive smelting with regard to DC plasma-arc furnace application:

- A mineralogical study of the actual slag, from the dumpsite to establish the phase with which cobalt is associated in slag (silicate or ferrite type). This would be used to formulate the chemical composition of slag with respect to cobalt.
- The rate of reduction of slags in plasma furnace reactors. From present study it was noticed that after about 30 minutes an inactive situation seemed to occur within the molten bath. The rate of reduction is associated with equilibrium conditions and so such a study would give an insight to the equilibrium reactions taking place.
- The effect of sulphur in the slag on the partitioning of cobalt and iron between slag and metal in reductive smelting.
- Equilibrium experiments to determine the activity coefficient of cobalt under reducing conditions in the slag studied this work.



## *References*

- Açma, E., Sesigur, H., Arslan, C., Addemir, O., and Tekin, A. **Production of Copper, Cobalt and Magnetic Iron oxide from the Ancient Copper slags**, *The Paul Queneau International Symposium Extractive Metallurgy of Copper, Nickel and Cobalt*, Vol. 1: Fundamental Aspects, Editor: R. G. Reddy and R. N. Weizenbach, The Minerals, Metals and Materials Society, pp. 1181-1193, 1993.
- Altudoğan, H. S., and Tümen F. **Metal Recovery from Copper Converter Slag by Roasting with Ferric Sulphate**. Elsevier-Hydrometallurgy 44 pp.261-267, 1997.
- Ammann, P. R., Kim, J. J., Crimes P. B., Brown, F. C. **The Kennecott Slag Cleaning Process: International Symposium On Copper Extraction and Refining, Extractive Metallurgy of Copper-Pyrometallurgy and Electrolytic Refining**. Editors Yannopoulos J. C. and Agarwal J. C., pp.331-350, 1976
- Banks, C. C., and Harrison, D. A, **The Recovery of Non-ferrous Metals from the Secondary Copper Smelter Discard Slags**, *Canadian Metallurgical Quarterly*, vol. 14 No.2, pp. 183-190, 1975.
- Biswas, A. K., Davenport W. G. **Extractive Metallurgy of Copper**, 2<sup>nd</sup> Ed. Pergamon Press, pp. 130, 1982.
- Clark B., **Cobalt (Co) a Welcome co-product**, Co-products and Minor Elements in Non-ferrous Smelting. *The Minerals, Metals and Materials Society*. pp. 98-101, 1995.
- Curr T. R., Barcza N. A., Maske K. U., and Mooney J. F., **The Design and Operation of Transferred-Arc Plasma Systems for Pyrometallurgical Application**, ISPC-6 Montreal, paper #A-6-2, 1983.
- Curr T. R., Maske K. U., Nicol K. C., **The attainment Of High Power Densities in Transferred Arc Plasma Smelting Processes**, ISPC-7 Eindhoven, paper # B-8-4, pp. 1186, 1985.

## References

- 
- Demetrio, S., Ahumada, J., Duran, M. A., Mast, E., Rojas, U., Sanchez, J., Reyes, P. and Morales, E. **Slag Cleaning: The Chilean Copper smelter Experience.** *JOM*, pp.20-25, 2000.
- Elliot J. F. and Mounier M., **Surface and Interfacial Tensions in Copper Matte-slag Systems, 1200°C,** *Canadian Metallurgical Quarterly*, Vol. 21, No. 4 pp. 415-428, 1982.
- Floyd, J. M., and Mackey, P. J. **Developments in Pyrometallurgical treatment of Slag: A Review of Current Technology and Physical Chemistry,** *Extractive Metallurgy, IMM London*, pp345-371, 1981.
- Gaskell, D. R., **Thermodynamic Models of Liquid Silicates,** *Canadian Metallurgical Quarterly*, Vol. 20, No. 1, pp3-19, 1981.
- Geological Survey Bulletin*, **1170**, pp 39-42, 72-73, 85-86.
- Gilchrist J. D., **Extraction Metallurgy**, 2Ed., Pergamon Press, pp. 210-233, 1980.
- Grimsey, E., J. and Toguri, J., M. **Cobalt in Silica Saturated fayalite Slags.** *Canadian Metallurgical Quarterly*, Vol. 27, No. 4, pp. 331-333, 1988.
- Hayes P.C., Okongwu D. A., and Toguri J. M. **Some Observations of the Reactions Between Molten Oxides and Solid Carbon.** *Canadian Metallurgical Quarterly*, vol. 34, No. 1 pp. 27-36, 1995.
- Hayes, P. Associate Professor of Extractive Metallurgy University of Queensland, **Personal Communication**, 2000.
- Hughes, S. **Applying Ausmelt Technology to Recover Cu, Ni and Co from slags.** *JOM*, pp. 30-33, 2000.
- Imriš, I. **Cobalt Distribution in Rokana Smelter.** *Transactions C: Mineral Processing and extractive Metallurgy IMM* vol. 91, pp C153-C161, 1982.
-



## References

---

- Jerome Feinman (Editor), **Plasma Technology in Metallurgical Processing**. Iron and Steel Society, AIME, 1987.
- Robinson, J. J., Editor **Nonferrous Metallurgy: Mineral Commodities Summaries, JOM**, pp. 5, 2000.
- Jones, R. T., Barcza, N. A. and Curr T. R, **Plasma Development in Africa**, <http://www.mintek.ac.za/pyromet/plasma.htm>, 1998.
- Jones, R. T., Hayman, D. A. and Denton, G. M. **Recovery of Cobalt, Nickel, and Copper from Slags, using DC-Arc Furnace Technology**, *Mintek paper # 8360*, 1996.
- Jones, R. T., la Grange, T. G., and Assis, G., **Influence of DC-arc furnace Geometry on a 'Cobalt from Slag Process**, *Mintek Paper #8389*, 1997.
- Khucharsky, M., Stubina, N. M., and Toguri, J. M. **Viscosity of Molten Fe-O-SiO<sub>2</sub>, Fe-O-CaO-SiO<sub>2</sub>, and Fe-O-MgO-SiO<sub>2</sub> Slags**. *Canadian Metallurgical Quarterly*, Vol. 28 no. 1 pp. 7-11, 1989.
- Kim G. H. and Sohn H. Y. **Effects of CaO, Al<sub>2</sub>O<sub>3</sub>, and MgO Additions on the Copper Solubility, Ferric/Ferrous Ratio, and Minor-Element Behaviour of Iron-Silicate Slags**. *Metallurgical and Materials Transactions B*. Vol. 29B, pp. 583-591, 1998.
- Kongoli, F., and Pelton A. D. **Model Prediction of Thermodynamic Properties of Co-Fe-Ni-S Mattes**. *Metallurgical Transactions B*. Vol. 30B, pp. 443-451, 1999.
- Kongoli, F., Yazawa, A. **Liquidus surface of FeO-Fe<sub>2</sub>O<sub>3</sub>-SiO<sub>2</sub>-CaO Slag Containing Al<sub>2</sub>O<sub>3</sub>, MgO and Cu<sub>2</sub>O at Various Oxygen Partial Pressures**. *Proceedings 6<sup>th</sup> International Conference on Slags, Fluxes and Molten Salts*, 2000
- Kor, G. J. W. **Equilibrium between Fe-Cu-Ni-Co-Mo Alloys and Slags of Varying Basicities at 1450°C**. (undated)

## References

---

- Mackenzie C. K., Minto R., and Davenport W. G., **Interfacial Energies in Pyrometallurgical Processes**, *Canadian Metallurgical Quarterly*, Vol. 14 No. 3, pp. 191-197, 1975
- Mackey, P. J. **The Physical Chemistry of Copper Smelting Slags-A review**. *Canadian Metallurgical Quarterly*, Vol. 21, no. 3, pp. 221-260, 1982.
- Matousek J. W. **The behaviour of Cobalt in Pyrometallurgical Processes**, *The Paul Queneau International Symposium Extractive Metallurgy of Copper, Nickel and Cobalt*, Vol. 1: Fundamental Aspects, Ed: R. G. Reddy and R. N. Weizenbach, The Minerals, Metals and Materials Society, pp. 129-142, 1993
- Matousek, J., W. **Oxygen Potential of Copper Smelting Slags**. *Canadian Metallurgical Quarterly*, Vol. 32, no. 2, pp. 97-101, 1993.
- Matuszewicz, R., and Mounsey, E. **Using Ausmelt Technology For the recovery of Cobalt from Smelter Slags**, Cobalt Recovery- a research summary, *JOM*, pp. 53-56, 1998.
- Mikhail S. A., and Webster A H. **Recovery of Nickel, Cobalt, and Copper from Industrial Slags-I. Extraction in Iron Sulphide Matte**. *Canadian Metallurgical Quarterly*, Vol. 31, No. 4, pp 269-281, 1992.
- Mills, K. C. **Structure of Liquid Slags**, *Slag Atlas*, Editor VDEh, pp. 1-8, 1995.
- Mining Weekly*, Vol. 5, No. 8, pp. 4-5, March 1999
- Minto R. and Davenport W. G., *Trans. IMM.* (Section C: Min. Proc. and Extr. Met.) Vol. 81 C36, (1972), Vol. 82 C59 (1973), Vol.83 C66 (1974)
- Norrish, K. and Hutton, J. T. **An accurate X-ray Spectrographic Method for the Analysis of a Wide Range of Geological Samples**. *Geochim. Cosmochim. Acta*, 33:, pp. 431-453, 1969.



## References

---

- Nzontta, M. M., Sichen Du, and Seetharaman, S. **A Study of Sulphide Capacities of Iron-oxide Containing Slags**, *Metallurgical and Materials Transactions B*, vol. 30B, pp 909-920, 1999.
- Pelton, A. D., **Solution Models**. *Advanced Physical Chemistry for Process Metallurgy*, Nobuo Sano, Wei-Kao Lu, Paul V. Reiboud, Editors. Academic Press, pp. 87-117, 1997.
- Pirard, E. **Quantitative Analysis of Co and Cu Distribution in Slags from Kure (Turkey)**, *CIM Bulletin, Mineral Processing*, Vol. 84, pp.87-90, 1991.
- Piret N. L, **Enhancing Cobalt Recovery from Primary and Secondary Sources**, Cobalt Recovery - a commentary, *JOM*, pp. 42-43, 1998.
- Piret N. L., **Cleaning Copper and Ni/Co Slags: The Technical, Economic and Environmental Aspects**. *JOM*, pp. 18, 2000.
- Qian F., Farouk B. and Mutharasan R., **Modeling of Fluid Flow and Heat Transfer in The Plasma Region of the Electric arc Furnace**, HTD-Vol. 248, Fundamentals of Heat Transfer in Electromagnetic, Electrostatic, Acoustic Fields, ASME, pp. 53-63, 1993,
- Radhanath P. Das, **Recovery of Cobalt from Secondary Sources in India**, *JOM*, pp. 52, 1998.
- Reddy, R. G. and Oden L. L. **Recovery of Copper from Industrial Copper Reverbaratory Slags**. 30 pgs, 1983.
- Reddy, R., G. and Healy, G., W. **Distribution of Cobalt Between Liquid Copper and Copper Silicate Slag at 1523 K**. *Metallurgical Transactions B* vol. 12B, September pp. 509-516, 1981.

## References

- 
- Reid, J. K., Moore, J. J., Murawa, J. M. **Plasma Reactor Engineering: Design Principles for the Application of Plasma Technology in Extractive Metallurgy.** *Mineral Resources Research Centre*, University of Minnesota. pp 87-111, 1987.
- Richardson, F. D. **Interfacial Phenomena in Metallurgical Processes.** *Canadian Metallurgical Quarterly*. vol. 21, No. 2, pp 7-11, 1982.
- Richardson, F., D. **Physical Chemistry of Melts in Metallurgy**, Academic Press, London, Vol. 1, pp. 99, 1974.
- Rosenqvist T, **Principles of Extractive Metallurgy**, 2<sup>nd</sup> Edition, McGraw-Hill International, pp. 299, 1983.
- Sano, N., **Thermodynamics of Slags** *Advanced Physical Chemistry for Process Metallurgy*, Editors Nobuo Sano, Wei-Kao Lu, Paul V Riboud, Academic press, pp 45-86, 1997.
- Soltanieh, M. Toguri, J. M. and Sridhar, R. **The Thermodynamics of the Fe-Co-S Ternary System.** *Canadian Metallurgical Quarterly*, Vol 38, No. 4 pp. 227-236, 1999
- Sorokin, M. L., Nikolaev A. G, and Komkov A. A. **Cobalt Behaviour at Smelting and Converting**, Co-products and minor elements in non-ferrous smelting, Ed. T. Lehner, Warrendale, PA: TMS ,pp 109-129, 1995.
- Steiler Jean-Marc, **Ironmaking Reactions.** *Advanced Physical Chemistry for Process Metallurgy*. Editors Nobuo Sano, Wei-Kao Lu, Paul V Riboud with Masafumi Maeda, Academic Press, 1997, pp 335-338.
- Teague, K., C., Swinbourne, D. R., Jahanshahi, S. **Thermodynamics of Cobalt Oxide in Iron Silicate-based Slags**, *The AusIMM Proceedings*, No. 1, pp 66-72, 2000.
- Warczok, A. and Utigard T. A. **Fayalite Slag Reduction by Solid Graphite.** *Canadian Metallurgical Quarterly*, vol. 37 No. 1 pp. 27-39, 1998.
-



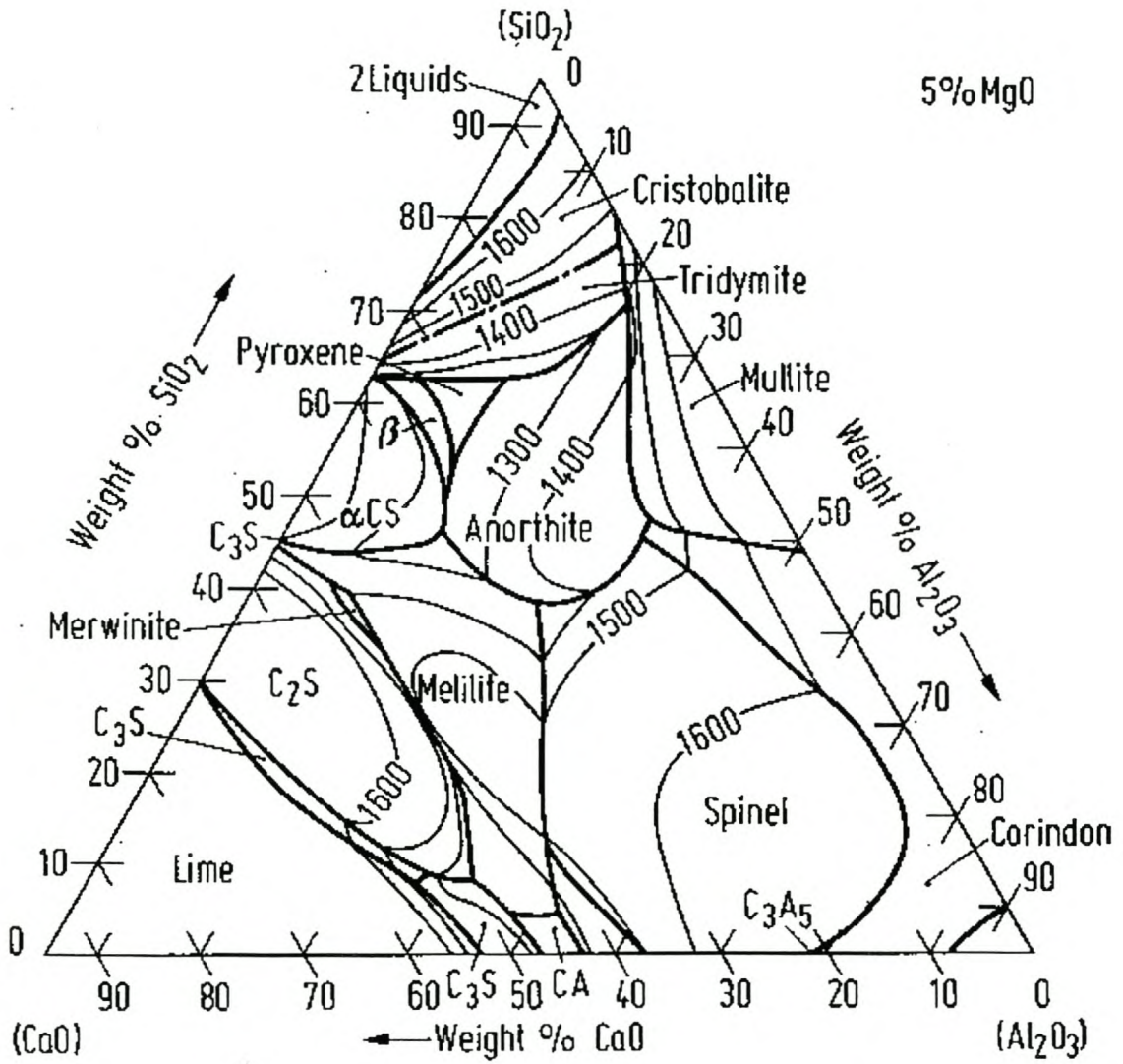
References

---

- Whyte, R. M., Orjans, J. R., Harris, G. B., Thomas, J. A. **Development of a Process for the Recovery of Electrolytic Copper and Cobalt from Rokana Converter Slag**, undated and publisher not indicated.
- Wright, S., Zhang, S., and Jahanshahi, S. **Viscosity of a CaO-MgO-Al<sub>2</sub>O<sub>3</sub>-SiO<sub>2</sub> Melt Containing Spinel Particles at 1646 K**. *Metallurgical and Materials Transactions B*, Vol. 31B, pp 97-104, 2000.
- Yucel, O., Addemir, O., Teking, A., and Nizamoglu, S. **Recovery of Cobalt from Copper Slags**, *Mineral Processing and Extractive Metallurgy Review*, vol. 10, pp. 99-107, 1992.
- Zhao, B. Jak, E. and Hayes, P. C. **The Effect of MgO on Liquidus Temperature of Fayalite Slags**. *Metallurgical and Materials Transactions B*. vol. 30B, pp1017-1026, December 1999.
- Zhao, B., Jak, E. and Hayes, P. C. **The effect of Al<sub>2</sub>O<sub>3</sub> on the Liquidus Temperature of Fayalite Slags**, *Metallurgical and Materials Transactions B*, **30B**, 597-605, 1999.

## Appendices

### Appendix A



**Figure 1A.** Liquidus surface in the system  $\text{Al}_2\text{O}_3$ - $\text{CaO}$ - $\text{MgO}$ - $\text{SiO}_2$  with 5 mass %  $\text{MgO}$  (Calvalier, Sandreo-Dendon, 1960)



## Appendix B



**Figure 1B** Setup of Tube Furnace



**Figure 2B.** Setup of crucible for Tube Furnace experiments



**Figure 3B** Muffle Furnace Setup used in the rate reduction determination






**Figure 4B** Induction Furnace Setup used in the rate reduction determination




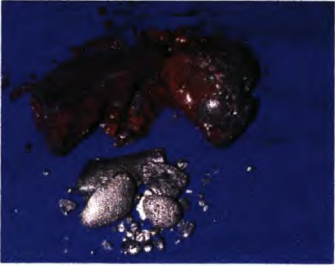





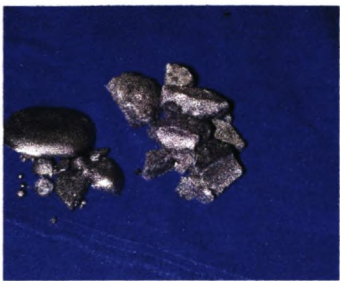
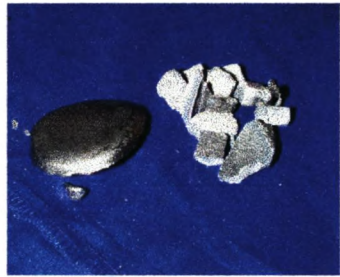
**Figure 5B** DC plasma-arc furnace setup used in the recovery of cobalt from slag

**Table 1A** Preparation of crucible and slag and the product of the plasma furnace

	Copper clippings placed at bottom centre of crucible.
	Slag placed around copper clippings and exposed to allow contact with electrode.
	Crucible with contents placed in the furnace in the anode slot..

	Furnace assembly. Roof of furnace on the left
	Adding feed to furnace once start up is initiated and is stable.
	No slag modifier added. Poor metal-slag separation with metal entrained in slag.
	Effect of small amounts of CaO on the metal and slag separation. Note the colour of the slag and the amount of metal granules. This is related to slag viscosity and interfacial energies.
	Effect of increased CaO on the metal and slag separation. Note the colour of the slag amount of metal granules which increased due to increased CaO addition.



	<p>Effect of <math>\text{TiO}_2</math> on the metal and slag separation. Note the colour of the slag</p>
	<p>Effect of <math>\text{CaF}_2</math> on the metal and slag separation. Note the colour of the slag and piece of alloy. The size of the metal alloy indicates how fluid the slag became with <math>\text{CaF}_2</math> addition..</p>

## Appendix C

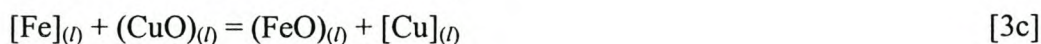
### *a) Calculation of Carbon Requirement for the Reduction of Slag in Tube Furnace*

The composition of actual slag was analysed by XRD technique. From this slag composition the amount of reducible oxides (CoO, CuO and FeO) was determined for the synthetic slag as shown in Table 1C. The total mass of the oxides was 1.555g and the rest was slag components (4.445g).

### *Assumptions*

- i) The equilibrium reactions at the slag/metal interface are
- ii) all the carbon only reacts with dissolved oxygen in slag

Therefore,



Number of moles from Equations 1c and 5c can be related as follows

$$N_{\text{FeO}} = \frac{1.333}{71.844} = 0.0185$$

$$N_{\text{CoO}} = \frac{0.111}{74.933} = 0.00148$$

$$N_{\text{CuO}} = \frac{0.111}{79.545} = 0.00139$$

therefore total moles = 0.0214 = number of moles of CO = number of moles of C.

mass of Carbon required therefore,

$$12.011 \times 0.0214 = \underline{0.257} \text{ grams}$$

mass of graphite therefore should be more than this since carbon content is only 99%

This value compared well with the point at which the metal recoveries were constant with further additions. That is

$$0.3\text{g} \times 99\% = \underline{0.297\text{g}}$$



---

For the actual slag experiments, the carbon calculated above was used a % of the total slag feed i.e.,  $0.3/6.0 * 100 = 5\%$

***b) Calculation of Carbon Requirement for the Reduction of Slag in Plasma arc Furnace***

The mass of feed (slag) was multiplied by 5% to obtain an equivalent carbon amount that was used in the tube furnace experiments, i.e.  $0.05 * 500 = 25\text{g}$ . This value was only 18.5g of carbon since anthracite contained 74% fixed carbon. However, in the experiments 100g of anthracite (11.1% in excess) was used because higher metal yields were achieved with this amount than when lesser amounts were used.

Table 1C Synthetic Slag Experiments Data

Flux				reductant Graphite 99.99%C			Slag Composition			mass	wt%	moles
CaO	wt%	moles	mass, g	mass	moles	wt%	<b>Feed wt in grams</b> (starting weight) mass of master slag mass of metal oxides <b>element grade</b> Co Cu Fe S	6.0	CaO	0.889	14.815	0.0159
	2.04	0.0022	0.25	0.2	0.0167	3.23			MgO	0.222	3.704	0.0055
	4.00	0.0045	0.50	0.3	0.0250	4.76			Al <sub>2</sub> O <sub>3</sub>	0.800	13.333	0.0078
	7.69	0.0089	0.75	0.4	0.0333	6.25			SiO <sub>2</sub>	2.444	40.741	0.0407
	11.11	0.0134	1.00	0.5	0.0417	7.69			FeO	1.333	22.222	0.0186
CaF <sub>2</sub>	wt%	moles	mass, g						CoO	0.111	1.852	0.0015
	2.04	0.0016	0.25						CuS	0.089	1.481	0.0009
	4.00	0.0032	0.50						CuO	0.111	1.852	0.0014
	7.69	0.0064	0.75									
	11.11	0.0096	1.00									
TiO <sub>2</sub>	wt%	moles	mass, g						<b>Master Slag Composition</b>			
	2.04	0.0016	0.25						mass	wt%		
	4.00	0.0031	0.50						CaO	20.000	20.408	
	7.69	0.0063	0.75						MgO	5.000	5.102	
	11.11	0.0094	1.00						Al <sub>2</sub> O <sub>3</sub>	18.000	18.367	
									SiO <sub>2</sub>	55.000	56.122	



**Table 2C** Feed size characterisation for DC plasma furnace Experiments

<b>Slag</b>				
<b>Size Range <math>\mu\text{m}</math></b>	<b>mm</b>	<b>mass, g</b>	<b>%</b>	<b>Cum %</b>
+4000	4.00	0.43	6.44	6.44
-4000 +3350	3.35	0.68	10.18	16.62
-3350 +2800	2.80	1.51	22.60	39.22
-2800 +1400	1.40	3.87	57.93	97.16
-1400 +1000	1.00	0.13	1.95	99.10
-1000	<1.00	0.06	0.90	100.00
<b>Total</b>		<b>6.68</b>	<b>100.00</b>	

<b>Coal</b>				
<b>Size Range <math>\mu\text{m}</math></b>	<b>mm</b>	<b>mass, g</b>	<b>%</b>	<b>Cum %</b>
+4000	4.00	0.83	23.71	23.71
-4000 +3350	3.35	0.52	14.86	38.57
-3350 +2800	2.80	0.74	21.14	59.71
-2800 +1400	1.40	1.33	38.00	97.71
-1400 +1000	1.00	0.08	2.29	100.00
-1000				
<b>Total</b>		<b>3.50</b>	<b>100.00</b>	

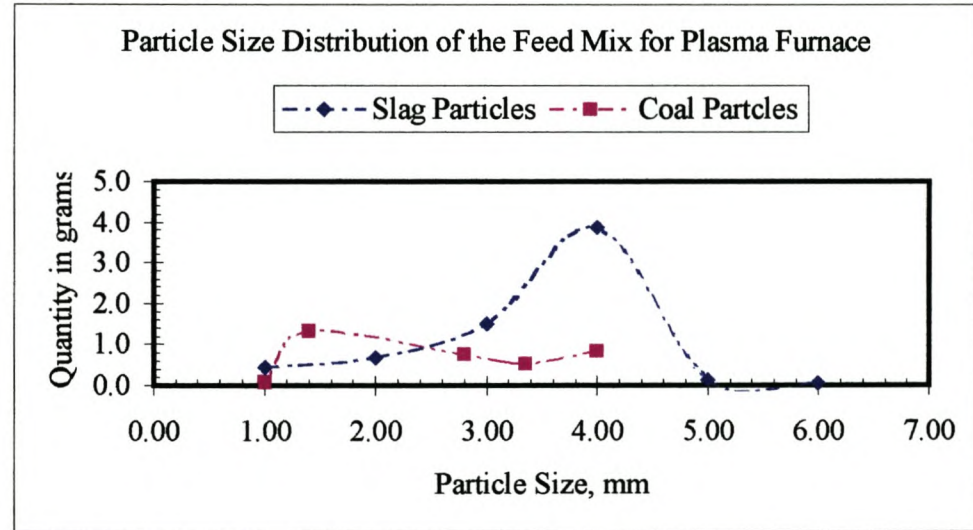


Table 3C Analytical Results

Sample	SiO <sub>2</sub>	TiO <sub>2</sub>	Al <sub>2</sub> O <sub>3</sub>	Cr <sub>2</sub> O <sub>3</sub>	e <sub>2</sub> O <sub>3</sub> (total)	FeO	Fe <sub>2</sub> O <sub>3</sub>	MnO	NiO	MgO	CaO	Na <sub>2</sub> O	K <sub>2</sub> O	P <sub>2</sub> O <sub>5</sub>	CuO	Co <sub>2</sub> O <sub>3</sub>
<i>Actual Slag after Experiments</i>																
#01 NK	44.38	0.58	24.04	0.12	4.35	3.87	0.48	0.12	0.01	2.86	15.89	0.85	3.22	0.00	0.05	0.03
#02 NK	50.91	0.62	17.32	0.15	10.06	nd	nd	0.13	0.01	3.18	12.34	0.71	4.05	0.01	0.14	0.06
#02A NK	50.43	0.62	17.82	0.14	10.00	nd	nd	0.14	0.01	3.21	12.15	0.35	4.07	0.01	0.08	0.04
#03 NK	50.56	0.93	16.33	0.14	11.85	nd	nd	0.13	0.01	3.22	10.51	0.26	4.14	0.01	0.10	0.05
#04 NK	50.14	0.68	17.44	0.13	13.94	10.53	3.41	0.15	0.01	3.25	10.42	0.00	4.38	0.02	0.13	0.07
#05 NK	50.36	0.64	22.40	0.14	6.91	5.58	1.33	0.15	0.01	3.38	14.88	0.00	4.04	0.00	0.09	0.04
#06 NK	50.81	0.96	18.04	0.14	12.26	9.63	2.63	0.14	0.01	3.25	10.68	0.00	4.17	0.02	0.11	0.05
#07 NK	46.68	0.60	17.52	0.13	10.59	nd	nd	0.13	0.01	2.74	17.30	0.52	3.80	0.02	0.09	0.04
#08 NK	51.35	0.63	15.27	0.14	11.76	nd	nd	0.14	0.01	3.13	12.71	0.32	4.20	0.03	0.09	0.07
#09 NK	51.57	0.59	18.65	0.14	11.74	nd	nd	0.14	0.01	3.33	10.93	0.00	4.28	0.00	0.13	0.05
#10 NK	45.53	0.64	22.11	0.11	11.25	nd	nd	0.13	0.01	2.53	16.94	0.00	3.66	0.02	0.03	0.03
#11 NK	45.24	0.62	27.63	0.12	3.59	nd	nd	0.11	0.01	2.54	17.31	0.97	2.70	0.00	0.05	0.02
#12 NK	45.24	0.86	18.65	0.14	10.25	nd	nd	0.12	0.01	2.96	19.68	0.00	3.80	0.00	0.11	0.05
#16 NK	56.58	0.69	16.58	0.10	7.02	6.39	0.63	0.14	0.01	3.52	11.64	0.60	4.66	0.03	0.15	0.09
#18 NK	47.64	0.59	16.19	0.13	18.24	14.40	3.84	0.13	0.01	2.93	9.72	0.15	3.96	0.05	0.16	0.12
#19 NK	49.71	0.62	16.89	0.15	13.48	nd	nd	0.15	0.01	3.14	10.50	0.98	4.12	0.03	0.14	0.11
<i>Synthetic Slag</i>																
#01	48.81	0.04	20.59	0.02	9.19	7.74	1.45	0.04	0.01	3.92	16.83	0.00	0.09	0.00	0.15	0.05
#02	50.85	0.04	21.85	0.01	5.26	4.50	0.76	0.04	0.01	4.10	17.58	0.00	0.09	0.00	0.17	0.10
#03	51.14	0.05	21.58	0.01	4.24	3.33	0.91	0.04	0.01	4.19	17.90	0.00	0.08	0.00	0.14	0.07
#04	49.45	0.04	22.94	0.01	4.25	3.69	0.56	0.03	0.01	3.98	17.48	0.00	0.09	0.00	0.33	0.08
#05	42.11	0.03	18.40	0.01	19.36	nd	nd	0.03	0.01	3.47	15.48	0.01	0.16	0.00	0.24	0.24
#07	48.21	0.04	20.97	0.01	4.37	nd	nd	0.04	0.01	3.71	21.00	0.06	0.17	0.00	0.12	0.05
#07a META	bd	0.01	0.00	0.00	79.90	nd	nd	0.01	0.01	0.00	0.00	0.01	0.00	0.00	11.27	9.14
#07b META	bd	0.01	0.02	0.00	80.05	nd	nd	0.03	0.02	0.00	0.01	0.01	0.00	0.00	11.38	8.79
#08	47.63	0.04	22.03	0.01	3.90	nd	nd	0.03	0.01	3.74	20.03	0.00	0.07	0.00	0.07	0.04
#09	48.37	4.69	22.22	0.01	3.91	nd	nd	0.04	0.01	3.81	16.84	0.00	0.05	0.00	0.14	0.06
#10	45.84	0.13	21.11	0.01	3.06	2.52	0.54	0.04	0.01	3.50	24.03	0.00	0.08	0.00	0.06	0.04
#11	43.16	0.07	25.00	0.01	2.27	1.89	0.38	0.04	0.01	3.40	21.40	0.00	0.09	0.00	0.05	0.02
#13	43.44	0.14	21.70	0.02	3.18	2.64	0.55	0.04	0.01	3.16	26.49	0.00	0.08	0.00	0.08	0.03
#15	40.74	12.12	19.96	0.02	8.14	nd	nd	0.03	0.01	3.44	14.64	0.00	0.01	0.00	0.16	0.05
#17	49.97	0.88	20.33	0.00	5.61	4.68	0.93	0.04	0.01	4.08	17.84	0.00	0.11	0.00	0.15	0.05
#18	42.90	0.19	22.59	0.02	2.80	nd	nd	0.03	0.01	3.19	26.12	0.00	0.07	0.00	0.07	0.02
#19	40.29	0.04	26.79	0.01	2.21	nd	nd	0.03	0.01	3.13	23.37	0.00	0.00	0.00	0.19	0.14
#20	41.14	0.08	22.33	0.01	4.87	nd	nd	0.03	0.01	2.82	28.42	0.00	0.02	0.00	0.06	0.04
#21	49.04	0.07	18.86	0.00	3.94	nd	nd	0.02	0.01	2.42	24.67	0.00	0.00	0.00	0.06	0.03
#22	36.45	0.04	29.80	0.02	1.53	nd	nd	0.03	0.01	2.79	23.96	0.00	0.05	0.00	0.04	0.01
#23	49.20	12.92	17.63	0.00	4.90	nd	nd	0.02	0.01	2.58	11.39	0.00	0.00	0.00	0.09	0.03
#24	48.11	2.75	22.02	0.01	5.02	nd	nd	0.04	0.01	3.88	16.78	0.00	0.10	0.00	0.25	0.13
#25	48.73	0.11	23.11	0.01	3.32	nd	nd	0.04	0.01	3.92	18.69	0.00	0.09	0.00	0.12	0.03
#26	49.07	0.06	18.46	0.00	7.02	5.76	1.26	0.03	0.01	4.03	20.19	0.00	0.00	0.00	0.08	0.05
<i>Master Slag</i>																
WB1a	55.61	0.03	18.92	0.01	0.10	nd	nd	0.02	0.01	4.56	19.42	0.06	0.11	0.00	bd	bd
WB1b	55.19	0.03	19.00	0.01	0.10	nd	nd	0.01	0.01	4.54	19.46	0.08	0.10	0.00	bd	bd
<i>Actual Slag</i>																
WB2a	41.97	0.52	7.96	0.12	30.92	23.67	7.25	0.12	0.02	2.77	9.24	0.00	3.53	0.21	1.65	1.77
WB2b	41.47	0.52	7.96	0.13	30.57	24.30	6.27	0.12	0.02	2.76	9.14	0.00	3.43	0.22	1.60	1.72
<i>Wustite</i>																
WB3a	0.00	0.07	0.00	0.01	98.42	73.35	25.07	0.10	0.02	0.07	0.01	0.00	0.00	0.00	bd	bd
WB3b	0.00	0.06	0.00	0.01	97.35	75.60	21.75	0.10	0.02	0.07	0.01	0.00	0.00	0.00	bd	bd

bd -below detection limit

nd - not determined

detection limit for all elements: 0.01%



**Table 4C** Recovery calculations for synthetic slag experiments in the tube furnace**Co recovery**

expt #	1	2	3	4	6	7	8	9	11	12	13	16	17	18	19	20	21	22	23
mass of feed slag	6.00	6.00	6.00	6.00	6.00	6.00	6.00	6.00	6.00	6.00	6.00	6.00	6.00	6.00	6.00	6.00	6.00	6.00	6.00
wt % of Co metal in feed slag	1.46	1.46	1.46	1.46	1.46	1.46	1.46	1.46	1.46	1.46	1.46	1.46	1.46	1.46	1.46	1.46	1.46	1.46	1.46
mass of Co metal in slag	0.09	0.09	0.09	0.09	0.09	0.09	0.09	0.09	0.09	0.09	0.09	0.09	0.09	0.09	0.09	0.09	0.09	0.09	0.09
Total mass of alloy recovered	0.52	0.77	0.79	0.82	0.93	0.84	0.94	0.92	0.61	0.71	0.86	0.88	0.64	0.95	0.49	0.78	0.94	0.77	0.84
wt% Co in alloy	8.58	7.09	7.58	7.21	7.15	7.59	7.56	6.46	6.62	8.91	7.88	6.73	7.13	6.30	7.61	6.77	6.74	7.96	8.83
mass of Co metal in alloy	0.04	0.05	0.06	0.06	0.07	0.06	0.07	0.06	0.04	0.06	0.07	0.06	0.05	0.06	0.04	0.05	0.06	0.06	0.07
<b>% Co Recovered</b>	<b>51.03</b>	<b>62.21</b>	<b>68.54</b>	<b>67.66</b>	<b>75.88</b>	<b>72.80</b>	<b>80.90</b>	<b>67.80</b>	<b>45.84</b>	<b>71.73</b>	<b>77.35</b>	<b>67.44</b>	<b>51.90</b>	<b>68.28</b>	<b>42.83</b>	<b>60.45</b>	<b>72.53</b>	<b>69.64</b>	<b>84.67</b>

**Cu Recovery**

expt #	1	2	3	4	6	7	8	9	11	12	13	16	17	18	19	20	21	22	23
mass of feed slag	6.00	6.00	6.00	6.00	6.00	6.00	6.00	6.00	6.00	6.00	6.00	6.00	6.00	6.00	6.00	6.00	6.00	6.00	6.00
wt % of Cu metal in feed slag	2.47	2.47	2.47	2.47	2.47	2.47	2.47	2.47	2.47	2.47	2.47	2.47	2.47	2.47	2.47	2.47	2.47	2.47	2.47
mass of Cu metal in slag	0.148	0.148	0.148	0.148	0.148	0.148	0.148	0.148	0.15	0.15	0.15	0.15	0.15	0.15	0.15	0.15	0.15	0.15	0.15
Total mass of alloy recovered	0.52	0.77	0.79	0.82	0.93	0.84	0.94	0.92	0.61	0.71	0.86	0.88	0.64	0.95	0.49	0.78	0.94	0.77	0.84
wt% Cu in alloy	16.25	14.16	15.71	15.04	15.40	15.11	14.72	13.83	13.00	17.76	15.21	13.15	13.78	12.47	15.11	13.33	13.75	15.58	11.15
mass of Cu metal in alloy	0.085	0.109	0.124	0.124	0.143	0.127	0.138	0.127	0.08	0.13	0.13	0.12	0.09	0.12	0.07	0.10	0.13	0.12	0.09
<b>% Cu Recovered</b>	<b>57.14</b>	<b>73.50</b>	<b>83.94</b>	<b>83.40</b>	<b>96.63</b>	<b>85.63</b>	<b>93.08</b>	<b>85.87</b>	<b>53.24</b>	<b>84.47</b>	<b>88.28</b>	<b>77.90</b>	<b>59.33</b>	<b>79.96</b>	<b>50.28</b>	<b>70.36</b>	<b>87.43</b>	<b>80.55</b>	<b>63.20</b>

**Fe Recovery**

expt #	1	2	3	4	6	7	8	9	11	12	13	16	17	18	19	20	21	22	23
mass of feed slag	6.00	6.00	6.00	6.00	6.00	6.00	6.00	6.00	6.00	6.00	6.00	6.00	6.00	6.00	6.00	6.00	6.00	6.00	6.00
wt % of Tot Fe metal in feed slag	17.27	17.72	17.72	17.72	17.72	17.72	17.72	17.72	17.72	17.72	17.72	17.72	17.72	17.72	17.72	17.72	17.72	17.72	17.72
mass of Tot Fe metal in slag	1.04	1.06	1.06	1.06	1.06	1.06	1.06	1.06	1.06	1.06	1.06	1.06	1.06	1.06	1.06	1.06	1.06	1.06	1.06
Total mass of alloy recovered	0.52	0.77	0.79	0.82	0.93	0.84	0.94	0.92	0.61	0.71	0.86	0.88	0.64	0.95	0.49	0.78	0.94	0.77	0.84
wt% Tot Fe in alloy	73.52	77.37	75.15	76.59	75.80	75.88	76.41	78.40	79.22	71.61	75.44	78.95	77.84	80.15	75.73	78.74	78.22	74.80	78.74
mass of Fe metal in alloy	0.38	0.60	0.60	0.63	0.70	0.64	0.72	0.72	0.48	0.50	0.65	0.69	0.50	0.76	0.37	0.62	0.74	0.57	0.66
<b>% Fe Recovered</b>	<b>36.97</b>	<b>55.96</b>	<b>55.98</b>	<b>59.21</b>	<b>66.30</b>	<b>59.95</b>	<b>67.34</b>	<b>67.84</b>	<b>45.23</b>	<b>47.49</b>	<b>61.02</b>	<b>65.20</b>	<b>46.71</b>	<b>71.62</b>	<b>35.12</b>	<b>57.92</b>	<b>69.30</b>	<b>53.89</b>	<b>62.21</b>

**S recovery**

expt #	1	2	3	4	6	7	8	9	11	12	13	16	17	18	19	20	21		22
mass of feed slag	6.00	6.00	6.00	6.00	6.00	6.00	6.00	6.00	6.00	6.00	6.00	6.00	6.00	6.00	6.00	6.00	6.00		6.00
wt % of S in feed slag	0.50	0.50	0.50	0.50	0.50	0.50	0.50	0.50	0.50	0.50	0.50	0.50	0.50	0.50	0.50	0.50	0.50		0.50
mass of S in slag	0.03	0.03	0.03	0.03	0.03	0.03	0.03	0.03	0.03	0.03	0.03	0.03	0.03	0.03	0.03	0.03	0.03		0.03
Total mass of alloy recovered	0.52	0.77	0.79	0.82	0.93	0.84	0.94	1.01	0.61	0.71	0.89	0.88	0.64	1.03	0.49	0.78	0.94		0.77
wt% S in alloy	1.64	1.38	1.56	1.16	1.65	1.42	1.30	1.31	1.17	1.72	1.47	1.17	1.25	1.08	1.54	1.15	1.29		1.65
mass of S alloy	0.01	0.01	0.01	0.01	0.02	0.01	0.01	0.01	0.01	0.01	0.01	0.01	0.01	0.01	0.01	0.01	0.01		0.01
<b>% S Recovered</b>	<b>28.55</b>	<b>35.25</b>	<b>41.31</b>	<b>31.92</b>	<b>51.27</b>	<b>39.64</b>	<b>40.63</b>	<b>44.06</b>	<b>23.57</b>	<b>40.40</b>	<b>43.50</b>	<b>34.32</b>	<b>26.68</b>	<b>37.11</b>	<b>25.33</b>	<b>30.04</b>	<b>40.38</b>		<b>42.18</b>



**Table 5C Recovery calculations for actual slag experiments in the tube furnace**

<b>Co Recovery</b>															
<b>expt #</b>	1	2	3	4	5	6	7	8	9	10	11	12	13	14	15
mass of feed slag	6.00	6.00	6.00	6.00	6.00	6.00	6.00	6.00	6.00	6.00	6.00	6.00	6.00	6.00	6.00
wt % of Co metal in feed slag	1.330	1.330	1.330	1.330	1.330	1.330	1.330	1.330	1.330	1.330	1.330	1.330	1.330	1.330	1.330
mass of Co metal in slag	0.08	0.08	0.08	0.08	0.08	0.08	0.08	0.08	0.08	0.08	0.08	0.08	0.08	0.08	0.08
Total mass of alloy recovered	0.70	0.85	0.76	0.62	0.99	0.70	0.70	1.05	0.75	0.65	0.81	0.63	0.93	0.52	0.56
wt% Co in alloy	7.42	7.05	7.56	7.90	6.69	7.20	7.44	6.19	7.45	7.67	4.86	7.71	6.27	10.15	7.30
mass of Co metal in alloy	0.05	0.06	0.06	0.05	0.07	0.05	0.05	0.06	0.06	0.05	0.04	0.05	0.06	0.05	0.04
<b>% Co Recovered</b>	<b>65.38</b>	<b>75.18</b>	<b>71.72</b>	<b>61.37</b>	<b>82.94</b>	<b>63.12</b>	<b>65.28</b>	<b>81.40</b>	<b>70.03</b>	<b>62.48</b>	<b>49.30</b>	<b>60.85</b>	<b>73.07</b>	<b>66.13</b>	<b>51.21</b>

**Cu Recovery**

<b>expt #</b>	1	2	3	4	5	6	7	8	9	10	11	12	13	14	15
mass of feed slag	6.00	6.00	6.00	6.00	6.00	6.00	6.00	6.00	6.00	6.00	6.00	6.00	6.00	6.00	6.00
wt % of Cu metal in feed slag	1.258	1.258	1.258	1.258	1.258	1.258	1.258	1.258	1.258	1.258	1.258	1.258	1.258	1.258	1.258
mass of Cu metal in slag	0.08	0.08	0.08	0.08	0.08	0.08	0.08	0.08	0.08	0.08	0.08	0.08	0.08	0.08	0.08
Total mass of alloy recovered	0.70	0.85	0.76	0.62	0.99	0.70	0.70	1.05	0.75	0.65	0.81	0.63	0.93	0.52	0.56
wt% Cu in alloy	7.51	7.17	7.50	7.54	6.79	7.03	7.64	6.53	7.38	7.54	5.46	7.51	7.09	9.93	7.55
mass of Cu metal in alloy	0.05	0.06	0.06	0.05	0.07	0.05	0.05	0.07	0.06	0.05	0.04	0.05	0.07	0.05	0.04
<b>% Cu Recovered</b>	<b>69.94</b>	<b>80.86</b>	<b>75.19</b>	<b>61.88</b>	<b>89.10</b>	<b>65.15</b>	<b>70.82</b>	<b>90.76</b>	<b>73.31</b>	<b>64.96</b>	<b>58.53</b>	<b>62.69</b>	<b>87.33</b>	<b>68.39</b>	<b>55.99</b>

**Fe Recovery**

<b>expt #</b>	1	2	3	4	5	6	7	8	9	10	11	12	13	14	15
mass of feed slag	6.00	6.00	6.00	6.00	6.00	6.00	6.00	6.00	6.00	6.00	6.00	6.00	6.00	6.00	6.00
wt % of Tot Fe metal in feed slag	23.194	23.194	23.194	23.194	23.194	23.194	23.194	23.194	23.194	23.194	23.194	23.194	23.194	23.194	23.194
mass of Tot Fe metal in slag	1.39	1.39	1.39	1.39	1.39	1.39	1.39	1.39	1.39	1.39	1.39	1.39	1.39	1.39	1.39
Total mass of alloy recovered	0.70	0.85	0.76	0.62	0.99	0.70	0.70	1.05	0.75	0.65	0.81	0.63	0.93	0.52	0.56
wt% Tot Fe in alloy	83.53	84.66	83.44	83.11	85.74	84.24	83.49	86.02	83.83	83.42	88.49	83.74	85.72	78.11	83.76
mass of Fe metal in alloy	0.59	0.72	0.63	0.52	0.85	0.59	0.58	0.90	0.63	0.54	0.72	0.53	0.80	0.41	0.47
<b>% Fe Recovered</b>	<b>42.20</b>	<b>51.77</b>	<b>45.39</b>	<b>37.03</b>	<b>60.99</b>	<b>42.37</b>	<b>42.00</b>	<b>64.90</b>	<b>45.18</b>	<b>38.96</b>	<b>51.50</b>	<b>37.91</b>	<b>57.28</b>	<b>29.18</b>	<b>33.71</b>



Table 6C Recovery calculations for actual slag experiments in the DC plasma arc furnace

Expt#	%Co	Cu%	Fe%	Si%	Ti%	C%	S%	Total	mass of alloy	%Co Alloy	%Co Slag	%Co Feed Slag	Rec Co%	%Cu Alloy	%Cu Slag	%Cu Feed Slag	Extra Cu%	Rec Cu%	%Fe Alloy	%Fe Slag	%Fe Feed Slag	Rec Fe%
Expt1	4.37	5.83	72.99	16.59	0.34	0.32	0.31	100.75	139.07	6.08	1.30	6.49	93.63	8.11	1.949629	9.75	1.106	83.17	101.51	23.595	117.98	86.04
Expt2	4.33	4.07	72.00	17.92	0.36	0.63	0.16	99.47	133.09	5.76			88.78	5.42				55.57	95.82			81.22
Expt3	4.54	4.48	72.12	16.45	0.44	0.91	0.20	99.14	119.73	5.44			83.74	5.36				55.02	86.35			73.19
Expt4	4.49	6.63	75.11	14.38	0.48	0.85	0.11	102.05	123.88	5.56			85.69	8.21				84.25	93.05			78.87
Expt5	4.27	5.44	71.63	15.23	0.32	0.55	0.23	97.67	136.72	5.84			89.94	7.44				76.30	97.93			83.01
Expt6	4.43	4.60	72.00	15.80	0.69	0.74	0.39	98.65	113.63	5.03			77.55	5.23				53.62	81.81			69.35
Expt7	4.07	4.94	77.97	15.94	0.46	0.31	0.17	103.86	126.15	5.13			79.10	6.23				63.93	98.36			83.37
Expt8	4.44	4.40	73.62	16.66	0.23	0.89	0.13	100.37	133.95	5.95			91.62	5.89				60.46	98.61			83.59
Expt9	4.25	3.71	72.18	15.91	0.67	0.72	0.23	97.67	144.79	6.15			94.80	5.37				55.10	104.51			88.58
Expt10	4.51	4.17	76.77	14.74	0.45	0.25	0.20	101.09	140.06	6.32			97.31	5.84				59.91	107.52			91.14
Expt11	4.21	4.44	72.92	16.45	0.36	0.34	0.58	99.30	143.66	6.05			93.17	6.38				65.43	104.76			88.79
Expt12	4.54	5.44	73.64	17.38	0.44	0.39	0.51	102.34	134.36	6.10			93.97	7.31				74.98	98.94			83.87

**d) Voltage Readings for the Plasma furnace Experiments.**

The Current in all the Tables was maintained at 0.45 kA (power unit) or 2.5 A (on regulator reading)

About 5.6g of 99.9% copper clipping was added for startup purposes in all the experiments

**Table 7C** DCV readings for plasma experiments

CaF2 Flux			Expt1			Expt2		Expt3		Expt4	
Time	Slag mass gram	Cumm slag mass	Flux type	Flux mass gram	DCV reading	Flux mass gram	DCV reading	Flux mass gram	DCV reading	Flux mass gram	DCV reading
0	100	100	CaF2	11	-	22	-	33	-	44	-
5	100	200			35		38		-		34
10	100	300			30		30		30		30
15	100	400			30		30		25		31
20	100	500			28		30		26		30
25					28		30		27		26
30					28		34		28		37
35					29		32		30		35
40					29		31		29		32
45					29		28		28		34
50					30		30		30		29
55					29		34		30		27
60					30		31		30		33
average DCV			29.58			31.5		28.45		31.5	
Average power at 0.45 kA		kVA	13.31			14.18		12.80		14.18	



**Table 8C** DCV readings for plasma experiments

CaO Flux			Expt1			Expt2		Expt3		Expt4	
Time	Slag mass gram	Cumm slag mass	Flux type	Flux mass gram	DCV reading	Flux mass Gram	DCV reading	Flux mass gram	DCV reading	Flux mass gram	DCV reading
0	100	100	CaO	11	-	22	-	33	-	44	-
5	100	200			39		34		39		37
10	100	300			20		27		30		31
15	100	400			28		30		27		30
20	100	500			27		27		28		29
25					26		30		28		26
30					27		28		31		26
35					28		25		28		27
40					26		24		25		26
45					25		25		33		28
50					24		24		33		27
55					23		26		30		30
60					25		25		30		25
average DCV			26.50			27.08		30.17		28.50	
Average power at 0.45 kA      kVA			11.93			12.19		13.58		12.82	

Table 9C DCV readings for plasma experiments

TiO2 Flux			Expt1			Expt2		Expt3		Expt4	
Time	Slag mass gram	Cumm slag mass	Flux type	Flux mass gram	DCV reading	Flux mass gram	DCV reading	Flux mass gram	DCV reading	Flux mass Gram	DCV reading
0	100	100	TiO2	11	-	22	-	33	-	44	-
5	100	200			37		30		40		38
10	100	300			30		28		27		33
15	100	400			27		28		27		32
20	100	500			28		29		27		31
25					26		25		26		30
30					25		26		26		31
35					24		23		23		32
40					23		24		29		30
45					22		24		27		30
50					22		27		21		30
55					23		25		23		27
60					25		24		20		25
average DCV			26.00			26.08		26.33		30.75	
Average power at 0.45 kA			11.70			11.74		11.84		13.83	
kVA											